# Interplay of Dengue Virus and the Human Immune Response

# Interplay of Dengue Virus and the Human Immune Response

A dissertation presented

by

**Ying Kai Chan**

to

**The Division of Medical Sciences**

in partial fulfillment of the requirements

for the degree of

Doctor of Philosophy

in the subject of

**Microbiology and Immunobiology**

Harvard University

Cambridge, Massachusetts

April 2015

Dissertation Advisor: Dr. Michaela U. Gack Ying Kai Chan

**Interplay of Dengue Virus and the Human Immune Response**

## ABSTRACT

RIG-I is a key cytosolic sensor of many RNA viruses, including dengue virus (DV), the most significant arboviral pathogen. Upon viral RNA binding, RIG-I signals via the adaptor protein MAVS, located at mitochondria, to induce the expression of interferons (IFNs), proinflammatory cytokines and interferon-stimulated genes (ISGs), thereby establishing an antiviral state. Among the ISGs, the IFITM proteins are critical for antiviral restriction of numerous pathogenic viruses including DV by inhibiting viral entry.

Here, we uncover how DV escapes RIG-I-mediated immunity. The NS3 protein of DV binds directly to 14-3-3ε, a mitochondrial-targeting protein that is essential for translocation of RIG-I from the cytosol to mitochondria. Specifically, NS3 blocks 14-3-3ε from forming a "translocon" complex with RIG-I and its upstream activator, TRIM25, thereby inhibiting RIG-I translocation to mitochondria for MAVS interaction and antiviral signaling. Furthermore, RIG-I that fails to translocate to mitochondria is degraded in a lysosome-dependent manner in DV-infected cells. Intriguingly, NS3 binds to 14-3-3ε using a phosphomimetic motif that resembles a canonical phospho-serine/threonine motif found in cellular 14-3-3-interaction partners. We engineer a recombinant DV encoding a mutant NS3 protein deficient in 14-3-3ε binding ($DV2_{KIKP}$) and find that this mutant virus is attenuated in replication compared to the parental virus. Strikingly, $DV2_{KIKP}$ fails to antagonize RIG-I and elicits high levels of IFNs,

proinflammatory cytokines and ISGs in human hepatocytes and monocytes. Taken together, our data reveal a novel phosphomimetic-based mechanism for viral antagonism of innate immunity and provide a foundation for DV vaccine development.

DV can infect cells directly, or complex with non-neutralizing antibodies to infect Fc-receptor-bearing cells in a secondary infection, which is associated with severe disease. While it has been shown that IFITMs restrict DV direct infection, it is unknown if the latter process, commonly termed antibody-dependent enhancement (ADE), might bypass IFITM-mediated restriction. Comparison of direct and ADE-mediated DV infection shows that IFITM proteins restrict both infection modes equally, suggesting that upregulation of IFITMs may be a therapeutic strategy.

In summary, our work elucidates several molecular aspects of the interplay of DV with the human immune response, which may guide the rational design of vaccines and antivirals.

## TABLE OF CONTENTS

## DEDICATION

I dedicate this thesis to my parents, Chee Tack Chan and Swee Juang Tan, who have supported me in every way they can.

## ACKNOWLEGEMENTS

I am deeply indebted to my mentors, Dr. Michaela Gack and Dr. Michael Farzan, for their invaluable guidance. Working with Michaela has taught me the utmost importance of focus, and how to strive for excellence. Michaela's attention for details has also greatly strengthened the quality of work I aim for. Mike has shown me how to "daydream" about science, and enhanced my appreciation for thinking out of the box. My graduate school experience would not have been half as rewarding without their support and advice.

My thesis committee, Dr. Lee Gehrke, Dr. Jim Cunningham and Dr. Jon Kagan, provided invaluable feedback and suggestions on my research direction. In particular, Lee and Jim generously guided me in my personal development. I would also like to thank my past mentors, Dr. Eng Eong Ooi and Dr. Robyn Klein, for numerous insights into graduate school. I am also immensely appreciative of the many people in the laboratory who provided intellectual discourse and shared technical expertise.

Finally, I would like to thank my family and friends who have been so encouraging throughout my time in graduate school. My parents, my sister Ying Xuan, my brother-in-law Patrick, and their three lovely children, have been a constant source of support and laughter. My friends also provided great perspective on career and life choices and several non-scientists even suggested project ideas. Life is so much more fulfilling when your loved ones are a part of the journey.

## ATTRIBUTIONS

### Chapter 1

Ying Kai Chan and Michaela Gack wrote the sections regarding RIG-I-like receptor regulation in virus infection and immunity. Ying Kai Chan wrote the rest of Chapter 1.

### Chapters 2 and 3

Ying Kai Chan performed all aspects of this study. Ying Kai Chan and Michaela Gack designed the study and wrote the manuscript (Chapter 2). Ying Kai Chan wrote Chapter 3.

### Chapter 4

Ying Kai Chan and Michael Farzan conceived and designed the experiments. Ying Kai Chan and I-Chueh Huang performed the experiments. Ying Kai Chan, I-Chueh Huang and Michael Farzan analyzed the data. I-Chueh Huang contributed reagents. Ying Kai Chan and Michael Farzan wrote the paper (Chapter 4).

### Chapter 5

Ying Kai Chan wrote Chapter 5.

# Chapter 1

## Introduction

Parts of this chapter were originally published as:

Chan YK, Gack MU (2015) RIG-I-like receptor regulation in virus infection and immunity. Curr Opin Virol 12C: 7-14.

## A PREAMBLE

Infectious agents and their hosts have been co-evolving since the dawn of life. While certain microbes and hosts share a mutually beneficial relationship known as symbiosis, other microbes replicate at the cost of their hosts and cause pathological outcomes. This has resulted in an arms race in which host immune responses restrict pathogens, and pathogens that acquire the ability to evade these countermeasures are in turn selected for. Understanding the basic mechanisms underlying these two sides of the coin is key to the rational design of antiviral therapeutics. This is especially true for dengue virus, the most significant arboviral pathogen, for which no therapeutics exist to-date. By elucidating several molecular aspects of the interplay of dengue virus with the human immune response, we hope to enhance our understanding of dengue pathogenesis and accelerate development of much needed anti-dengue therapeutics.

## DENGUE VIRUS (DV)

### DV epidemiology and disease

Dengue virus (DV) is responsible for ~390 million infections annually, and 2.5 billion people live in areas at risk for dengue transmission, making DV a highly significant arboviral pathogen [1-3]. DV belongs to the *Flaviviridae* family, which consists of many other significant human pathogens, including West Nile virus (WNV), yellow fever virus (YFV), Japanese encephalitis virus (JEV), tick-borne encephalitis virus (TBEV) and hepatitis C virus (HCV).

DV is spread by the bite of infected mosquitoes, most notably *Aedes aegypti* and *Aedes albopictus*. The four serotypes of DV co-circulate in many tropical and sub-tropical regions and continue to expand their range. DV infection can cause the acute febrile disease known as

dengue fever (DF), which is characterized by fever, joint pain, rashes and other non-specific symptoms [4]. While DF is thought to be self-limiting, some DV-infected patients acquire potentially lethal dengue hemorrhagic fever (DHF), which manifests as high fever, liver damage, hemorrhage tendency, and thrombocytopenia [5]. DHF can further progress to dengue shock syndrome (DSS) during which patients experience a sudden drop in blood pressure due to extensive vascular leakage [6].

Primary DV infection generally confers long-lasting immunity to the infecting serotype [7]. However, epidemiological studies suggest that secondary infection with a heterologous serotype increases the chance of acquiring severe dengue disease [8]. Furthermore, primary infection of infants breast-feeding from dengue-immune mothers also result in higher risk for severe dengue disease [9]. The dominant theory explaining these phenomena is known as antibody-dependent enhancement (ADE), and is described in greater detail later.

**DV pathogenesis**

During a blood meal, DV-infected mosquitoes transmit the virus subcutaneously and it is thought that skin-resident macrophages and dendritic cells (DCs) are the initial targets of infection [6]. These infected cells can recruit monocytes and DCs to the dermis and infect them [10], or migrate to lymph nodes and disseminate the virus to monocytes and macrophages [11], which amplifies the infection and finally results in viremia. In agreement, autopsy and clinical studies indicate that mononuclear phagocytes (monocytes, macrophages and DCs) are the primary sites of DV replication, although the virus can also be detected in other tissues such as spleen and liver [12-14].

As the key targets of DV are phagocytic cells of the immune system, severe dengue disease is thought to be a consequence of immunopathogenesis. Infected phagocytes secrete

large amounts of proinflammatory cytokines such as TNF-α and IL-6, which perturb vascular endothelial cells and result in increased capillary permeability and hemorrhage tendency [15-17]. While it is unclear what triggers this cytokine storm in primary DV infections, extensive research suggests that ADE can drive immunopathogenesis in secondary infections. Pre-existing, non-neutralizing antibodies bind to the infecting heterologous DV serotype and mediate efficient uptake of DV-antibody complexes into Fcγ receptor-bearing monocytes, macrophages and DCs, thereby leading to increased viral replication and enhanced cytokine release [3].

**DV therapeutics**

Currently, there are no FDA approved therapies against dengue. In particular, vaccination efforts are challenging due to the need to simultaneously protect against 4 distinct serotypes. Recently, a live-attenuated tetravalent vaccine based on chimeric YFV-DV completed two phase III clinical trials and provided ~80% protection from risk of hospitalization [18,19]. However, the vaccine showed weak to moderate efficacy against the widely prevalent DV serotype 2 (DV2). Several other vaccine candidates, including live-attenuated vaccines, subunit, DNA and purified inactivated vaccines, are also being pursued but are at earlier stages of clinical testing. Due to the lack of DV therapeutics, patients generally receive supportive treatment, and vector control through the use of insecticides remains the principal tool for combatting DV transmission [20].

**DV life cycle**

DV is a single-strand, positive sense RNA virus (reviewed in [21]). The ~11 kb long genome encodes 10 proteins: 3 structural proteins [capsid (C), membrane (M), envelope (E)] and 7 nonstructural proteins (NS1, NS2A, NS2B, NS3, NS4A, NS4B and NS5). DV virions are ~50

nm in diameter and enter cells via clathrin-mediated endocytosis. The drop in pH triggers membrane fusion in the late endosomes, releasing DV RNA into the cytoplasm. As the genome is positive sense, it acts like host mRNA and is translated by ribosomes at the rough endoplasmic reticulum (ER) membrane. Translation results in a large polyprotein that is subsequently cleaved by host proteases and the DV NS2B/3 protease complex into the 10 individual proteins.

Upon translation, DV forms replication complexes (RCs) by inducing large membrane alterations on the ER (reviewed in [22]). These RCs consist of the transmembrane NS proteins (NS2B, NS4A and NS4B), the RNA-dependent RNA polymerase NS5, the serine protease NS3, and viral RNA. While the transmembrane NS proteins are thought to be important for inducing membrane rearrangements such as invaginations, NS5 is the key enzyme that generates a complementary negative strand of the viral genome, which is then used as a template to produce more positive sense capped viral RNA. Apart from proteolytic processing of the translated polyprotein, NS3 is also an essential component of RCs due to its RNA helicase activity.

Newly generated viral RNA associates with C to form nucleocapsids, which bud into the ER lumen and are packaged into virions by prM and E. These immature virions then pass through the trans-golgi network (TGN) during which prM is cleaved by furin and glycans found on E are further modified. The mature infectious virion is then secreted extracellularly for dissemination.

## INNATE IMMUNE SENSORS AND IMMUNE EVASION

### Classes of PRRs and viral PAMPs

Mammalian cells possess pattern-recognition receptors (PRRs) that recognize foreign

molecules, such as viral replication products or structural components of the virion, commonly known as pathogen-associated molecular patterns (PAMPs). Upon non-self-recognition, the infected host cell rapidly mounts an innate immune response, characterized by induction of type I and III interferons (IFNs), interferon-stimulated genes (ISGs) and proinflammatory cytokines, to restrict viral replication and direct adaptive immune responses [23].

Of the innate immune sensors that recognize foreign nucleic acids, members of the Toll-like receptor family (TLR3, TLRs7-9 and TLR13) detect RNA or DNA in the lumen of endosomes or lysosomes. These TLRs are single transmembrane proteins found on the endosomal membrane, and are highly expressed mainly in immune cells (reviewed in [24]). Another class of PRRs known as the RIG-I like receptors (RLRs) sense viral RNA in the cytoplasm. In contrast to the TLRs, RLRs are expressed in most cell types. As viruses usurp host machinery for replication, a hallmark of pathogenic viruses is their ability to invade the cytoplasm and replicate. Thus, RLRs are well positioned to sense a pathogenic viral infection and trigger an innate immune response. More recently, several innate immune sensors that detect foreign DNA have been discovered and characterized. For example, cyclic GMP-AMP synthase (cGAS) senses DNA in the cytosol while interferon-inducible protein 16 (IFI16) recognizes DNA both in the cytoplasm and in the nucleus (reviewed in [25]). Other proposed DNA sensors include RNA polymerase III (pol III), DNA-dependent activator of IFN-regulatory factors (DAI), DDX41, DNA-dependent protein kinase (DNA-PK) and stimulator of interferon genes (STING). The detection of foreign nucleic acids by these PRRs triggers a signaling cascade that generally leads to the transcriptional upregulation of IFNs and proinflammatory cytokines, thereby inducing an antiviral state. In this chapter, I focus on the RLRs and how they are regulated.

**RLR structure and signaling**

The RLR family, comprising RIG-I, MDA5 and LGP2, detects viral RNA in the cytosol of most cell types. The RLRs possess a central DExD/H-box helicase domain and a C-terminal domain (CTD), which are important for binding viral RNA. RIG-I and MDA5 further harbor two N-terminal caspase activation and recruitment domains (CARDs), which are responsible for downstream signaling. LGP2 lacks the CARDs and is generally thought to play a regulatory role in RLR signaling (reviewed in [26]).

RIG-I and MDA5 recognize structurally distinct viral RNA species. RIG-I senses RNAs possessing both panhandle structures and a 5'triphosphate moiety, while MDA5 is thought to recognize long dsRNA or web-like RNA aggregates (reviewed in [27]). In addition, a recent study indicated that a 5'diphosphate moiety in the viral RNA can also be recognized by RIG-I [28]. Extensive functional studies have demonstrated the importance of RIG-I and MDA5 in sensing RNA virus infections, with RIG-I playing a critical role in the detection of orthomyxo-, rhabdo- and arenaviruses, and MDA5 preferentially detecting picornaviruses. Moreover, many viruses (flaviviruses, paramyxoviruses and reoviruses) are sensed by both RIG-I and MDA5 [29]. Upon RNA ligand binding, RIG-I and MDA5 bind to their common adaptor MAVS/Cardif/IPS-1/VISA through CARD-CARD interactions. This leads, via TRAF3 or TRAF6, to the activation of several well-studied kinases of the IKK family, namely IKKε and TBK1 as well as the IKKα/β/γ complex. Through phosphorylation steps, these kinases ultimately activate the transcription factors IFN-regulatory factor 3 and 7 (IRF3/7), NF-κB, and ATF2/c-Jun, which then induce the transcription of IFNs and proinflammatory cytokines [30]. Subsequently, secreted IFNs bind to their respective receptors and induce the expression of hundreds of ISGs, leading to an antiviral state.

While antiviral and proinflammatory cytokines are key to controlling viral infection, they also lead to inflammation and tissue damage and hence must be tightly regulated. In the following sections we review the key molecular and cellular processes that regulate RLR signaling, with emphasis given to recently published work.

**RIG-I activation and homeostasis**

**i) RLR regulation by posttranslational modifications**

In the past several years, it has become evident that the activation of RIG-I and MDA5 is a multi-step process consisting of viral RNA binding, conformational changes, and a series of posttranslational modifications (PTMs). Furthermore, regulatory PTMs ensure that aberrant RLR signal transduction does not occur in the absence of a viral infection (Figure 1.1). In uninfected cells, RIG-I is kept in an auto-repressed state due to the masking of its CARDs by the helicase domain [31,32]. In addition, RIG-I and MDA5 undergo phosphorylation at multiple residues, which prevents aberrant downstream signaling: S8 and T170 as well as T770 and S854/S855 in the RIG-I CARDs and CTD, respectively; and S88 in the MDA5 CARDs [33]. RIG-I is kept phosphorylated at these CARD and CTD sites by protein kinase C α/β (PKCα/β) and casein kinase II (CKII), respectively, while the kinase(s) for MDA5 phosphorylation is still unknown [32,34]. An RNAi screen against the human phosphatome recently revealed that two highly homologous isoenzymes of phosphoprotein phosphatase 1 (PP1α and PP1γ) are responsible for RIG-I and MDA5 dephosphorylation, thereby triggering their activation [35]. In response to viral RNA binding, PP1α/γ binds and dephosphorylates both RIG-I (S8 and T170) and MDA5 (S88) in the CARDs, allowing for MAVS binding, likely through a rearrangement of the tandem CARD after dephosphorylation. The phosphatase(s) for the removal of the phosphorylation marks in the RIG-I CTD is currently unknown. As PP1α and PP1γ dephosphorylate numerous

substrates in the cell, current studies are focused on elucidating the mechanism of PP1's substrate specificity for RLRs in infected cells.

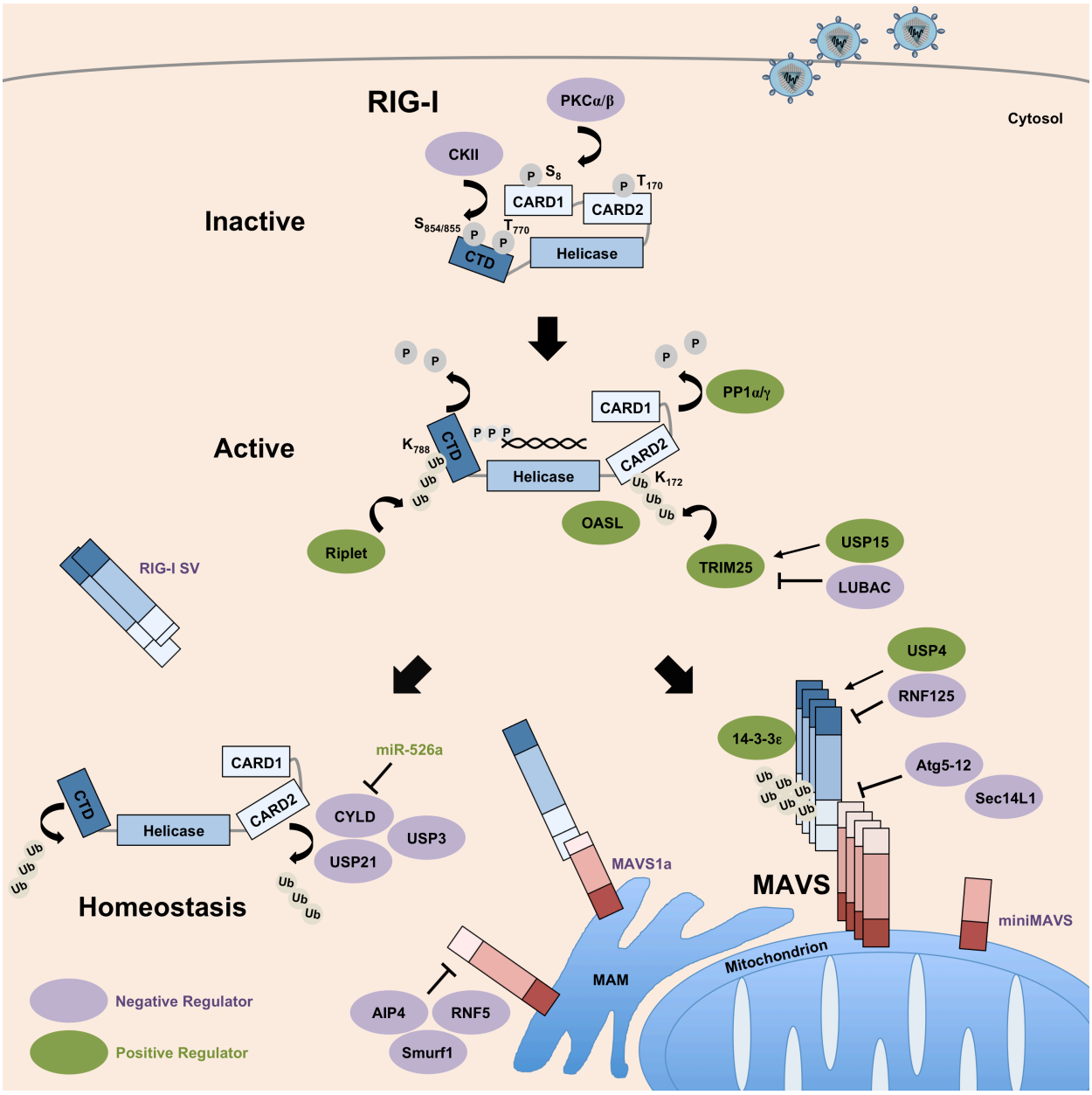


**Figure 1.1. Regulation of RLR signaling, as exemplified by RIG-I.** RIG-I is kept in an inactive phosphorylated state in resting cells by PKCα/β and CKII. Upon engagement of viral RNA, RIG-I undergoes a conformational change and is dephosphorylated by PP1α/γ. Subsequently, activation of RIG-I is mediated by K63-linked ubiquitination of the CTD and CARD domains by Riplet and TRIM25, respectively, promoting RIG-I tetramerization. OASL can mimic ubiquitination to promote RIG-I activation. The adaptor protein 14-3-3ε mediates translocation of the active RIG-I-TRIM25 complex to the mitochondrion/MAM-localized MAVS, leading to downstream signal transduction that results in type I IFN gene expression (not illustrated). The deubiquitinating enzymes CYLD, USP21 and USP3 remove K63-linked polyubiquitin chains from RIG-I as a form of homeostatic regulation to prevent aberrant IFN induction. The expression of CYLD is suppressed by miR-526a. TRIM25, RIG-I and MAVS are further regulated by degradative K48-linked ubiquitination mediated by LUBAC, RNF125, and AIP4, Smurf1, and RNF5, respectively. Conversely, USP15 and USP4 deubiquitinate TRIM25 and RIG-I, respectively, to stabilize the proteins. The Atg5-Atg12 conjugate and Sec14L1 block the RIG-I-MAVS interaction to prevent antiviral signaling. Finally, a RIG-I splice variant (RIG-I SV), MAVS splice variant (MAVS1a) and miniMAVS further contribute to prevent excessive signaling. (Adapted from *Chan and Gack, Curr Opin Virol, 2015*.)

Recent data demonstrated that, in the case of RIG-I, there is crosstalk between phosphorylation and K63-linked ubiquitination, a polyubiquitin linkage that does not trigger proteasomal degradation but facilities signal transduction events. Biochemical studies demonstrated that in cells without viral infection, RIG-I is robustly phosphorylated but minimally ubiquitinated in its CARDs and CTD. However, upon stimulation of RIG-I by viral RNA binding, dephosphorylation occurs and this triggers robust K63-ubiquitination of RIG-I by two critical E3 ligases, TRIM25 and Riplet. Mechanistically, the E3 ligase Riplet first induces K63-linked ubiquitination of K788 in the CTD of RIG-I [36]. This appears to trigger a conformational change that exposes the CARDs, enabling TRIM25 to bind and to attach K63-linked ubiquitin chains to K172 in RIG-I CARD2, ultimately leading to RIG-I oligomerization and MAVS binding [37]. K63-linked ubiquitination of CARD2 is critical for RIG-I activation as loss of TRIM25 severely hampers RIG-I signaling. Furthermore, K63-linked ubiquitin chains have also been shown to bind to the CARDs non-covalently to promote RIG-I oligomerization and activation [38]. Thus, it has been unclear for quite some time how both covalent and non-covalent K63-polyubiquitin mediate RIG-I activation. This question was recently addressed by structural analysis of the RIG-I CARDs, which showed that the RIG-I CARDs form a helical tetramer adopting a 'lock-washer configuration', in which three K63-diubiquitins are wrapped around the outer rim of the CARD tetramer [39]. This study further showed that K172 is within the covalent linkage distance to ubiquitin (< 20 Å), strongly indicating that this residue is indeed covalently ubiquitinated. Biochemical studies comparing the activation capacity of covalent versus non-covalent K63-diubiquitin showed that, while both induced RIG-I tetramerization and MAVS activation, covalent K63-diubiquitin had a stronger RIG-I activation capacity than unanchored K63-ubiquitin [39]. It has been recently shown that RIG-I can be also activated in an

ubiquitin-independent manner. Specifically, the IFN-inducible oligoadenylate synthetases-like (OASL) protein, which contains two tandem ubiquitin-like domains, binds to RIG-I and mimics K63-ubiquitination, thereby enhancing RIG-I activation [40]. This study proposed a model in which TRIM25- and Riplet-mediated K63-linked ubiquitination is essential for RIG-I activation early during infection, while OASL activates RIG-I at later time points.

The importance of K63-linked ubiquitination for RIG-I activation was further strengthened by the identification of several deubiquitinating (DUB) enzymes that remove this ubiquitin mark from RIG-I to inhibit its signaling. CYLD (cylindromatosis) deubiquitinates RIG-I and several downstream molecules to prevent premature RIG-I activation in uninfected cells [41], while USP3 deubiquitinates RIG-I specifically after viral infection, likely serving as a negative feedback regulator [42]. In contrast, USP21 has been shown to bind and deubiquitinate RIG-I independent of viral infection [43]. Together, these studies establish K63-linked ubiquitination as a crucial activation mark for RIG-I. In contrast, the role of K63-linked ubiquitin polymers in MDA5 activation is still a subject of debate. In general, our knowledge of PTMs that regulate the signaling activity of MDA5 lags significantly. As described above, dephosphorylation by PP1$\alpha$/$\gamma$ has been shown to be critical for MDA5 activation [35]. In addition, SUMOylation of the MDA5 CTD by the ubiquitin E3 ligase PIAS2$\beta$ facilitates MDA5-mediated antiviral signaling; however, the precise mechanism of this activation mode remains unknown [44].

In contrast to K63-linked ubiquitination that serves as an activation mark, K48-linked ubiquitination triggers proteasomal degradation to regulate the turnover of cellular proteins, including key molecules in the RLR pathway. The RING-finger protein 125 (RNF125) induces K48-linked ubiquitination and proteasomal degradation of RIG-I, MDA5 and MAVS, thereby

preventing excessive RLR signaling [45]. Conversely, USP4 removes K48-linked ubiquitination from RIG-I to stabilize it [46]. The stability of TRIM25, a key regulator of RIG-I activation, is tightly regulated by K48-linked ubiquitination mediated by the linear ubiquitin assembly complex (LUBAC), consisting of the two E3 ligases HOIL-1L and HOIP [47]. Conversely, USP15 has been recently identified as a DUB enzyme that stabilizes TRIM25, thereby ensuring effective viral clearance through sustained IFN-β production [48]. The abundance of MAVS is also delicately controlled by degradative K48-linked ubiquitination mediated by the E3 ligases AIP4 (also called ITCH), Smurf1 (SMAD ubiquitin regulatory factor 1), and RNF5 [49-51]. However, how MAVS stability is dynamically regulated by these three E3 ligases, or whether they act in a temporal or cell type-specific manner, is currently unknown.

**ii) RLR regulation by posttranscriptional mechanisms**

Several posttranscriptional mechanisms modulating the RLR signal-transducing activities have been identified, including alternative splicing, alternative translation as well as microRNAs (miRNAs), small noncoding RNAs that lead to the degradation or translational repression of target mRNAs by binding to complementary sequences in their 3' untranslated region. In most cases, posttranscriptional mechanisms are part of a negative feedback loop to dampen RLR signaling to prevent excessive or sustained production of antiviral and inflammation-inducing proteins (Figure 1.1).

Alternative splicing has been shown to play an important role in modulating the activities of RIG-I and MAVS. A splice variant of RIG-I (RIG-I SV) is specifically induced upon viral infection or IFN stimulation [52]. RIG-I SV carries a short deletion (amino acids 36-80) in CARD1 and is therefore unable to bind TRIM25 for downstream activation. RIG-I SV suppresses RIG-I activation in a dominant negative manner by hetero-oligomerizing with full-length RIG-I, which prevents MAVS binding. Similarly, a splice variant of MAVS (MAVS1a) strongly binds to RIG-I and inhibits its interaction with full-length MAVS for signal transduction [53]. Furthermore, it has been recently reported that the MAVS mRNA is bicistronic and that alternative translation gives rise to a smaller MAVS protein termed "miniMAVS" [54]. MiniMAVS dampens IFN induction, but promotes cell death comparably to full-length MAVS; The precise mechanism of how miniMAVS acts is however unknown.

Innate immune signaling triggered by virus infection also leads to the upregulation of several miRNAs, which in turn modulate RIG-I activity and IFN induction. For example, miR-526a is induced in monocytes upon vesicular stomatitis virus (VSV) infection and directly suppresses the expression of CYLD, hence enhancing K63-linked ubiquitination of RIG-I and its

activation [55]. VSV infection also induces the expression of miR-146a in macrophages in a RIG-I-dependent manner. MiR-146a then acts as a negative-feedback regulator in the RLR-mediated IFN induction pathway by targeting several important downstream signaling molecules, including TRAF6 [56]. Furthermore, miR-466l directly binds to the 3'UTR of IFN-α mRNAs and reduces their expression during VSV infection [57].

**iii) Regulation of RLR-MAVS signal transduction by subcellular localization and autophagy**

Apart from molecular regulatory mechanisms, cellular processes control and shape the signaling activities of RLRs and MAVS. RLRs are traditionally thought to be "free floating" cytosolic molecules, though recent studies indicated that RLRs are localized to cytoplasmic bodies induced by PKR and DHX36, known as antiviral stress granules (avSGs) [58]. It has been proposed that avSGs provide a platform for RLRs, other antiviral proteins (PKR, RNAseL, and OAS1), and viral RNA to interact, hence augmenting RLR signaling. Further studies are, however, required to determine the contribution of soluble versus avSG-associated RLRs to antiviral immunity, and whether other subcellular compartments are used by RLRs for initiating signal transduction.

In contrast to the RLRs, the regulation of MAVS by subcellular localization is better characterized due to its membrane-bound nature. MAVS resides in multiple subcellular regions, including the outer mitochondrial membrane, mitochondrial-associated ER membranes (MAMs; a specialized sub-domain of the ER located adjacent to mitochondria) and peroxisomes [59-61]. Functionally, while cytosolic MAVS is unable to signal, mitochondrial and MAM-associated MAVS are responsible for type I IFN induction [60]. Furthermore, recent work indicated that peroxisomal MAVS preferentially induces type III IFNs [62].

Upon PAMP recognition, cytosolic RLRs must interact with membrane-bound MAVS; however, how this translocation event occurs was not known until recently. It has been shown that the activated RIG-I-TRIM25 complex requires binding to the adaptor protein 14-3-3ε to translocate to mitochondria/MAMs for MAVS interaction and downstream activation [63]. It is unclear if MDA5 also requires 14-3-3ε for translocation, and if other adaptor proteins control RLR translocation to other MAVS locations such as the peroxisomes.

Autophagy, a degradation process well-known for its role in the removal of protein aggregates and organelles, also plays a critical role in innate immunity by either degrading intracellular pathogens, or by homeostatic regulation of innate immune signaling (reviewed in [64]. It has been reported that cells deficient in Atg5, a key regulatory protein of autophagy, are defective in autophagosome formation and accumulated damaged mitochondria, leading to increased RLR stimulation, likely due to increased release of reactive oxygen species (ROS) [65]. Another line of evidence also supports the negative regulation of RLR signaling by Atg5; however, this study suggested a different mechanism, specifically that Atg5-Atg12 conjugate suppresses IFN induction by directly interacting with RIG-I and MAVS through their CARDs [66]. Similarly, Sec14L1, a protein that is not implicated in autophagy, inhibits the CARD-CARD interaction of RIG-I and MAVS [67].

**Pathogenic viruses target RLR regulation for immune evasion**

Viruses and their hosts are in an active “arms race”, driving continuous co-evolution. Given the importance of RLRs for an effective innate immune response, viral pathogens have evolved means to manipulate various RLR regulatory mechanisms for immune evasion (Figure 1.2). Many viruses have been shown to dysregulate the PTMs of RLRs. For example, measles and Nipah virus, both members of the paramyxovirus family, antagonize the phosphatases

PP1α/γ to prevent RLR dephosphorylation and hence activation. Mechanistically, their V protein, a well-known IFN-antagonist, interacts with PP1α/γ and sequesters these phosphatases away from MDA5, hence keeping it in the CARD-phosphorylated, inactive state [68]. Furthermore, in dendritic cells, measles virus targets PP1α/γ through a V-independent mechanism that was due to measles-induced DC-SIGN signaling and formation of a negative-regulatory PP1 complex, hence inhibiting both RIG-I and MDA5 [69]. Previously, multiple studies have demonstrated that the V proteins of several paramyxoviruses, including parainfluenza virus 5 (PIV5), antagonize MDA5 through a direct interaction with its helicase domain, thereby blocking its ATPase activity [70,71]. VP35 of Ebola virus (EboV) and NS1 of influenza A virus (IAV) specifically inhibit the ATPase activity of RIG-I that is stimulated by PACT (PKR activator) [72,73].

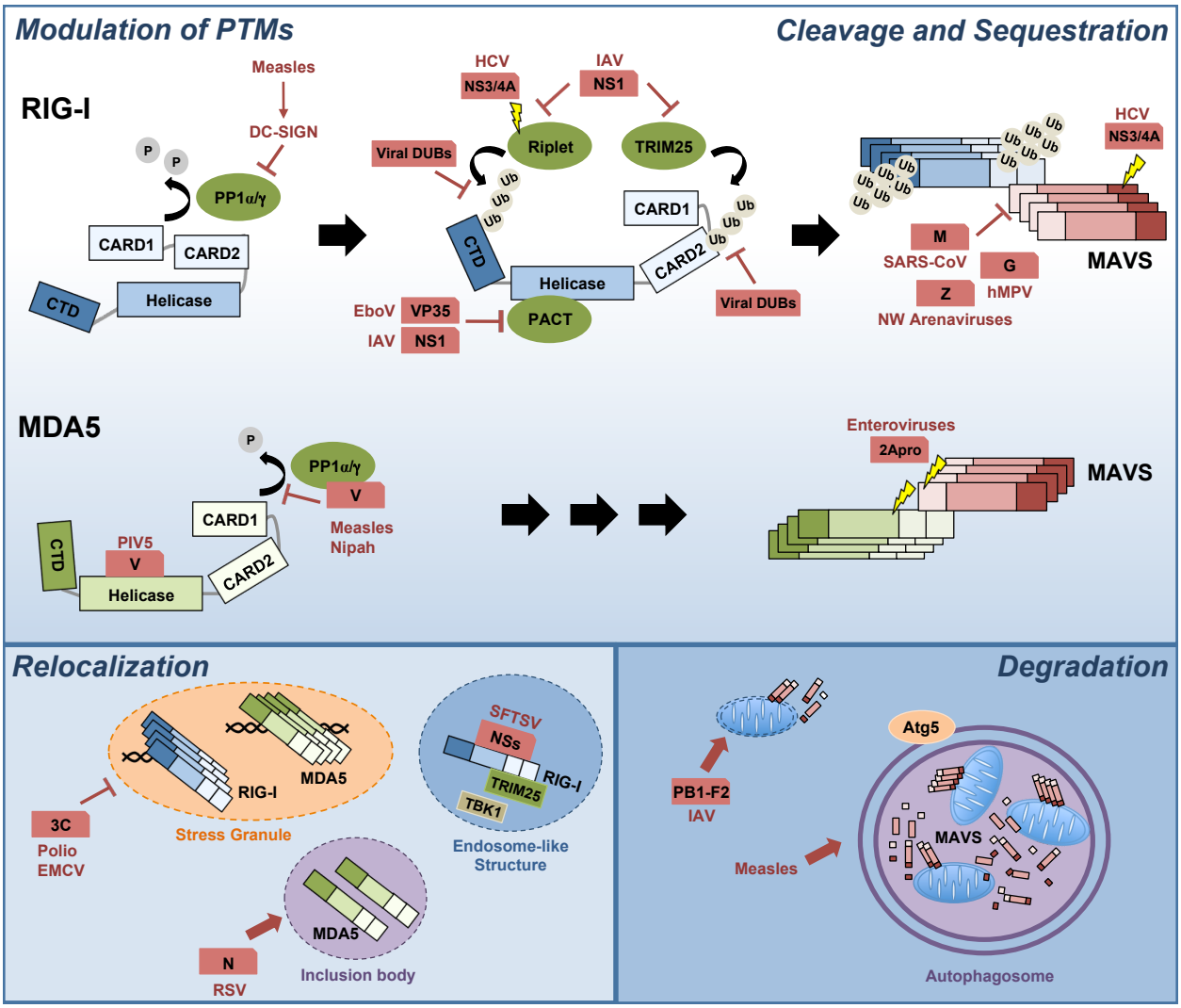


**Figure 1.2. Pathogenic viruses target RLR regulation for immune evasion.** There are five general strategies used by viruses to target RLR-MAVS signaling: *(1)* modulation of PTMs of RLRs, *(2)* cleavage of RLR pathway components, *(3)* sequestration of RLRs, *(4)* modulation of RLR localization, and *(5)* degradation of MAVS and other RLR downstream signaling molecules. The details of the viral antagonistic mechanisms are described in the text. (Adapted from *Chan and Gack, Curr Opin Virol, 2015*.)

With regards to K63-linked ubiquitination of RIG-I, the NS1 protein of IAV binds to the ubiquitin E3 ligase TRIM25 to block ubiquitination of the RIG-I CARDs [74]. Furthermore, the NS1 proteins of some IAV strains were shown to also bind human Riplet to inhibit ubiquitination of the RIG-I CTD [75]. A recent study indicated that the NS3/4A protease complex of HCV cleaves not only MAVS but also Riplet to prevent RIG-I activation [36,61,76]. Viruses also act directly on RIG-I by encoding enzymes that deubiquitinate RIG-I and hence inactivate it. Orf64, a viral DUB of Kaposi's sarcoma-associated herpesvirus (KSHV), removes K63-ubiquitin chains from the RIG-I CARDs [77]. The papain-like protease (PLP) of severe acute respiratory syndrome coronavirus (SARS-CoV) and the leader proteinase ($L^{pro}$) of foot-and-mouth disease virus (FMDV) also deubiquitinate RIG-I and other innate immune signaling molecules [78,79]. Finally, arteriviruses and nairoviruses encode proteins with ovarian tumor (OTU)-type DUB enzymatic activities to remove K63-polyubiquitin from RIG-I [80].

Another viral strategy to escape the RLR response is the induction of specific miRNAs that target critical regulatory proteins in the RLR pathway. For example, the 3C protein of Enterovirus 71 (EV71) blocks the up-regulation of miR-526a in infected cells, which leads to increased expression of CYLD and hence RIG-I inhibition via deubiquitination [55].

Viruses are also equipped with proteins that modulate the subcellular localization of RLRs, or actively degrade components of the RLR pathway. For example, poliovirus and encephalomyocarditis virus (EMCV) use their 3C proteases to prevent the formation of RLR-containing avSGs through cleavage of the Ras-Gap SH3 domain binding protein 1 (G3BP1) [81,82]. Other proteins sequester RLRs from MAVS. The M protein of SARS-CoV, the Z protein of New World (NW) arenaviruses, and the glycoprotein G of human metapneumovirus (hMPV) bind to RIG-I to sequester it from MAVS. Furthermore, the N protein of respiratory

syncytial virus (RSV) binds specifically to MDA5, relocalizing it to large inclusion bodies [83-86]. Furthermore, the NSs protein of severe fever with thrombocytopenia syndrome virus (SFTSV) has been recently shown to interact with RIG-I, TRIM25 and TBK1 to relocalize them into cytoplasmic endosome-like structures for sequestration [87]. Moreover, PB1-F2 of IAV reduces the inner membrane potential of mitochondria, leading to fragmentation of these organelles and inhibition of innate immune signaling [88,89].

Another important evasion strategy employed by several viruses is cleavage of RIG-I, MDA5 and/or MAVS. For example, enteroviruses cleave both MDA5 and MAVS using their protease 2Apro, thereby blunting IFN-β induction [90,91]. Measles virus infection triggers selective autophagy to degrade mitochondria (a process termed "mitophagy"), resulting in decreased MAVS abundance and disruption of RLR signaling [92]. Finally, the NS1 and NS2 proteins of RSV have been recently shown to trigger the degradation of RIG-I, IRF3 and many other molecules in the IFN induction pathway by assembling a large degradative complex on the mitochondria [93].

**Immune evasion strategies used by DV**

DV has evolved to evade or subvert the human immune response extensively. DV escapes immune detection by PRRs by replicating in intracellular membrane structures, which allows it to partially shield double-stranded RNA (dsRNA) from PRRs [94]. In contrast, infection with the related flavivirus JEV results in exposed dsRNA early in infection, giving rise to IFN induction and a self-limiting infection.

DV also actively antagonizes the IFN response by inhibiting both IFN induction and IFN-receptor signaling. DCs infected with DV secrete little type I IFN when compared to other RNA virus infections [95,96]. With regards to IFN induction, the NS2B/3 protease complex has been

shown to be responsible for blocking IFN induction. Recently, two groups showed that NS2B/3 cleaves STING, an adaptor protein downstream of cytosolic DNA sensors [97,98]. It is currently unclear how STING plays a role in IFN induction during RNA virus infection, though some evidence suggests that STING is able to interact with RIG-I and MAVS in the RNA sensing pathway [99]. In contrast, a lot more is known about how DV inhibits type I IFN-receptor (IFNAR) signaling (reviewed in [100]). NS2A, NS4A and NS4B associate with cellular membranes and inhibit STAT1 phosphorylation, while NS5 induces proteasomal degradation of STAT2. More recently, non-coding subgenomic flaviviral RNA (sfRNA) of DV has been shown to antagonize RNA-binding proteins that are required for translation of ISG mRNAs ([101].

Furthermore, DV inhibits several antiviral cellular processes in order to replicate. DV has been shown to block formation of antiviral stress granules (SGs), thereby facilitating viral RNA synthesis [102]. DV also subverts autophagy, which is typically an antiviral process, by manipulating autophagy for increased viral replication while avoiding lysosomal degradation [103-106]. In addition, DV induces the unfolded protein response (UPR) to avoid translational inhibition and to prevent cell death [107,108]. Finally, non-neutralizing antibodies increase infectivity of heterologous DV serotypes, and ADE has also been suggested to downregulate antiviral and inflammatory cytokines to allow increased viral replication [109,110].

## ANTIVIRAL INTERFERON-STIMULATED GENES (ISGs)

Upon detecting PAMPs, PRRs signal to induce type I and III IFN production. These secreted IFNs then engage their cognate receptors and signal via the JAK-STAT pathway to promote the transcription of hundreds of antiviral ISGs (reviewed in [111]). While some ISGs have been extensively characterized in terms of antiviral activity and mode of action, the

molecular mechanisms of many ISGs are still not well understood. Here, I discuss selected ISGs with an emphasis on their impact on flavivirus replication.

In general, **ISGs** target conserved aspects of viral replication (reviewed in [112]), including virus entry, viral nucleic acids, protein translation and virus egress. **IFITM proteins** (interferon-induced transmembrane proteins), consisting of IFITM1-3 in humans, inhibit viral replication by blocking entry of several pathogenic viruses including DV and WNV [113]. IFITMs primarily restrict viruses that enter via the endocytic pathway and fuse in the late endosomes or lysosomes, although there are exceptions to this rule. Several mechanisms have been proposed to explain IFITM's mode of action, and they mostly suggest that IFITM proteins modify the physical properties of cellular membranes to prevent formation of fusion pores, such as cholesterol accumulation in endosomal membranes and deformation of endosomal membrane curvature [114-116].

With regards to ISGs that target viral nucleic acids, **OAS proteins** recognize dsRNA and generate 2',5'-oligoadenylates which activate **RNAseL** to degrade viral RNA (reviewed in [117]). **APOBEC3G** is a cytidine deaminase and restricts retroviruses such as HIV by catalyzing the deamination of cytidine to uridine in reverse transcribed viral DNA [118]. Other ISGs modulate protein translation to thwart viral replication. **PKR** is activated by dsRNA and phosphorylates EIF2A to inhibit both cellular and viral mRNA translation, thereby shutting down viral replication (reviewed in [119]). PKR also triggers inflammation and induces apoptosis to further inhibit viral spread. While PKR is known to be critical for controlling WNV replication [120], a recent study suggests that PKR may downregulate IFN production during DV infection, indicating that DV may subvert PKR activity for its replication [120]. **IFIT** (interferon-induced protein with tetratricopeptide repeats) family proteins, consisting of IFIT1-3

and 5 in humans, prevent viral replication by non-specifically inhibiting translation or directly binding and sequestering viral RNA (reviewed in [121]). IFIT3 has a protective role against DV infection, while other work shows that NS5 2'-O-methylates DV RNA which may facilitate evasion of IFIT-mediated restriction [122,123]. In addition, **tetherin**, which is also an ISG, prevents virus egress by tethering virions to the cell surface and preventing their spread (reviewed in [124]). Tetherin has been shown to target retroviruses such as HIV and filoviruses such as Ebola, as well as DV recently [125].

Hundreds of ISGs are upregulated by IFN to create an antiviral state. These ISGs target multiple steps of the viral life cycle through diverse mechanisms. While some pathogens have evolved to escape the action of certain ISGs, the collective effect of ISGs is likely to be effective against most viruses. Deciphering the antiviral activity and mode of action of poorly characterized ISGs may be useful for the development of novel antivirals, especially against pathogens like DV for which no therapies exist.

## REFERENCES


1. Bhatt S, Gething PW, Brady OJ, Messina JP, Farlow AW, et al. (2013) The global distribution and burden of dengue. Nature 496: 504-507.

2. Gubler DJ (1998) Dengue and dengue hemorrhagic fever. Clin Microbiol Rev 11: 480-496.

3. Halstead SB (2007) Dengue. Lancet 370: 1644-1652.

4. Whitehorn J, Simmons CP (2011) The pathogenesis of dengue. Vaccine 29: 7221-7228.

5. Vaughn DW, Green S, Kalayanarooj S, Innis BL, Nimmannitya S, et al. (2000) Dengue viremia titer, antibody response pattern, and virus serotype correlate with disease severity. J Infect Dis 181: 2-9.

6. St John AL, Abraham SN, Gubler DJ (2013) Barriers to preclinical investigations of anti-dengue immunity and dengue pathogenesis. Nat Rev Microbiol 11: 420-426.

7. Halstead SB (2003) Neutralization and antibody-dependent enhancement of dengue viruses. Adv Virus Res 60: 421-467.

8. Huy NT, Van Giang T, Thuy DH, Kikuchi M, Hien TT, et al. (2013) Factors associated with dengue shock syndrome: a systematic review and meta-analysis. PLoS Negl Trop Dis 7: e2412.

9. Halstead SB, Lan NT, Myint TT, Shwe TN, Nisalak A, et al. (2002) Dengue hemorrhagic fever in infants: research opportunities ignored. Emerg Infect Dis 8: 1474-1479.

10. Schmid MA, Harris E (2014) Monocyte recruitment to the dermis and differentiation to dendritic cells increases the targets for dengue virus replication. PLoS Pathog 10: e1004541.

11. Martina BE, Koraka P, Osterhaus AD (2009) Dengue virus pathogenesis: an integrated view. Clin Microbiol Rev 22: 564-581.

12. Jessie K, Fong MY, Devi S, Lam SK, Wong KT (2004) Localization of dengue virus in naturally infected human tissues, by immunohistochemistry and in situ hybridization. J Infect Dis 189: 1411-1418.

13. Aye KS, Charngkaew K, Win N, Wai KZ, Moe K, et al. (2014) Pathologic highlights of dengue hemorrhagic fever in 13 autopsy cases from Myanmar. Hum Pathol 45: 1221-1233.

14. Balsitis SJ, Coloma J, Castro G, Alava A, Flores D, et al. (2009) Tropism of dengue virus in mice and humans defined by viral nonstructural protein 3-specific immunostaining. Am J Trop Med Hyg 80: 416-424.

15. Pang T, Cardosa MJ, Guzman MG (2007) Of cascades and perfect storms: the immunopathogenesis of dengue haemorrhagic fever-dengue shock syndrome (DHF/DSS). Immunol Cell Biol 85: 43-45.

16. Chakravarti A, Kumaria R (2006) Circulating levels of tumour necrosis factor-alpha & interferon-gamma in patients with dengue & dengue haemorrhagic fever during an outbreak. Indian J Med Res 123: 25-30.

17. Juffrie M, Meer GM, Hack CE, Haasnoot K, Sutaryo, et al. (2001) Inflammatory mediators in dengue virus infection in children: interleukin-6 and its relation to C-reactive protein and secretory phospholipase A2. Am J Trop Med Hyg 65: 70-75.

18. Villar L, Dayan GH, Arredondo-Garcia JL, Rivera DM, Cunha R, et al. (2014) Efficacy of a Tetravalent Dengue Vaccine in Children in Latin America. N Engl J Med.

19. Capeding MR, Tran NH, Hadinegoro SR, Ismail HI, Chotpitayasunondh T, et al. (2014) Clinical efficacy and safety of a novel tetravalent dengue vaccine in healthy children in Asia: a phase 3, randomised, observer-masked, placebo-controlled trial. Lancet 384: 1358-1365.

20. Luz PM, Vanni T, Medlock J, Paltiel AD, Galvani AP (2011) Dengue vector control strategies in an urban setting: an economic modelling assessment. Lancet 377: 1673-1680.

21. Acosta EG, Kumar A, Bartenschlager R (2014) Revisiting dengue virus-host cell interaction: new insights into molecular and cellular virology. Adv Virus Res 88: 1-109.

22. Chatel-Chaix L, Bartenschlager R (2014) Dengue virus- and hepatitis C virus-induced replication and assembly compartments: the enemy inside--caught in the web. J Virol 88: 5907-5911.

23. Ivashkiv LB, Donlin LT (2014) Regulation of type I interferon responses. Nat Rev Immunol 14: 36-49.

24. Kagan JC, Barton GM (2014) Emerging Principles Governing Signal Transduction by Pattern-Recognition Receptors. Cold Spring Harb Perspect Biol 7.

25. Wu J, Chen ZJ (2014) Innate immune sensing and signaling of cytosolic nucleic acids. Annu Rev Immunol 32: 461-488.

26. Rodriguez KR, Bruns AM, Horvath CM (2014) MDA5 and LGP2: accomplices and antagonists of antiviral signal transduction. J Virol 88: 8194-8200.

27. Schlee M (2013) Master sensors of pathogenic RNA - RIG-I like receptors. Immunobiology 218: 1322-1335.

28. Goubau D, Schlee M, Deddouche S, Pruijssers AJ, Zillinger T, et al. (2014) Antiviral

immunity via RIG-I-mediated recognition of RNA bearing 5'-diphosphates. Nature 514: 372-375.

29. Goubau D, Deddouche S, Reis e Sousa C (2013) Cytosolic sensing of viruses. Immunity 38: 855-869.

30. Chiang JJ, Davis ME, Gack MU (2014) Regulation of RIG-I-like receptor signaling by host and viral proteins. Cytokine Growth Factor Rev.

31. Kowalinski E, Lunardi T, McCarthy AA, Louber J, Brunel J, et al. (2011) Structural basis for the activation of innate immune pattern-recognition receptor RIG-I by viral RNA. Cell 147: 423-435.

32. Maharaj NP, Wies E, Stoll A, Gack MU (2012) Conventional protein kinase C-alpha (PKC-alpha) and PKC-beta negatively regulate RIG-I antiviral signal transduction. J Virol 86: 1358-1371.

33. Gack MU, Nistal-Villan E, Inn KS, Garcia-Sastre A, Jung JU (2010) Phosphorylation-mediated negative regulation of RIG-I antiviral activity. J Virol 84: 3220-3229.

34. Sun Z, Ren H, Liu Y, Teeling JL, Gu J (2011) Phosphorylation of RIG-I by casein kinase II inhibits its antiviral response. J Virol 85: 1036-1047.

35. Wies E, Wang MK, Maharaj NP, Chen K, Zhou S, et al. (2013) Dephosphorylation of the RNA sensors RIG-I and MDA5 by the phosphatase PP1 is essential for innate immune signaling. Immunity 38: 437-449.

36. Oshiumi H, Miyashita M, Matsumoto M, Seya T (2013) A distinct role of Riplet-mediated K63-Linked polyubiquitination of the RIG-I repressor domain in human antiviral innate immune responses. PLoS Pathog 9: e1003533.

37. Gack MU, Shin YC, Joo CH, Urano T, Liang C, et al. (2007) TRIM25 RING-finger E3 ubiquitin ligase is essential for RIG-I-mediated antiviral activity. Nature 446: 916-920.

38. Zeng W, Sun L, Jiang X, Chen X, Hou F, et al. (2010) Reconstitution of the RIG-I pathway reveals a signaling role of unanchored polyubiquitin chains in innate immunity. Cell 141: 315-330.

39. Peisley A, Wu B, Xu H, Chen ZJ, Hur S (2014) Structural basis for ubiquitin-mediated antiviral signal activation by RIG-I. Nature 509: 110-114.

40. Zhu J, Zhang Y, Ghosh A, Cuevas RA, Forero A, et al. (2014) Antiviral activity of human OASL protein is mediated by enhancing signaling of the RIG-I RNA sensor. Immunity 40: 936-948.

41. Friedman CS, O'Donnell MA, Legarda-Addison D, Ng A, Cardenas WB, et al. (2008) The

tumour suppressor CYLD is a negative regulator of RIG-I-mediated antiviral response. EMBO Rep 9: 930-936.

42. Cui J, Song Y, Li Y, Zhu Q, Tan P, et al. (2014) USP3 inhibits type I interferon signaling by deubiquitinating RIG-I-like receptors. Cell Res 24: 400-416.

43. Fan Y, Mao R, Yu Y, Liu S, Shi Z, et al. (2014) USP21 negatively regulates antiviral response by acting as a RIG-I deubiquitinase. J Exp Med 211: 313-328.

44. Fu J, Xiong Y, Xu Y, Cheng G, Tang H (2011) MDA5 is SUMOylated by PIAS2beta in the upregulation of type I interferon signaling. Mol Immunol 48: 415-422.

45. Arimoto K, Takahashi H, Hishiki T, Konishi H, Fujita T, et al. (2007) Negative regulation of the RIG-I signaling by the ubiquitin ligase RNF125. Proc Natl Acad Sci U S A 104: 7500-7505.

46. Wang L, Zhao W, Zhang M, Wang P, Zhao K, et al. (2013) USP4 positively regulates RIG-I-mediated antiviral response through deubiquitination and stabilization of RIG-I. J Virol 87: 4507-4515.

47. Inn KS, Gack MU, Tokunaga F, Shi M, Wong LY, et al. (2011) Linear ubiquitin assembly complex negatively regulates RIG-I- and TRIM25-mediated type I interferon induction. Mol Cell 41: 354-365.

48. Pauli EK, Chan YK, Davis ME, Gableske S, Wang MK, et al. (2014) The Ubiquitin-Specific Protease USP15 Promotes RIG-I-Mediated Antiviral Signaling by Deubiquitylating TRIM25. Sci Signal 7: ra3.

49. You F, Sun H, Zhou X, Sun W, Liang S, et al. (2009) PCBP2 mediates degradation of the adaptor MAVS via the HECT ubiquitin ligase AIP4. Nat Immunol 10: 1300-1308.

50. Wang Y, Tong X, Ye X (2012) Ndfip1 negatively regulates RIG-I-dependent immune signaling by enhancing E3 ligase Smurf1-mediated MAVS degradation. J Immunol 189: 5304-5313.

51. Zhong B, Zhang Y, Tan B, Liu TT, Wang YY, et al. (2010) The E3 ubiquitin ligase RNF5 targets virus-induced signaling adaptor for ubiquitination and degradation. J Immunol 184: 6249-6255.

52. Gack MU, Kirchhofer A, Shin YC, Inn KS, Liang C, et al. (2008) Roles of RIG-I N-terminal tandem CARD and splice variant in TRIM25-mediated antiviral signal transduction. Proc Natl Acad Sci U S A 105: 16743-16748.

53. Lad SP, Yang G, Scott DA, Chao TH, Correia Jda S, et al. (2008) Identification of MAVS splicing variants that interfere with RIGI/MAVS pathway signaling. Mol Immunol 45: 2277-2287.

54. Brubaker SW, Gauthier AE, Mills EW, Ingolia NT, Kagan JC (2014) A bicistronic MAVS transcript highlights a class of truncated variants in antiviral immunity. Cell 156: 800-811.

55. Xu C, He X, Zheng Z, Zhang Z, Wei C, et al. (2014) Downregulation of microRNA miR-526a by enterovirus inhibits RIG-I-dependent innate immune response. J Virol 88: 11356-11368.

56. Hou J, Wang P, Lin L, Liu X, Ma F, et al. (2009) MicroRNA-146a feedback inhibits RIG-I-dependent Type I IFN production in macrophages by targeting TRAF6, IRAK1, and IRAK2. J Immunol 183: 2150-2158.

57. Li Y, Fan X, He X, Sun H, Zou Z, et al. (2012) MicroRNA-466l inhibits antiviral innate immune response by targeting interferon-alpha. Cell Mol Immunol 9: 497-502.

58. Yoo JS, Takahasi K, Ng CS, Ouda R, Onomoto K, et al. (2014) DHX36 enhances RIG-I signaling by facilitating PKR-mediated antiviral stress granule formation. PLoS Pathog 10: e1004012.

59. Seth RB, Sun L, Ea CK, Chen ZJ (2005) Identification and characterization of MAVS, a mitochondrial antiviral signaling protein that activates NF-kappaB and IRF 3. Cell 122: 669-682.

60. Dixit E, Boulant S, Zhang Y, Lee AS, Odendall C, et al. (2010) Peroxisomes are signaling platforms for antiviral innate immunity. Cell 141: 668-681.

61. Horner SM, Liu HM, Park HS, Briley J, Gale M, Jr. (2011) Mitochondrial-associated endoplasmic reticulum membranes (MAM) form innate immune synapses and are targeted by hepatitis C virus. Proc Natl Acad Sci U S A 108: 14590-14595.

62. Odendall C, Dixit E, Stavru F, Bierne H, Franz KM, et al. (2014) Diverse intracellular pathogens activate type III interferon expression from peroxisomes. Nat Immunol 15: 717-726.

63. Liu HM, Loo YM, Horner SM, Zornetzer GA, Katze MG, et al. (2012) The mitochondrial targeting chaperone 14-3-3epsilon regulates a RIG-I translocon that mediates membrane association and innate antiviral immunity. Cell Host Microbe 11: 528-537.

64. Deretic V, Saitoh T, Akira S (2013) Autophagy in infection, inflammation and immunity. Nat Rev Immunol 13: 722-737.

65. Tal MC, Sasai M, Lee HK, Yordy B, Shadel GS, et al. (2009) Absence of autophagy results in reactive oxygen species-dependent amplification of RLR signaling. Proc Natl Acad Sci U S A 106: 2770-2775.

66. Jounai N, Takeshita F, Kobiyama K, Sawano A, Miyawaki A, et al. (2007) The Atg5 Atg12

conjugate associates with innate antiviral immune responses. Proc Natl Acad Sci U S A 104: 14050-14055.

67. Li MT, Di W, Xu H, Yang YK, Chen HW, et al. (2013) Negative regulation of RIG-I-mediated innate antiviral signaling by SEC14L1. J Virol 87: 10037-10046.

68. Davis ME, Wang MK, Rennick LJ, Full F, Gableske S, et al. (2014) Antagonism of the phosphatase PP1 by the measles virus V protein is required for innate immune escape of MDA5. Cell Host Microbe 16: 19-30.

69. Mesman AW, Zijlstra-Willems EM, Kaptein TM, de Swart RL, Davis ME, et al. (2014) Measles virus suppresses RIG-I-like receptor activation in dendritic cells via DC-SIGN-mediated inhibition of PP1 phosphatases. Cell Host Microbe 16: 31-42.

70. Rodriguez KR, Horvath CM (2013) Amino acid requirements for MDA5 and LGP2 recognition by paramyxovirus V proteins: a single arginine distinguishes MDA5 from RIG-I. J Virol 87: 2974-2978.

71. Motz C, Schuhmann KM, Kirchhofer A, Moldt M, Witte G, et al. (2013) Paramyxovirus V Proteins Disrupt the Fold of the RNA Sensor MDA5 to Inhibit Antiviral Signaling. Science.

72. Luthra P, Ramanan P, Mire CE, Weisend C, Tsuda Y, et al. (2013) Mutual antagonism between the Ebola virus VP35 protein and the RIG-I activator PACT determines infection outcome. Cell Host Microbe 14: 74-84.

73. Tawaratsumida K, Phan V, Hrincius ER, High AA, Webby R, et al. (2014) Quantitative proteomic analysis of the influenza A virus nonstructural proteins NS1 and NS2 during natural cell infection identifies PACT as an NS1 target protein and antiviral host factor. J Virol 88: 9038-9048.

74. Gack MU, Albrecht RA, Urano T, Inn KS, Huang IC, et al. (2009) Influenza A virus NS1 targets the ubiquitin ligase TRIM25 to evade recognition by the host viral RNA sensor RIG-I. Cell Host Microbe 5: 439-449.

75. Rajsbaum R, Albrecht RA, Wang MK, Maharaj NP, Versteeg GA, et al. (2012) Species-specific inhibition of RIG-I ubiquitination and IFN induction by the influenza A virus NS1 protein. PLoS Pathog 8: e1003059.

76. Li XD, Sun L, Seth RB, Pineda G, Chen ZJ (2005) Hepatitis C virus protease NS3/4A cleaves mitochondrial antiviral signaling protein off the mitochondria to evade innate immunity. Proc Natl Acad Sci U S A 102: 17717-17722.

77. Inn KS, Lee SH, Rathbun JY, Wong LY, Toth Z, et al. (2011) Inhibition of RIG-I-mediated signaling by Kaposi's sarcoma-associated herpesvirus-encoded deubiquitinase ORF64. J Virol 85: 10899-10904.

78. Clementz MA, Chen Z, Banach BS, Wang Y, Sun L, et al. (2010) Deubiquitinating and interferon antagonism activities of coronavirus papain-like proteases. J Virol 84: 4619-4629.

79. Wang D, Fang L, Li P, Sun L, Fan J, et al. (2011) The leader proteinase of foot-and-mouth disease virus negatively regulates the type I interferon pathway by acting as a viral deubiquitinase. J Virol 85: 3758-3766.

80. van Kasteren PB, Bailey-Elkin BA, James TW, Ninaber DK, Beugeling C, et al. (2013) Deubiquitinase function of arterivirus papain-like protease 2 suppresses the innate immune response in infected host cells. Proc Natl Acad Sci U S A 110: E838-847.

81. Ng CS, Jogi M, Yoo JS, Onomoto K, Koike S, et al. (2013) Encephalomyocarditis virus disrupts stress granules, the critical platform for triggering antiviral innate immune responses. J Virol 87: 9511-9522.

82. White JP, Cardenas AM, Marissen WE, Lloyd RE (2007) Inhibition of cytoplasmic mRNA stress granule formation by a viral proteinase. Cell Host Microbe 2: 295-305.

83. Siu KL, Kok KH, Ng MH, Poon VK, Yuen KY, et al. (2009) Severe acute respiratory syndrome coronavirus M protein inhibits type I interferon production by impeding the formation of TRAF3.TANK.TBK1/IKKepsilon complex. J Biol Chem 284: 16202-16209.

84. Fan L, Briese T, Lipkin WI (2010) Z proteins of New World arenaviruses bind RIG-I and interfere with type I interferon induction. J Virol 84: 1785-1791.

85. Bao X, Kolli D, Ren J, Liu T, Garofalo RP, et al. (2013) Human metapneumovirus glycoprotein G disrupts mitochondrial signaling in airway epithelial cells. PLoS One 8: e62568.

86. Bao X, Liu T, Shan Y, Li K, Garofalo RP, et al. (2008) Human metapneumovirus glycoprotein G inhibits innate immune responses. PLoS Pathog 4: e1000077.

87. Santiago FW, Covaleda LM, Sanchez-Aparicio MT, Silvas JA, Diaz-Vizarreta AC, et al. (2014) Hijacking of RIG-I signaling proteins into virus-induced cytoplasmic structures correlates with the inhibition of type I interferon responses. J Virol 88: 4572-4585.

88. Varga ZT, Grant A, Manicassamy B, Palese P (2012) Influenza virus protein PB1-F2 inhibits the induction of type I interferon by binding to MAVS and decreasing mitochondrial membrane potential. J Virol 86: 8359-8366.

89. Yoshizumi T, Ichinohe T, Sasaki O, Otera H, Kawabata S, et al. (2014) Influenza A virus protein PB1-F2 translocates into mitochondria via Tom40 channels and impairs innate immunity. Nat Commun 5: 4713.

90. Wang B, Xi X, Lei X, Zhang X, Cui S, et al. (2013) Enterovirus 71 protease 2Apro targets MAVS to inhibit anti-viral type I interferon responses. PLoS Pathog 9: e1003231.

91. Feng Q, Langereis MA, Lork M, Nguyen M, Hato SV, et al. (2014) Enterovirus 2Apro targets MDA5 and MAVS in infected cells. J Virol 88: 3369-3378.

92. Xia M, Gonzalez P, Li C, Meng G, Jiang A, et al. (2014) Mitophagy enhances oncolytic measles virus replication by mitigating DDX58/RIG-I-like receptor signaling. J Virol 88: 5152-5164.

93. Goswami R, Majumdar T, Dhar J, Chattopadhyay S, Bandyopadhyay SK, et al. (2013) Viral degradasome hijacks mitochondria to suppress innate immunity. Cell Res 23: 1025-1042.

94. Uchida L, Espada-Murao LA, Takamatsu Y, Okamoto K, Hayasaka D, et al. (2014) The dengue virus conceals double-stranded RNA in the intracellular membrane to escape from an interferon response. Sci Rep 4: 7395.

95. Rodriguez-Madoz JR, Belicha-Villanueva A, Bernal-Rubio D, Ashour J, Ayllon J, et al. (2010) Inhibition of the type I interferon response in human dendritic cells by dengue virus infection requires a catalytically active NS2B3 complex. J Virol 84: 9760-9774.

96. Rodriguez-Madoz JR, Bernal-Rubio D, Kaminski D, Boyd K, Fernandez-Sesma A (2010) Dengue virus inhibits the production of type I interferon in primary human dendritic cells. J Virol 84: 4845-4850.

97. Aguirre S, Maestre AM, Pagni S, Patel JR, Savage T, et al. (2012) DENV inhibits type I IFN production in infected cells by cleaving human STING. PLoS Pathog 8: e1002934.

98. Yu CY, Chang TH, Liang JJ, Chiang RL, Lee YL, et al. (2012) Dengue virus targets the adaptor protein MITA to subvert host innate immunity. PLoS Pathog 8: e1002780.

99. Maringer K, Fernandez-Sesma A (2014) Message in a bottle: lessons learned from antagonism of STING signalling during RNA virus infection. Cytokine Growth Factor Rev 25: 669-679.

100. Morrison J, Aguirre S, Fernandez-Sesma A (2012) Innate immunity evasion by Dengue virus. Viruses 4: 397-413.

101. Bidet K, Dadlani D, Garcia-Blanco MA (2014) G3BP1, G3BP2 and CAPRIN1 are required for translation of interferon stimulated mRNAs and are targeted by a dengue virus non-coding RNA. PLoS Pathog 10: e1004242.

102. Emara MM, Brinton MA (2007) Interaction of TIA-1/TIAR with West Nile and dengue virus products in infected cells interferes with stress granule formation and processing body assembly. Proc Natl Acad Sci U S A 104: 9041-9046.

103. Lee YR, Lei HY, Liu MT, Wang JR, Chen SH, et al. (2008) Autophagic machinery activated by dengue virus enhances virus replication. Virology 374: 240-248.

104. Khakpoor A, Panyasrivanit M, Wikan N, Smith DR (2009) A role for autophagolysosomes in dengue virus 3 production in HepG2 cells. J Gen Virol 90: 1093-1103.

105. Panyasrivanit M, Khakpoor A, Wikan N, Smith DR (2009) Co-localization of constituents of the dengue virus translation and replication machinery with amphisomes. J Gen Virol 90: 448-456.

106. Mateo R, Nagamine CM, Spagnolo J, Mendez E, Rahe M, et al. (2013) Inhibition of cellular autophagy deranges dengue virion maturation. J Virol 87: 1312-1321.

107. Yu CY, Hsu YW, Liao CL, Lin YL (2006) Flavivirus infection activates the XBP1 pathway of the unfolded protein response to cope with endoplasmic reticulum stress. J Virol 80: 11868-11880.

108. Umareddy I, Pluquet O, Wang QY, Vasudevan SG, Chevet E, et al. (2007) Dengue virus serotype infection specifies the activation of the unfolded protein response. Virol J 4: 91.

109. Chareonsirisuthigul T, Kalayanarooj S, Ubol S (2007) Dengue virus (DENV) antibody-dependent enhancement of infection upregulates the production of anti-inflammatory cytokines, but suppresses anti-DENV free radical and pro-inflammatory cytokine production, in THP-1 cells. J Gen Virol 88: 365-375.

110. Modhiran N, Kalayanarooj S, Ubol S (2010) Subversion of innate defenses by the interplay between DENV and pre-existing enhancing antibodies: TLRs signaling collapse. PLoS Negl Trop Dis 4: e924.

111. Hoffmann HH, Schneider WM, Rice CM (2015) Interferons and viruses: an evolutionary arms race of molecular interactions. Trends Immunol 36: 124-138.

112. Schoggins JW (2014) Interferon-stimulated genes: roles in viral pathogenesis. Curr Opin Virol 6: 40-46.

113. Brass AL, Huang IC, Benita Y, John SP, Krishnan MN, et al. (2009) The IFITM proteins mediate cellular resistance to influenza A H1N1 virus, West Nile virus, and dengue virus. Cell 139: 1243-1254.

114. John SP, Chin CR, Perreira JM, Feeley EM, Aker AM, et al. (2013) The CD225 domain of IFITM3 is required for both IFITM protein association and inhibition of influenza A virus and dengue virus replication. J Virol 87: 7837-7852.

115. Amini-Bavil-Olyaee S, Choi YJ, Lee JH, Shi M, Huang IC, et al. (2013) The antiviral effector IFITM3 disrupts intracellular cholesterol homeostasis to block viral entry. Cell Host Microbe 13: 452-464.

116. Li K, Markosyan RM, Zheng YM, Golfetto O, Bungart B, et al. (2013) IFITM proteins restrict viral membrane hemifusion. PLoS Pathog 9: e1003124.

117. Kristiansen H, Gad HH, Eskildsen-Larsen S, Despres P, Hartmann R (2011) The oligoadenylate synthetase family: an ancient protein family with multiple antiviral activities. J Interferon Cytokine Res 31: 41-47.

118. Sheehy AM, Gaddis NC, Choi JD, Malim MH (2002) Isolation of a human gene that inhibits HIV-1 infection and is suppressed by the viral Vif protein. Nature 418: 646-650.

119. Pindel A, Sadler A (2011) The role of protein kinase R in the interferon response. J Interferon Cytokine Res 31: 59-70.

120. Samuel MA, Whitby K, Keller BC, Marri A, Barchet W, et al. (2006) PKR and RNase L contribute to protection against lethal West Nile Virus infection by controlling early viral spread in the periphery and replication in neurons. J Virol 80: 7009-7019.

121. Zhou X, Michal JJ, Zhang L, Ding B, Lunney JK, et al. (2013) Interferon induced IFIT family genes in host antiviral defense. Int J Biol Sci 9: 200-208.

122. Hsu YL, Shi SF, Wu WL, Ho LJ, Lai JH (2013) Protective roles of interferon-induced protein with tetratricopeptide repeats 3 (IFIT3) in dengue virus infection of human lung epithelial cells. PLoS One 8: e79518.

123. Dong H, Chang DC, Hua MH, Lim SP, Chionh YH, et al. (2012) 2'-O methylation of internal adenosine by flavivirus NS5 methyltransferase. PLoS Pathog 8: e1002642.

124. Neil SJ (2013) The antiviral activities of tetherin. Curr Top Microbiol Immunol 371: 67-104.

125. Pan XB, Han JC, Cong X, Wei L (2012) BST2/tetherin inhibits dengue virus release from human hepatoma cells. PLoS One 7: e51033.

# Chapter 2

## A Phosphomimetic-based Mechanism for Antagonism of Antiviral Innate Immunity

Ying Kai Chan and Michaela U. Gack

Department of Microbiology and Immunobiology, Harvard Medical School, Boston, MA 02115, USA

Originally submitted as:

Chan YK and Gack MU. (submitted, Mar 2015) A Phosphomimetic-based Mechanism for Antagonism of Antiviral Innate Immunity.

**ABSTRACT**

14-3-3 proteins regulate a myriad of biological processes by binding to phospho-serine/threonine (pS/pT) motifs of numerous cellular proteins. Among them, 14-3-3ε is crucial for innate immunity to RNA virus infection by mediating the cytosol-to-mitochondrial-membrane translocation of the pathogen sensor RIG-I. Here we show that the NS3 protein of dengue virus (DV), a significant arthropod-borne viral pathogen, binds to 14-3-3ε and prevents RIG-I translocation to the mitochondrion-localized adaptor protein MAVS, thereby blocking antiviral signaling. Intriguingly, a highly conserved phosphomimetic RxEP motif in NS3 is essential for 14-3-3ε binding. We engineered a recombinant DV encoding a mutant NS3 deficient in 14-3-3ε binding and found that the mutant virus is impaired in RIG-I antagonism and elicits markedly higher levels of interferon (IFN), IFN-stimulated genes, and proinflammatory cytokines. Our work reveals a novel phosphomimetic-based mechanism for viral antagonism of 14-3-3-mediated immunity, which may guide the rational design of vaccines and antivirals.

**INTRODUCTION**

Dengue virus (DV) is responsible for ~390 million infections annually, and 2.5 billion people live in areas at risk for dengue transmission, making DV a highly significant arthropod-borne viral pathogen. DV infection can lead to the debilitating febrile disease known as dengue fever, or the more severe and potentially lethal dengue hemorrhagic fever/dengue shock syndrome (DHF/DSS). Four serotypes of DV exist and infection by one serotype only confers long-lasting immunity to that particular serotype. Currently, there are no FDA-approved therapies against DV infection. A promising tetravalent vaccine candidate recently completed

two phase III clinical trials but showed weak to moderate protection against the widely prevalent DV serotype 2 (DV2) [1,2]. Hence, there is a pressing need to better understand dengue pathogenesis in order to aid the design of broadly effective vaccines and antivirals.

The innate immune system is the first line of defense against invading pathogens and is essential for early restriction of viral replication and for directing adaptive immune responses. Germline-encoded pattern recognition receptors (PRRs) detect viral nucleic acid or conserved structural components of the virion, and subsequently trigger an antiviral response [3,4]. Among the PRRs, RIG-I (retinoic acid-inducible gene-I) has emerged as a key sensor of many RNA viruses, including DV, by recognizing cytosolic viral RNA species harboring a 5' tri- or di-phosphate moiety and/or poly(U/UC) motifs [5,6]. Upon viral RNA binding to the helicase and C-terminal domain (also called repressor domain), RIG-I undergoes a conformational change followed by K63-linked ubiquitination at its N-terminal caspase activation and recruitment domains (CARDs) mediated by the E3 ubiquitin ligase TRIM25 [7-9]. Ubiquitination of RIG-I facilitates its tetramerization, and the activated RIG-I tetramer subsequently translocates from the cytosol to MAVS (also called Cardif, IPS-1, or VISA), which is found at the outer mitochondrial membrane, mitochondrial-associated membranes (MAMs), and peroxisomes [10-12]. MAVS then assembles a multi-protein signaling complex that leads to the activation of the transcription factors IRF3/7 and NF-κB to induce the gene expression of type I IFNs (mainly IFNα/β), proinflammatory cytokines, and antiviral interferon-stimulated genes (ISGs) [13,14]. Recently, the mitochondrial-targeting chaperone protein 14-3-3ε has been identified as a crucial mediator of the redistribution of RIG-I from the cytosol to mitochondrion/MAM-associated MAVS by forming a 'translocon' complex with RIG-I and TRIM25, ultimately triggering an antiviral immune response [15].

DV has evolved to evade or inhibit both innate and adaptive immune responses, allowing it to replicate unchecked and disseminate [16]. DV antagonizes IFN-mediated innate immunity by suppressing both type I IFN induction and IFNα/β receptor (IFNAR) signal transduction through a variety of strategies [17]. Specifically, DV NS5 protein blocks IFNAR signaling by inducing the proteasomal degradation of STAT2 [18]. With regards to suppression of IFN induction, the NS2B-NS3 protease complex (NS2B/3), which is essential for DV polyprotein processing and hence DV replication, has been demonstrated to be the main viral antagonist [19]. NS2B/3 has been shown to cleave stimulator of interferon genes (STING) [20,21], an adaptor protein downstream of cytosolic DNA sensors. However, how DV escapes innate immune detection by RIG-I is unknown.

Here, we uncover that the NS3 protein of DV antagonizes the RIG-I-mediated IFN response through a proteolysis-independent mechanism. NS3 binds to the trafficking molecule 14-3-3ε, blocking the translocation of RIG-I to mitochondria/MAMs and thereby inhibiting antiviral signal transduction. Intriguingly, NS3 binds to 14-3-3ε using a highly conserved four-amino-acid sequence that mimics a canonical phospho-serine/threonine (pS/pT) motif found in cellular interaction partners of 14-3-3 proteins. We further show that a recombinant DV encoding a mutant NS3 protein deficient in 14-3-3ε binding loses the ability to antagonize RIG-I and elicits an augmented innate immune response.

## RESULTS

### The NS3 protein of DV interacts with 14-3-3ε

We hypothesized that NS3 and NS5, two major IFN-antagonistic proteins of DV, inhibit

the innate host defense via previously unidentified mechanisms. To address this, we sought to identify novel cellular interaction partners of NS3 and NS5 by utilizing affinity purification and mass spectrometry (MS) analysis of defined FLAG-tagged domains of both viral proteins: the NS3 protease (amino acids (aa) 1-179) and helicase (aa 169-619) domains (FLAG-NS3-Pro and FLAG-NS3-Hel), as well as the NS5 methyltransferase (aa 1-319) and polymerase (aa 297-901) domains (FLAG-NS5-MTase and FLAG-NS5-Pol). MS analysis showed that 14-3-3ε, a ~30kDa mitochondrial-targeting chaperone protein, was specifically present in complex with FLAG-NS3-Pro, but not with FLAG-NS3-Hel, FLAG-NS5-MTase or FLAG-NS5-Pol (Figure 2.1A and data not shown).

Using co-immunoprecipitation (Co-IP) assay, we first confirmed that c-myc-tagged 14-3-3ε specifically bound to NS3-Pro, but not to NS3-Hel (Figure 2.1B). Furthermore, in agreement with our MS results, ectopically expressed FLAG-14-3-3ε interacted specifically with NS3 (fused to Glutathione *S*-transferase; GST-NS3), but not GST-NS5 or GST alone (Figure 2.1C). The interaction between NS3 and 14-3-3ε was specific as 14-3-3σ, another member of the 14-3-3 protein family which shares ~75% homology with 14-3-3ε, did not bind GST-NS3 (Figure 2.1D). Furthermore, exogenously expressed NS3 of DV strongly interacted with endogenous 14-3-3ε (Figure 2.1E); in contrast, the NS3 proteins of Yellow Fever virus (YFV) and Hepatitis C virus (HCV), two related viruses that also belong to the family *Flaviviridae*, did not bind 14-3-3ε (Figure 1E). We next addressed whether NS3 binds to 14-3-3ε during DV infection by determining the interaction of endogenous 14-3-3ε and NS3 in DV-infected human hepatoma cells (Huh7) by Co-IP. NS3 efficiently formed a complex with endogenous 14-3-3ε during DV infection (Figure 2.1F). Furthermore, laser scanning confocal microscopy of DV-infected Huh7 cells showed that 14-3-3ε was expressed throughout the cytoplasm, while DV NS3, as previously

reported, formed perinuclear cytoplasmic speckles, which are indicative of DV replication complexes at ER-derived membranes [22]. NS3 co-localized extensively with 14-3-3ε in these perinuclear bodies, which also co-stained with NS4A, a key component of the DV replication complex [23] (Figures 2.1G and 2.1H). Finally, we assessed whether NS3 directly binds to 14-3-3ε by performing an *in vitro* binding assay (Figure 2.1I). This showed that GST-NS3 immobilized on glutathione agarose beads, but not GST alone, efficiently interacted with bacterially-purified recombinant (r) 14-3-3ε, demonstrating a direct interaction between NS3 and 14-3-3ε. Taken together, our results indicate that DV NS3 and 14-3-3ε bind directly to each other and form a complex during DV infection.

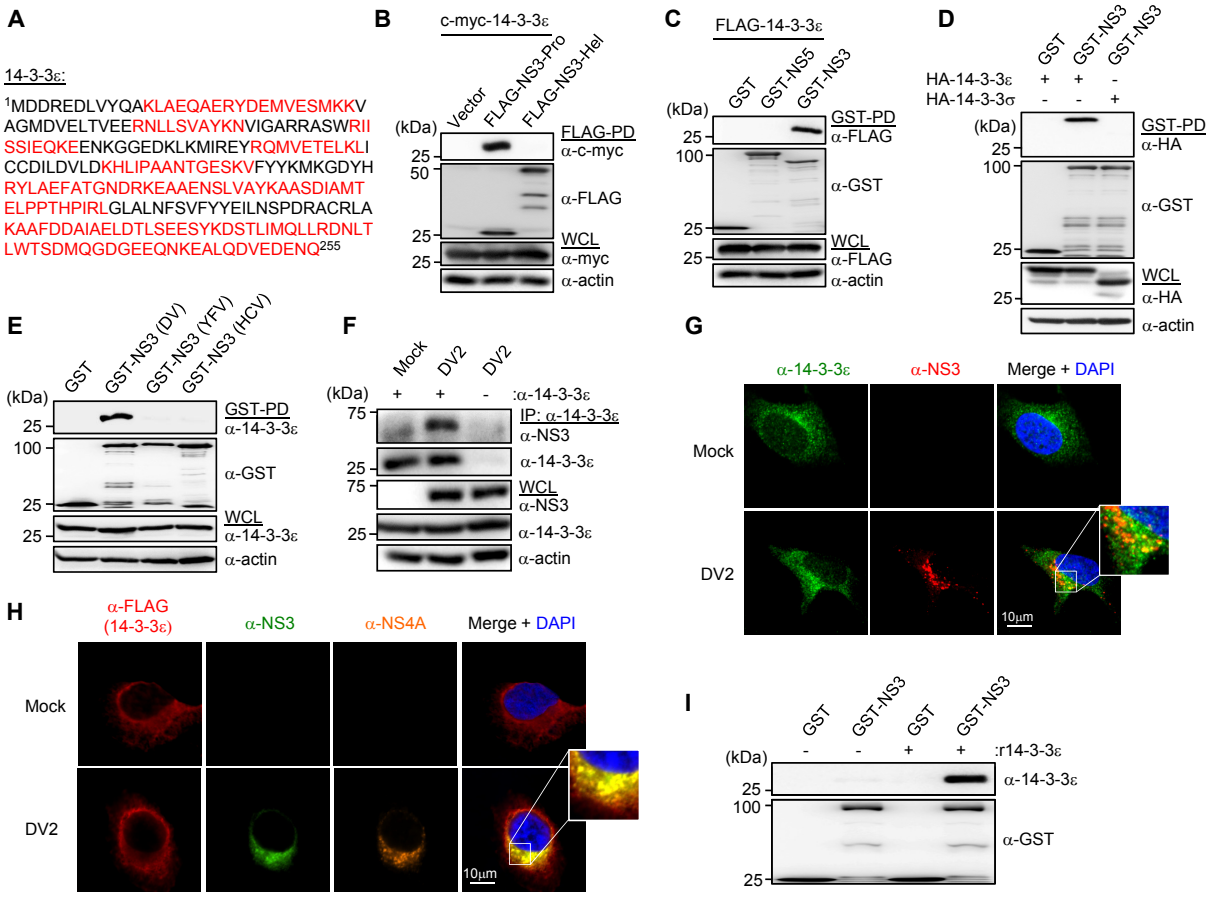


**Figure 2.1. The NS3 protein of DV interacts with 14-3-3ε. (A)** Amino acid sequence of 14-3-3ε and specific peptides (red) identified by MS upon affinity purification of FLAG-NS3-Pro (DV2, strain NGC) from HEK293T cells. Peptide coverage was ~64.3%. Numbers indicate amino acids. **(B)** HEK293T cells were transfected with c-myc-tagged 14-3-3ε and FLAG-tagged NS3-Pro or NS3-Hel. 48 h later, WCLs were subjected to FLAG-pulldown (FLAG-PD), followed by IB with anti-c-myc and anti-FLAG. **(C)** Binding of FLAG-14-3-3ε and GST, GST-NS5, or GST-NS3, assessed in 293T cells by GST-PD and IB with anti-FLAG and anti-GST antibodies. **(D)** HEK293T cells were transfected with HA-tagged 14-3-3ε or 14-3-3σ together with GST or GST-NS3. WCLs were subjected to GST-PD, followed by IB with anti-HA and anti-GST. **(E)** Binding of endogenous 14-3-3ε and GST, or GST-NS3 of DV2 (NGC), YFV (strain 17D), or HCV (strain Con1) in transfected 293T cells, assessed by GST-PD and IB with anti-14-3-3ε antibody. **(F)** Huh7 cells were mock-infected or infected with DV2 NGC (MOI 1) for 28 h. WCLs were subjected to immunoprecipitation (IP) with anti-14-3-3ε antibody, followed by IB with anti-NS3 and anti-14-3-3ε. **(G)** Huh7 cells were mock-infected, or infected with DV2 (NGC) at MOI 0.2 for 24 h. Cells were stained for endogenous 14-3-3ε (green) and NS3 (red) and imaged by confocal microscopy. Nuclei were stained with DAPI (blue). **(H)** Huh7 cells were transfected with FLAG-14-3-3ε and subsequently mock-infected, or infected with DV2 (NGC) at MOI 1 for 24 h. Cells were stained for FLAG (14-3-3ε; red), NS3 (green) and NS4A (orange) and imaged by confocal microscopy. Nuclei were stained with DAPI (blue). **(I)** *In vitro* binding of recombinant 14-3-3ε and purified GST or GST-NS3 determined by IB with anti-14-3-3ε antibody.

**14-3-3ε is critical for controlling DV replication**

Previously, it has been shown that 14-3-3ε assembles a translocon complex which mediates the redistribution of RNA-bound RIG-I in complex with TRIM25 from the cytosol to mitochondria/MAMs for MAVS interaction and antiviral signaling. Viral infection studies demonstrated that 14-3-3ε is required for an effective IFN-mediated antiviral response against Sendai virus (SeV), vesicular stomatitis virus (VSV), and HCV, all of which are sensed by RIG-I [15]. To assess whether 14-3-3ε is also critical for controlling DV infection, we first determined the effect of ectopically expressed 14-3-3ε on DV replication in Huh7 cells. 14-3-3ε expression potently suppressed DV2 replication (Figure 2.2A). 14-3-3ε overexpression also significantly inhibited the replication of four other DV strains representing all four serotypes (DV1-4), but had no effect on herpes simplex virus-1 (HSV-1), an unrelated DNA virus (Figure 2.2B). To determine the relevance of 14-3-3ε in restricting DV replication, we silenced endogenous 14-3-3ε in Huh7 cells using short interfering RNAs (siRNAs). Gene targeting of 14-3-3ε had significant cytotoxic effects in Huh7 cells as well as in HEK293T cells (data not shown), impeding assessment of DV replication in these cell types. In contrast, siRNA-mediated depletion of 14-3-3ε was better tolerated in K562 myeloid cells, which are also commonly used to study DV infection. Knockdown of 14-3-3ε in K562 cells significantly enhanced DV replication as compared to non-targeting control siRNA (si.C) (Figure 2.2C), supporting a role for 14-3-3ε in controlling DV replication.

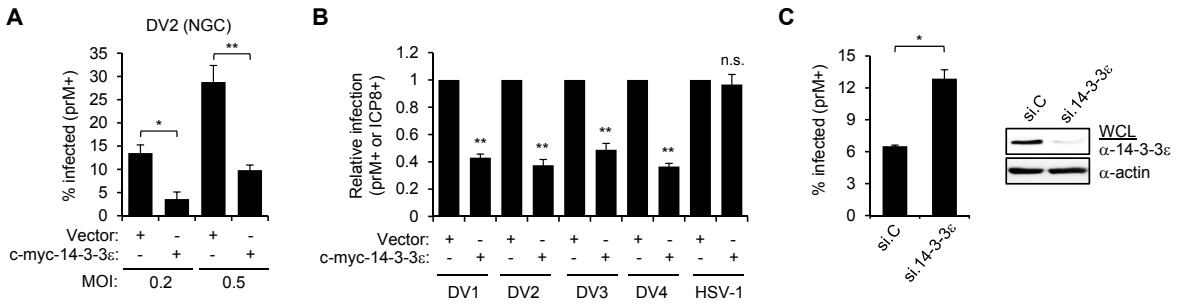


**Figure 2.2. 14-3-3ε is critical for controlling DV replication. (A)** Huh7 cells were transfected with empty vector or c-myc-tagged 14-3-3ε and subsequently infected with DV2 (NGC) at the indicated MOIs, as determined by titration on Vero cells. 72 h later, cells were stained for intracellular DV prM and analyzed by flow cytometry. The results are expressed as means ± SD (n = 3). *p<0.05; **p<0.005. **(B)** Huh7 cells were transfected with vector or c-myc-tagged 14-3-3ε, and subsequently infected with the indicated DV serotypes (MOI 0.05), or HSV-1 (MOI 0.2). Infected cells were determined by intracellular prM (DV) or ICP8 (HSV-1) staining at 72 and 24 h.p.i, respectively. The infectivity for each virus was normalized to vector-transfected cells. The results are expressed as means ± SD (n = 3). **p<0.005. n.s.; not significant. **(C)** K562 cells were transfected with 14-3-3ε-specific siRNA or non-targeting siRNA (si.C). 48 h later, cells were infected with DV2 (NGC) at MOI 1. 48 h later, DV prM-positive cells were determined by flow cytometry. The results are expressed as means ± SD (n = 3). *p<0.05. Knockdown of 14-3-3ε was confirmed by IB.

**NS2B/3 inhibits RIG-I activation independent of proteolytic activity**

Given the role of 14-3-3ε in RIG-I translocation and our results indicating that 14-3-3ε is critical for restricting DV infection, we postulated that the interaction of NS3 with 14-3-3ε might interfere with 14-3-3ε-mediated RIG-I antiviral signal transduction. NS3 in complex with NS2B forms the DV protease, and for most flaviviruses it is believed that proteolytic activity of the viral protease is important for antagonizing antiviral immunity. DV NS2B/3 has been shown to cleave STING [20,21]. Furthermore, the NS3/4A protease of HCV cleaves MAVS and thereby dampens RIG-I signaling [24,25]. Therefore, we first asked whether NS3 in complex with NS2B can cleave 14-3-3ε. Immunoblot (IB) analysis showed that overexpression of a proteolytically-active NS2B/3 construct did not result in any cleavage products of co-expressed FLAG-14-3-3ε (Figure 2.3). In support of this, endogenous 14-3-3ε protein levels were unchanged during DV infection (Figures 2.2F and 2.5D), strongly suggesting that DV NS2B/3 does not cleave 14-3-3ε. Furthermore, NS2B/3 did not cleave TRIM25 or RIG-I, the two other essential components of the 14-3-3ε translocon complex (Figure 2.3). In contrast, NS2B/3 readily cleaved co-expressed STING, which served as a positive control.

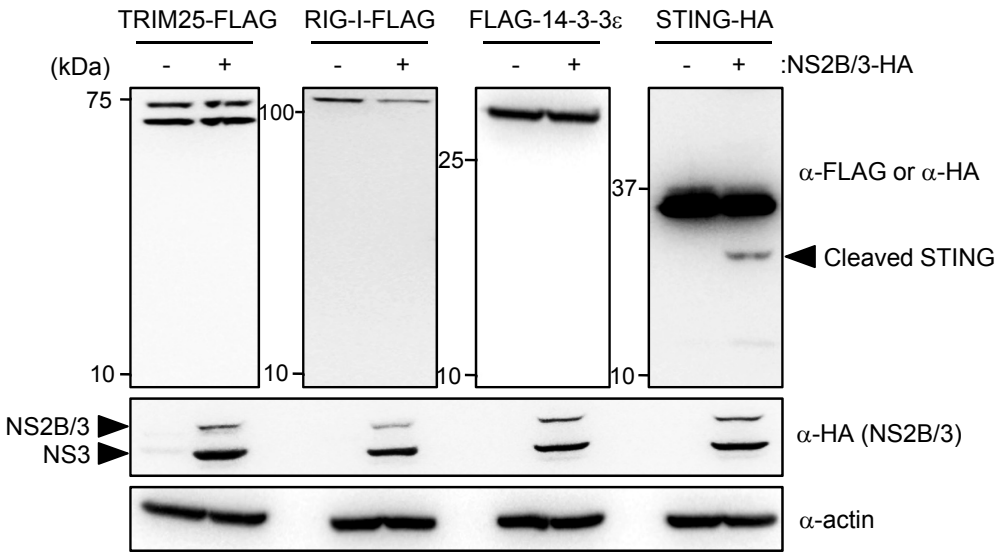


**Figure 2.3. NS2B/3 does not cleave 14-3-3ε, RIG-I or TRIM25.** HEK293T cells were transfected with TRIM25-FLAG, RIG-I-FLAG, FLAG-14-3-3ε, or STING-HA together with empty vector or HA-tagged NS2B/3. 48 h later, WCLs were subjected to IB with anti-HA, anti-FLAG, and anti-actin antibodies.

We next asked whether NS3 inhibits RIG-I signaling in a cleavage-dependent or -independent manner. To address this question, we generated a catalytically-inactive mutant of NS2B/3 (NS2B/$3_{S135A}$) [26], which, in contrast to WT NS2B/3, was unable to cleave itself or STING (Figure 2.4A). Ectopic expression of both NS2B/3 and NS2B/$3_{S135A}$ potently suppressed IFN-β induction mediated by ectopic expression of RIG-I 2CARD, the constitutively active signaling module of RIG-I (Figures 2.4B and 2.4C). In contrast, only WT NS3/4A of HCV suppressed RIG-I 2CARD-mediated IFN-β induction, while the inactive mutant NS3/$4A_{S139A}$ failed to do so (Figure 2.4B). Importantly, NS3 alone, which has no proteolytic activity without its co-factor NS2B [27] (Figure 2.4A), blocked RIG-I 2CARD- and SeV-induced IFN-β promoter activation as potently as NS2B/3 WT and NS2B/$3_{S135A}$ (Figures 2.4C and 2.4D). Consistent with this finding, NS3 overexpression also markedly inhibited endogenous IRF3 dimerization and ISG induction triggered by SeV infection (Figures 2.4E and 2.4F). These results indicate that DV NS3 inhibits RIG-I- and 14-3-3ε-mediated signaling in a cleavage-independent manner.

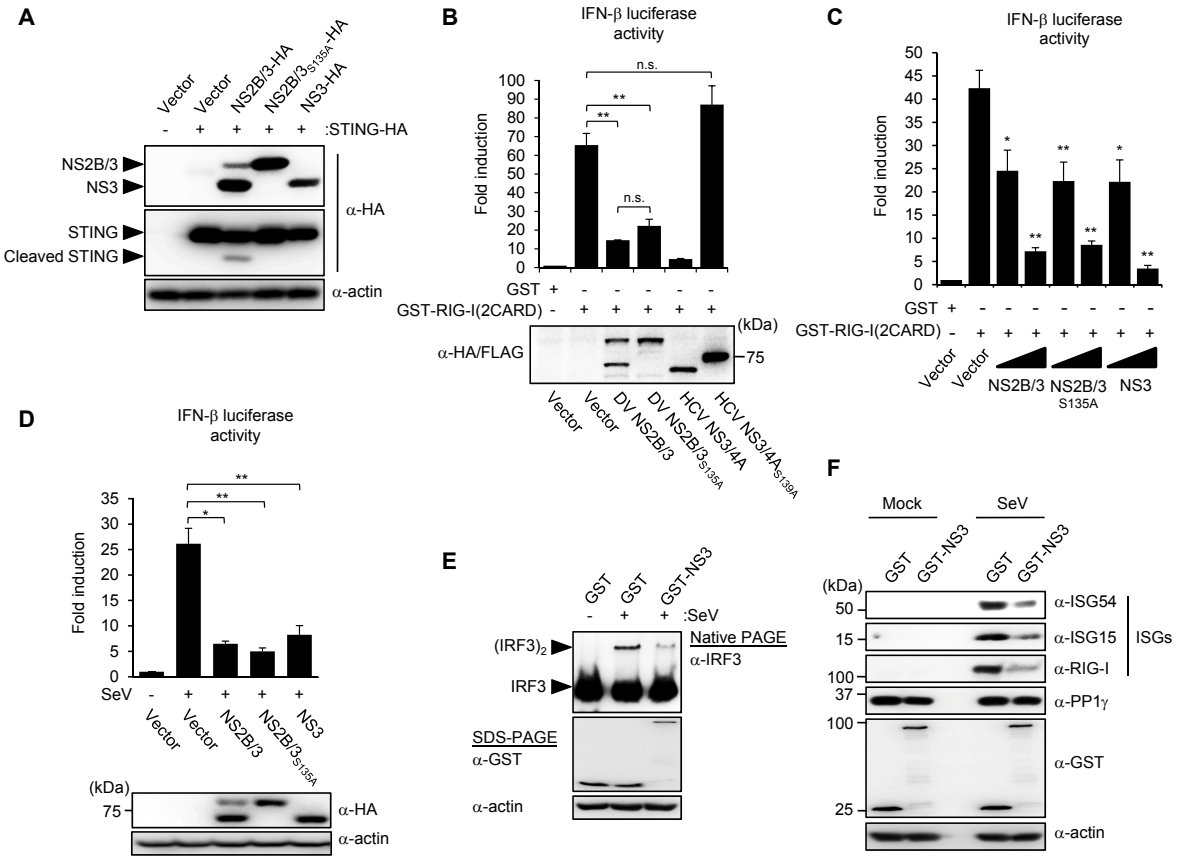


**Figure 2.4. NS2B/3 inhibits RIG-I activation independent of proteolytic activity. (A)** HEK293T cells were transfected with HA-tagged NS2B/3 WT, NS2B/3$_{S135A}$, or NS3, together with STING-HA. WCLs were analyzed by IB with anti-HA and anti-actin antibodies. **(B)** IFN-β luciferase activity in 293T cells transfected with GST or GST-RIG-I 2CARD together with vector, DV NS2B/3 WT or S135A, or HCV NS3/4A WT or S139A, normalized to constitutive pGK-β-gal. Viral protein expressions were determined by IB. The results are expressed as means ± SD (n = 3). **p<0.005. n.s.; not significant. **(C)** IFN-β luciferase activity in 293T cells transfected with GST or GST-RIG-I 2CARD together with vector, or increasing amounts of DV NS2B/3 WT, NS2B/3 S135A, or NS3, normalized to constitutive pGK-β-gal. The results are expressed as means ± SD (n = 3). *p<0.05; **p<0.005. **(D)** 293T cells, that had been transfected with vector, DV NS2B/3 WT, NS2B/3 S135A, or NS3, were subsequently infected with SeV (50 HAU/ml) for 18 h. Luciferase and β-gal activities were determined as in (B). Representative IB of viral protein expressions is shown. The results are expressed as means ± SD (n = 3). *p<0.05; **p<0.005. **(E)** GST or GST-NS3 was transfected into HEK293T cells. 48 h later, cells were infected with SeV (50 HAU/ml) for 16 h. WCLs were subjected to native PAGE, followed by IB with anti-IRF3 antibody. WCLs were further used for SDS-PAGE, followed by IB with the indicated antibodies. **(F)** Similar to (E), except WCLs were analyzed by IB 22 h after SeV infection with the indicated antibodies. Expression of PP1γ (not an ISG) was also determined by IB.

**NS3 prevents binding of the RIG-I-TRIM25 complex to 14-3-3ε, thereby inhibiting the translocation of activated RIG-I to mitochondria/MAMs**

To gain further insights into the mechanism by which the interaction of NS3 with 14-3-3ε suppresses RIG-I-mediated IFN induction, we asked whether NS3 *(i)* blocks the K63-linked ubiquitination of RIG-I, *(ii)* interferes with the complex formation of 14-3-3ε, RIG-I and TRIM25, or *(iii)* inhibits the translocation of RIG-I to mitochondria/MAMs, all of which are critical steps of RIG-I activation. Efficient ubiquitination of FLAG-RIG-I upon SeV infection was detected in both GST and GST-NS3 co-expressing cells (Figure 2.5A). Importantly, we detected robust ubiquitination of endogenous RIG-I during both DV and SeV infection, indicating that DV does not inhibit the ubiquitination of RIG-I (Figure 2.5B). To test whether NS3 inhibits the assembly of the 14-3-3ε-TRIM25-RIG-I ternary complex, we determined the binding of endogenous RIG-I to 14-3-3ε or TRIM25 upon SeV infection in the presence or absence of exogenous NS3. While SeV infection robustly triggered both 14-3-3ε and TRIM25 binding to RIG-I, expression of GST-NS3, but not GST alone, profoundly reduced 14-3-3ε binding to RIG-I, but did not affect the virus-induced interaction between TRIM25 and RIG-I (Figure 2.5C). In support of this, DV infection induced the complex formation of endogenous RIG-I and TRIM25 as efficiently as SeV infection (Figure 2.5D). However, the interaction between 14-3-3ε and RIG-I during DV infection was minimal and comparable to the interaction observed in mock-infected cells. In contrast, SeV infection induced robust 14-3-3ε-RIG-I binding (Figure 2.5D). These results indicate that NS3 does not affect TRIM25 binding and K63-linked ubiquitination of RIG-I, but instead specifically blocks the interaction of RIG-I with 14-3-3ε. In support of this, while both RIG-I and TRIM25 form a ternary complex with 14-3-3ε in infected cells [15], only RIG-I-FLAG, but not TRIM25-FLAG, interacted with bacterially-

purified r14-3-3ε in an *in vitro* binding assay (Figure 2.5E). Taken together, this supports a model in which 14-3-3ε directly binds to RIG-I upon viral infection, and NS3-14-3-3ε binding specifically prevents RIG-I from accessing 14-3-3ε.

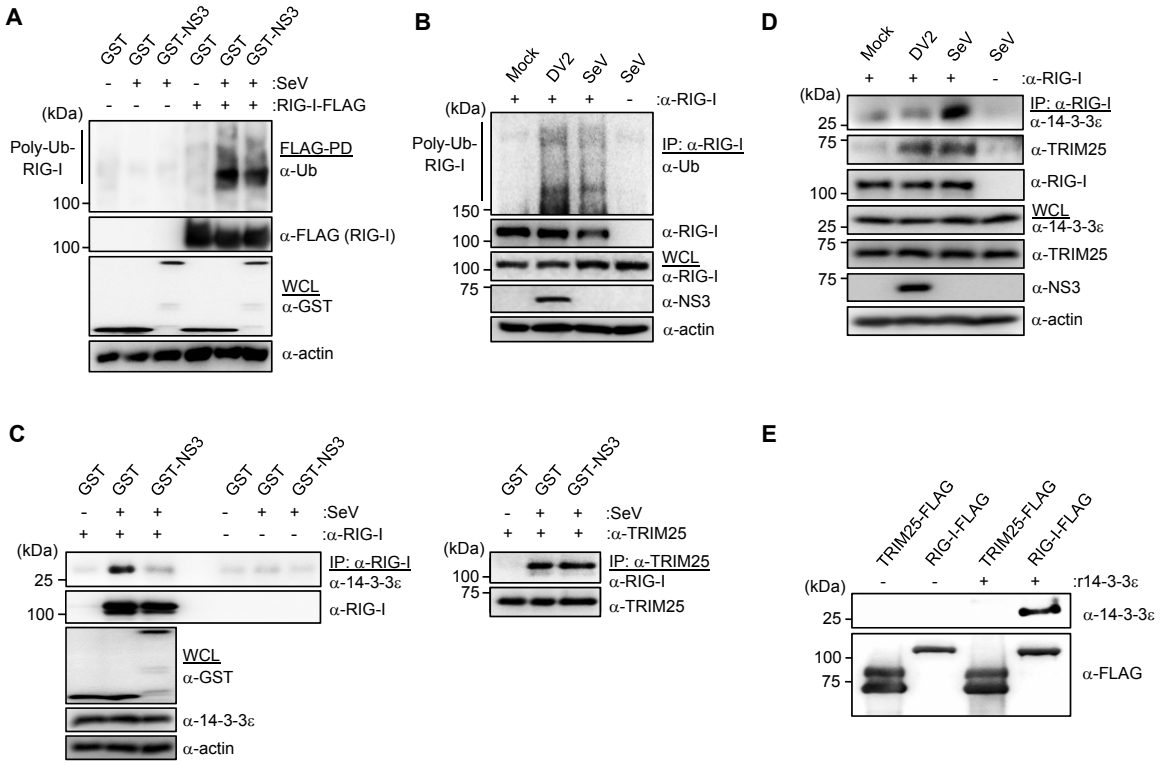


**Figure 2.5. NS3 inhibits binding of RIG-I to 14-3-3ε. (A)** HEK293T cells were transfected with empty vector or RIG-I-FLAG together with GST or GST-NS3. 48 h later, cells were infected with SeV (50 HAU/ml) for 19 h. WCLs were subjected to FLAG-PD, followed by IB with anti-ubiquitin (Ub) and anti-FLAG antibodies. **(B)** Huh7 cells were mock infected, or infected with DV2 NGC (MOI 1) or SeV (50 HAU/ml) for 18 h. WCLs were subjected to IP with anti-RIG-I, followed by IB with anti-Ub and anti-RIG-I. **(C)** HEK293T cells were transfected with GST or GST-NS3. 48 h later, cells were infected with SeV (50 HAU/ml) for 23 h. WCLs were subjected to IP with anti-RIG-I (left), or anti-TRIM25 (right), followed by IB with anti-14-3-3ε, anti-TRIM25 and anti-RIG-I antibodies. **(D)** Huh7 cells were mock-infected, or infected with DV2 NGC (MOI 1) or SeV (50 HAU/ml) for 18 h. WCLs were subjected to IP with anti-RIG-I, followed by IB with anti-14-3-3ε, anti-TRIM25 and anti-RIG-I. **(E)** *In vitro* binding assay was performed by incubating purified TRIM25-FLAG or RIG-I-FLAG with bacterially-purified recombinant (r) human 14-3-3ε. Binding was determined by IB with anti-14-3-3ε and anti-FLAG antibodies.

To address whether NS3 inhibits 14-3-3ε-mediated translocation of RIG-I to mitochondria/MAMs, we performed fractionation studies of DV- or SeV-infected Huh7 cells. In mock-infected cells, RIG-I was present almost exclusively in the cytosolic fraction, whereas in SeV-infected cells, RIG-I was abundant in the mitochondrial fraction, along with MAVS, indicating its translocation from the cytosol to mitochondria/MAMs. In striking contrast, RIG-I failed to translocate to the MAVS-containing mitochondrial fraction during DV infection (Figure 2.6A). The defect in RIG-I translocation was attributable to NS3 as ectopic expression of GST-NS3, but not GST alone, markedly diminished RIG-I amounts in the mitochondrial fraction of SeV-infected cells (Figure 2.6B). Together, these results indicate that binding of NS3 blocks 14-3-3ε from interacting with the activated RIG-I-TRIM25 complex, thereby preventing RIG-I from translocating to mitochondria/MAMs to initiate antiviral signaling.

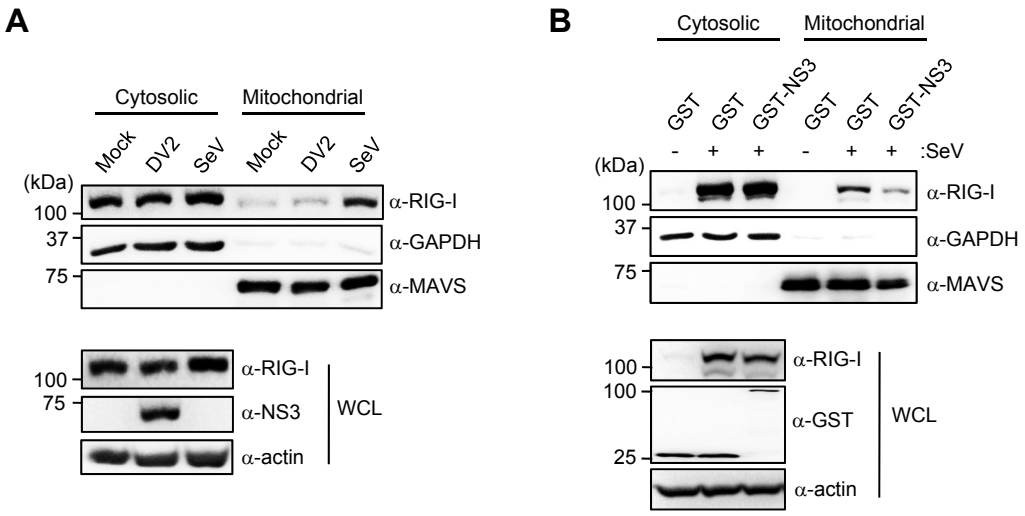


**Figure 2.6. NS3 prevents the translocation of activated RIG-I to mitochondria/MAMs. (A)** Huh7 cells were mock infected, or infected with DV2 NGC (MOI 1) or SeV (50 HAU/ml) for 22 h. WCLs were subjected to cytosol/mitochondria fractionation, followed by IB with anti-RIG-I, anti-MAVS and anti-GAPDH antibodies. Expression of RIG-I and NS3 was further determined in the WCL. **(B)** HEK293T cells were transfected with GST or GST-NS3. 48 h later, cells were infected with SeV (50 HAU/ml) for 20 h, followed by mitochondria fractionation assay and IB analysis. Furthermore, WCLs were analyzed for RIG-I, GST, GST-NS3, and actin protein expressions.

**NS3 binds to 14-3-3ε using a phosphomimetic RxEP motif**

To identify the binding site of 14-3-3ε in the protease domain of NS3 (NS3-Pro), we constructed GST-fused NS3-Pro truncation fragments and tested them for their abilities to bind endogenous 14-3-3ε by Co-IP. Full-length GST-NS3 served as a positive control (Figures 2.7A and 2.7B). We observed that full-length GST-NS3, GST-$NS3_{1\text{-}92}$ and GST-$NS3_{43\text{-}92}$ efficiently interacted with endogenous 14-3-3ε, while other NS3 fragments did not bind 14-3-3ε under the same conditions.

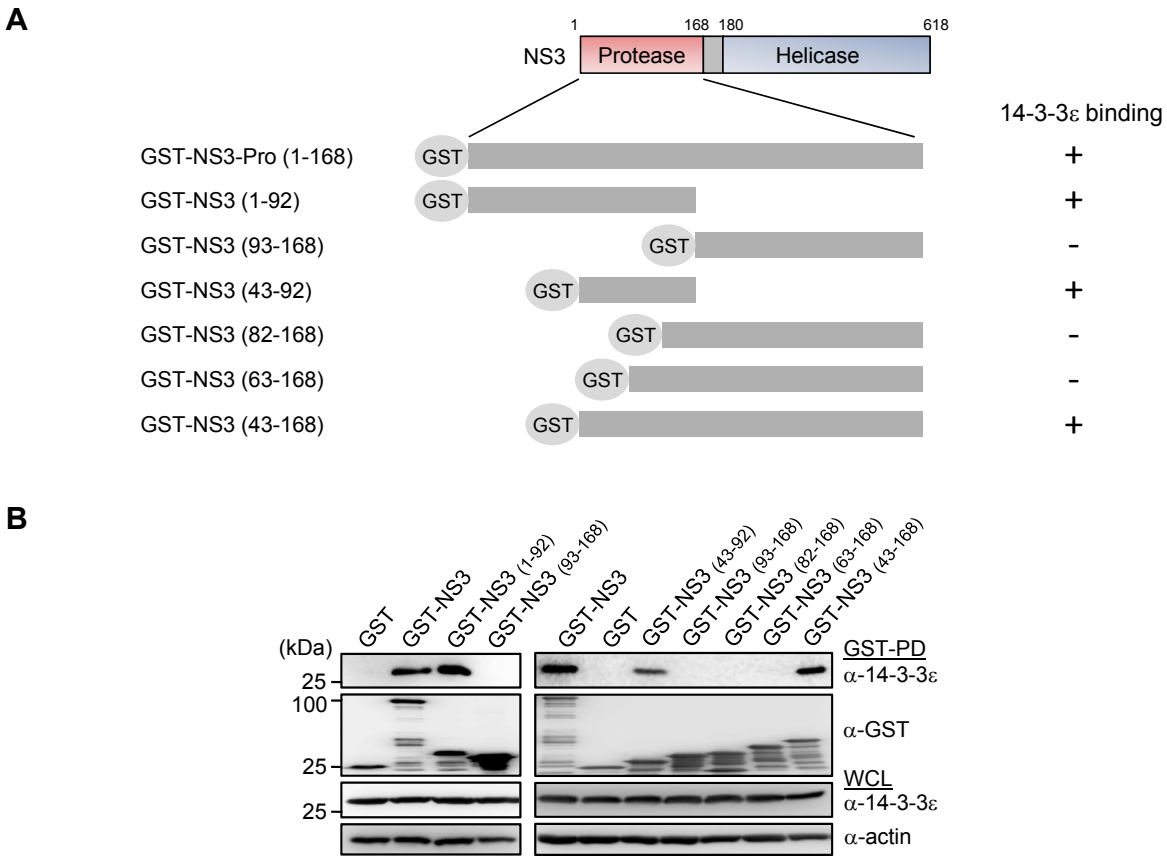


**Figure 2.7. Mapping the interaction of NS3 and 14-3-3ε. (A)** Schematic representation of the domain structure of NS3 as well as GST-fused NS3 truncation mutants. Furthermore, a summary of the results from the 14-3-3ε binding studies shown in (B) is provided. Numbers indicate amino acids. **(B)** 293T cells were transfected with the indicated GST-fused NS3 truncation constructs. 48 h later, WCLs were subjected to GST-PD, followed by IB with anti-14-3-3ε and anti-GST antibodies.

A hallmark of many cellular proteins that bind to 14-3-3 family members is the presence of a canonical high-affinity binding motif, such as Rxx(pS/pT)xP, where x denotes any residue and pS/pT indicates a phosphorylated serine/threonine residue [28]. Phosphorylation of S/T in Rxx(pS/pT)xP has been shown to be essential for 14-3-3 binding, as dephosphorylation of this residue abrogates 14-3-3 interaction [29]. A closer examination of $NS3_{43-92}$, which is sufficient for 14-3-3 binding (Figure 2.7B), revealed a "compact" $^{64}$RIEP$^{67}$ motif bearing close similarity to the cellular Rxx(pS/pT)xP motif but harboring a charged Glu$^{66}$ (E$^{66}$) residue in place of pS/pT (Figure 2.8A). Based on the crystal structure of the DV NS3 protein [30], which revealed an elongated shape of NS3 in which the linker region between the Pro and Hel domains adopts an extended conformation, this $^{64}$RIEP$^{67}$ motif is likely exposed for 14-3-3ε binding without steric hindrance (Figure 2.8B). Furthermore, the $^{64}$RIEP$^{67}$ motif is conserved between the DV2 strains NGC and 16681, while DV1, 3 and 4 harbor a similar motif, $^{64}$RLEP$^{67}$ (Figure 2.8A), suggesting that the $^{64}$RxEP$^{67}$ motif is conserved across various DV strains. Indeed, bioinformatics analysis aligning more than 3000 NS3 sequences derived from fully-sequenced DV1-4 strains showed that the $^{64}$RxEP$^{67}$ motif is conserved in all except two analyzed NS3 sequences, while adjacent residues show substantially more polymorphisms (Figure 2.8C).

Since E is a negatively charged residue which is often used to mimic pS/pT in molecular biology experiments, we hypothesized that DV NS3 may utilize the phosphomimetic E$^{66}$ residue in $^{64}$RxEP$^{67}$ for 14-3-3ε binding. To test this, we transplanted the corresponding motif from DV1, 3 and 4 (RLEP), or WNV (RLDP), both harboring phosphomimetic residues at position 66 (E$^{66}$ or D$^{66}$), into full-length NS3 derived from DV2 (NGC strain, which contains RIEP). In addition, we also transplanted the corresponding motif from YFV (KLIP), harboring an uncharged hydrophobic residue at position 66 (I$^{66}$), into DV2 NS3. Chimeric NS3 proteins containing RLEP

and RLDP ($NS3_{RLEP}$ and $NS3_{RLDP}$), which harbor $E^{66}$ or $D^{66}$, were both able to bind 14-3-3ε. In contrast, $NS3_{KLIP}$ showed strongly diminished binding (Figure 2.8D), which is consistent with our results that YFV NS3 does not bind 14-3-3ε (Figure 2.1E). This suggests that $D^{66}$, which is also a phosphomimetic residue, can substitute for $E^{66}$, and that $I^{65}$ and $L^{65}$ are functionally equivalent.

To further probe the importance of the phosphomimetic $E^{66}$ residue in NS3 for 14-3-3ε binding, we replaced $E^{66}$ with Lys ($K^{66}$), a positively charged amino acid ($NS3_{RIKP}$). $NS3_{RIKP}$ exhibited profoundly diminished binding to 14-3-3ε, indicating that the phosphomimetic $E^{66}$ (or $D^{66}$) is critical for 14-3-3ε interaction. Furthermore, additional mutation of $R^{64}$ to $K^{64}$ ($NS3_{KIKP}$) led to a near-complete loss of 14-3-3ε binding, demonstrating the importance of $E^{66}$ and $R^{64}$ for NS3 interaction with 14-3-3ε (Figure 2.8E). Collectively, these results indicate that instead of utilizing a canonical pS/pT-containing 14-3-3-binding motif, DV NS3 binds 14-3-3ε using a compact RxEP motif that contains a phosphomimetic ($E^{66}$) residue.

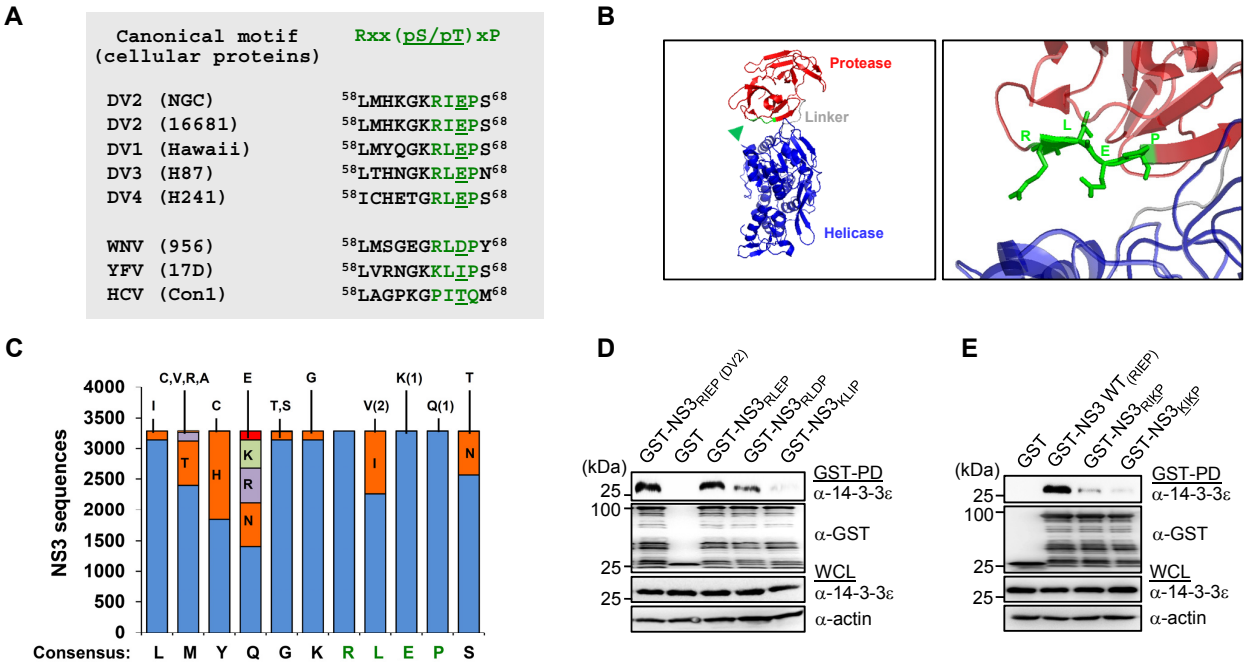


**Figure 2.8. NS3 binds to 14-3-3ε using a phosphomimetic RxEP motif. (A)** Amino acid sequence of the NS3 region harboring the 14-3-3 binding motif (green) from DV (serotypes 1-4), and WNV, YFV and HCV. **(B)** (Left) Ribbon representation of the crystal structure of DV4 NS3 protein. Protease domain is shown in red, linker in grey, and helicase domain in blue. The RLEP motif (arrow) is illustrated in green. (Right) Closed up view of the RLEP motif. **(C)** Bioinformatics analysis of 3280 known DV NS3 protein sequences. The most common residue for each position is shown as the consensus sequence (bottom) and is represented in blue in the bar graph. Polymorphisms for each position are represented by different colors. One polymorphism for $E^{66}$ or $P^{67}$ each was identified, as indicated in parenthesis. **(D and E)** 293T cells were transfected with GST, GST-NS3, or the indicated GST-NS3 mutants. 48 h later, WCLs were subjected to GST-PD, followed by IB with anti-14-3-3ε and anti-GST.

**The 14-3-3ε-binding deficient $NS3_{KIKP}$ mutant protein is impaired in suppression of RIG-I translocation and IFN-β induction**

To determine the role of 14-3-3ε binding for IFN antagonism by the DV NS3 protein, we functionally characterized the $NS3_{KIKP}$ mutant protein that exhibited a near-complete loss of 14-3-3ε binding. We first compared the inhibitory effect of WT NS3 and the $NS3_{KIKP}$ mutant on the complex formation of endogenous RIG-I and 14-3-3ε triggered by SeV infection. While WT NS3 potently inhibited SeV-induced RIG-I-14-3-3ε binding, $NS3_{KIKP}$ did not affect their interaction (Figure 2.9A). In line with this, while WT NS3 potently blocked the translocation of endogenous RIG-I to MAVS-containing mitochondrial fractions, $NS3_{KIKP}$ expression did not inhibit RIG-I translocation (Figure 2.9B). Furthermore, expression of WT NS3, but not $NS3_{KIKP,}$ significantly suppressed SeV-mediated IFN-β transcriptional activation and ISG protein expressions (Figures 2.9C and 2.9D). These data show that a mutant NS3 protein that is deficient in 14-3-3ε binding is unable to inhibit RIG-I-14-3-3ε binding and RIG-I translocation to mitochondria/MAMs, and thus has an impaired ability to suppress IFN and ISG induction. Together, this demonstrates that NS3's capacity to block the RIG-I-14-3-3ε interaction and RIG-I translocation is contingent on its ability to bind 14-3-3ε.

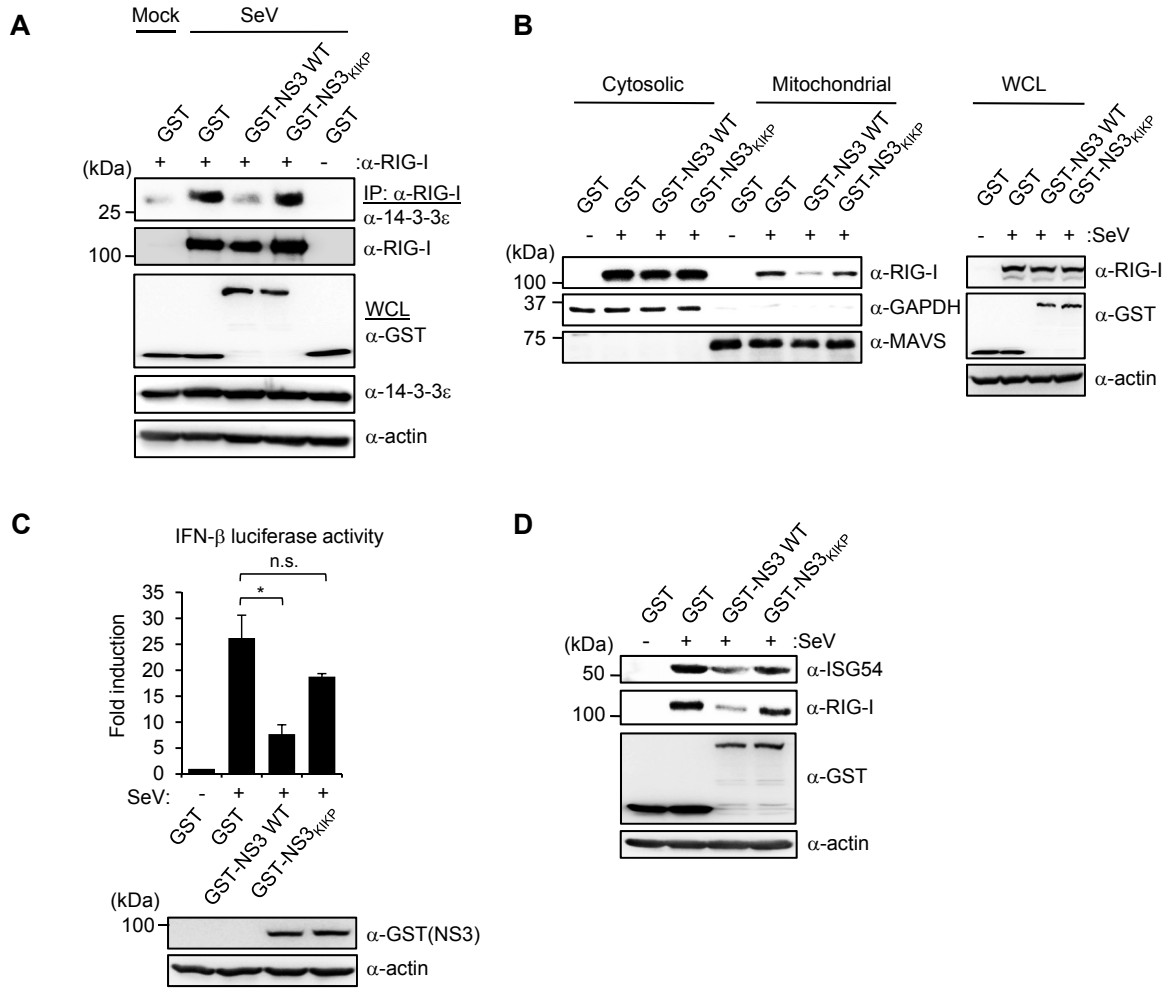


**Figure 2.9. The $NS3_{KIKP}$ mutant protein is impaired in inhibiting the RIG-I-14-3-3ε interaction, RIG-I translocation, and virus-mediated IFN and ISG induction. (A)** HEK293T cells were transfected with GST, GST-NS3 WT, or GST-$NS3_{KIKP}$. 48 h later, cells were infected with SeV (50 HAU/ml) for 20 h. WCLs were subjected to IP with anti-RIG-I antibody, followed by IB with anti-14-3-3ε and anti-RIG-I antibodies. **(B)** HEK293T cells were transfected with GST, GST-NS3 WT, or GST-$NS3_{KIKP}$. 48 h later, cells were infected with SeV (50 HAU/ml). 20 h later, cells were harvested for WCLs or subjected to mitochondria fractionation assay, followed by IB analysis. **(C)** HEK293T cells were transfected with IFN-β luciferase and pGK-β-gal, together with GST, GST-NS3 WT, or GST-$NS3_{KIKP}$. 48 h later, cells were infected with SeV (50 HAU/ml) for 18 h and subjected to luciferase assay. WCLs were analyzed for GST-NS3 expression by IB. The results are expressed as means ± SD (n = 3). *$p<0.05$. n.s., statistically not significant. **(D)** GST, GST-NS3 WT, or GST-$NS3_{KIKP}$ was transfected into HEK293T cells. 48 h later, cells were infected with SeV (50 HAU/ml) for 22 h. ISG (ISG54 or RIG-I) protein expression in the WCLs was determined by IB with the indicated antibodies.

**A recombinant DV encoding a $NS3_{KIKP}$ mutant protein is attenuated in replication and elicits enhanced levels of IFNs, ISGs and proinflammatory cytokines**

To determine the physiological relevance of the disruption of 14-3-3ε-mediated RIG-I translocation by NS3, we sought to construct a recombinant DV encoding the $NS3_{KIKP}$ mutant protein that is impaired in 14-3-3ε binding and RIG-I antagonism. Since NS3, as part of the NS2B/3 protease complex, processes the viral polyprotein and is therefore essential for DV replication, we first assessed if a $NS2B/3_{KIKP}$ mutant protein retains proteolytic activity. IB analysis showed that similar to WT NS2B/3, $NS2B/3_{KIKP}$ was able to induce self-cleavage (Figure 2.10A), which confirms an intact proteolytic activity and further suggests that a recombinant DV encoding $NS2B/3_{KIKP}$ would be viable. Using reverse genetics, we introduced the $R^{64}\rightarrow K^{64}$ and $E^{66}\rightarrow K^{66}$ mutations in an infectious clone originally derived from DV2 16681 [31,32], thereby engineering a recombinant mutant DV encoding $NS3_{KIKP}$ (subsequently referred to as $DV2_{KIKP}$).

Assessment of virus replication in Vero cells, which are deficient in type I IFN responses [33], showed that $DV2_{KIKP}$ exhibited reduced replication capacity compared to the parental virus ($DV2_{WT}$), resulting in approximately 1-log lower viral loads of $DV2_{KIKP}$ compared to $DV2_{WT}$ at 48 h and 72 h postinfection (Figures 2.10B and 2.10C). A decreased replication efficiency of $DV2_{KIKP}$, compared to WT virus, was also observed in mosquito (C6/36) and hamster (BHK21) cells (data not shown), indicating that the slightly attenuated replication capacity of $DV2_{KIKP}$ is independent of the host type I IFN system.

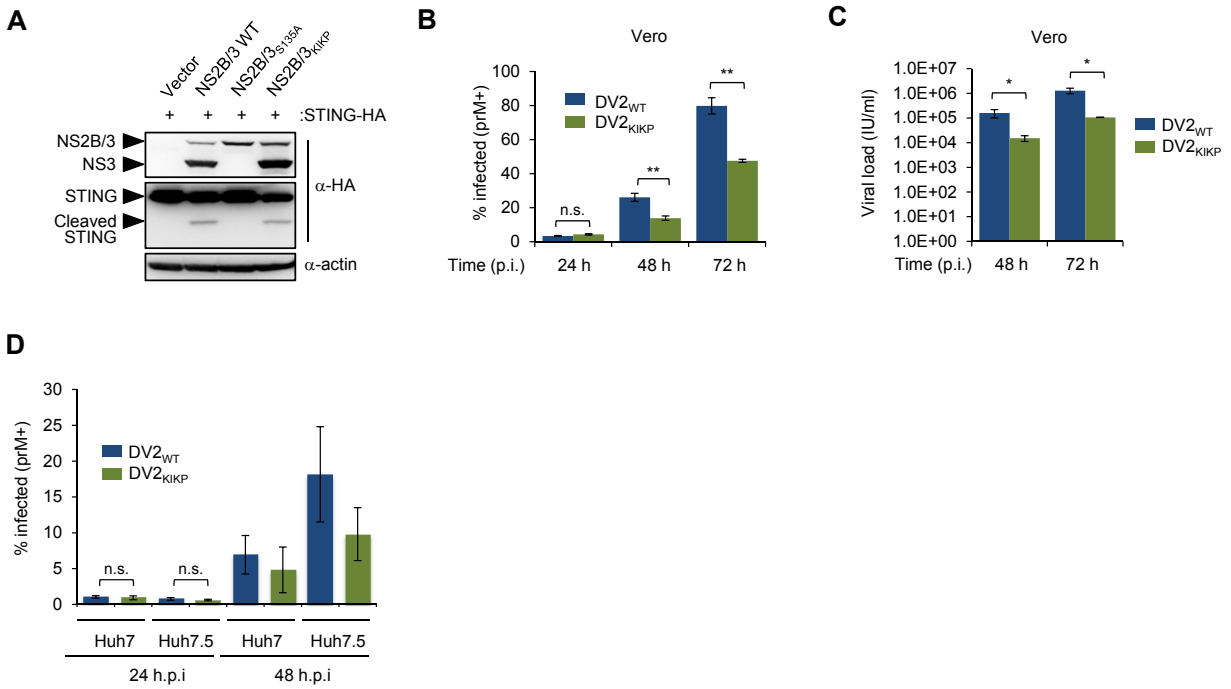


**Figure 2.10. A recombinant DV virus encoding a $NS3_{KIKP}$ mutant protein is attenuated in replication. (A)** The $NS2B/3_{KIKP}$ mutant protein is catalytically active. HEK293T cells were transfected with HA-tagged STING together with empty vector, or HA-tagged NS2B/3 WT, $NS2B/3_{S135A}$, or $NS2B/3_{KIKP}$. 48 h later, WCLs were analyzed by IB with anti-HA and anti-actin antibodies. **(B and C)** Replication of $DV2_{WT}$ and $DV2_{KIKP}$ in Vero cells. Vero cells were infected with $DV2_{WT}$ or $DV2_{KIKP}$ at an MOI of 0.02, as determined by titration on Veri cells. Cells were harvested for intracellular prM staining at the indicated time points and analyzed by flow cytometry (B). Furthermore, viral titers were determined in the supernatants (C). The results are expressed as means ± SD (n = 3). *$p<0.05$. **$p<0.005$. **(D)** Replication of $DV2_{WT}$ and $DV2_{KIKP}$ in Huh7 and Huh7.5 cells. Huh7 or Huh7.5 cells were infected with $DV2_{WT}$ or $DV2_{KIKP}$ at an MOI of 0.01. Cells were harvested for intracellular prM staining and analyzed by flow cytometry. The results are from 2 independent experiments and expressed as means ± SD (n = 6).

Next, we tested the replication of $DV2_{WT}$ and $DV2_{KIKP}$ in Huh7 cells, which have an intact type I IFN response. The replication rates of both $DV2_{WT}$ and $DV2_{KIKP}$ were similar 24 h after infection (Figure 2.10D); however, at 72 h postinfection, the replication of $DV2_{KIKP}$ was strongly suppressed, while $DV2_{WT}$ replicated efficiently (Figure 2.11A). To determine if the strongly diminished replication of $DV2_{KIKP}$ is due to its inability to antagonize RIG-I, we determined the replication of $DV2_{KIKP}$ in Huh7.5 cells, a sub-cell line of Huh7 naturally harboring a RIG-I mutant protein (RIG-I T55I) that is defective in TRIM25 binding and thus ubiquitination-mediated RIG-I activation [34,35]. We found that $DV2_{KIKP}$ replicated almost as efficiently as $DV2_{WT}$ in Huh7.5 cells (Figure 2.11A), indicating that the failure of $DV2_{KIKP}$ to replicate in Huh7 cells is predominantly due to RIG-I activation. Interestingly, $DV2_{WT}$ showed only a marginal increase in replication in Huh7.5 cells as compared to Huh7 cells (Figure 2.11A), suggesting that RIG-I signaling is effectively antagonized by $DV2_{WT}$.

To assess whether the reduced replication capacity of $DV2_{KIKP}$ in Huh7 cells, as compared to $DV2_{WT}$, is due to its inability to block IFN induction, we determined the gene upregulation of IFN-β, ISGs, and proinflammatory cytokines upon infection with $DV2_{KIKP}$ or $DV2_{WT}$. To account for the differences in replication efficiency, we infected Huh7 cells with $DV2_{WT}$ or $DV2_{KIKP}$ using MOIs (MOI 0.3 and 1, respectively) that resulted in comparable infectivity (~75% of cells infected at 2 d postinfection as determined by flow cytometry [data not shown]). We found that $DV2_{KIKP}$ elicited markedly higher levels of *IFNB1*, ISGs (*ISG15, IFIH1* and *MX1*), and proinflammatory cytokines (*TNF, IL6* and *CCL5*) than $DV2_{WT}$ (Figure 2.11B). In line with this, $DV2_{KIKP}$ infection of A549 cells robustly induced ISG protein expression (ISG54 and RIG-I) in neighboring non-infected cells as determined by confocal immunofluorescence microscopy. In contrast, ISG protein induction was low in response to $DV2_{WT}$ infection (Figure

2.11C). Crucially, we found that the higher *IFNB1* induction by $DV2_{KIKP}$, as compared to $DV2_{WT}$, was mediated by RIG-I activation, as Huh7.5 cells that are defective in RIG-I signaling exhibited low *IFNB1* induction following $DV2_{KIKP}$ infection (Figure 2.11D). To rule out the possibility that the impaired capacity of $DV2_{KIKP}$ to inhibit ISG induction was due to a potential defect in its ability to degrade STAT2, we tested the degradation of endogenous STAT2 in infected Huh7 cells. Both $DV2_{WT}$ and $DV2_{KIKP}$ were able to effectively degrade STAT2 (Figure 2.11E). Furthermore, a loss of STING antagonism could not account for the higher IFN response induced by $DV2_{KIKP}$, as both WT NS2B/3 and $NS2B/3_{KIKP}$ efficiently cleaved STING (Figure 2.10A). Mechanistically, we confirmed that cells infected with $DV2_{KIKP}$ exhibited efficient RIG-I translocation to the mitochondrial fraction. In contrast, $DV2_{WT}$ infection marginally induced RIG-I translocation (Figure 2.11F). Taken together, our results indicate that the 14-3-3ε-binding-deficient $DV2_{KIKP}$ virus fails to antagonize RIG-I and thus elicits enhanced induction of IFNs, ISGs and proinflammatory cytokines. This augmented immune response in turn contributes to restriction of $DV2_{KIKP}$ replication.

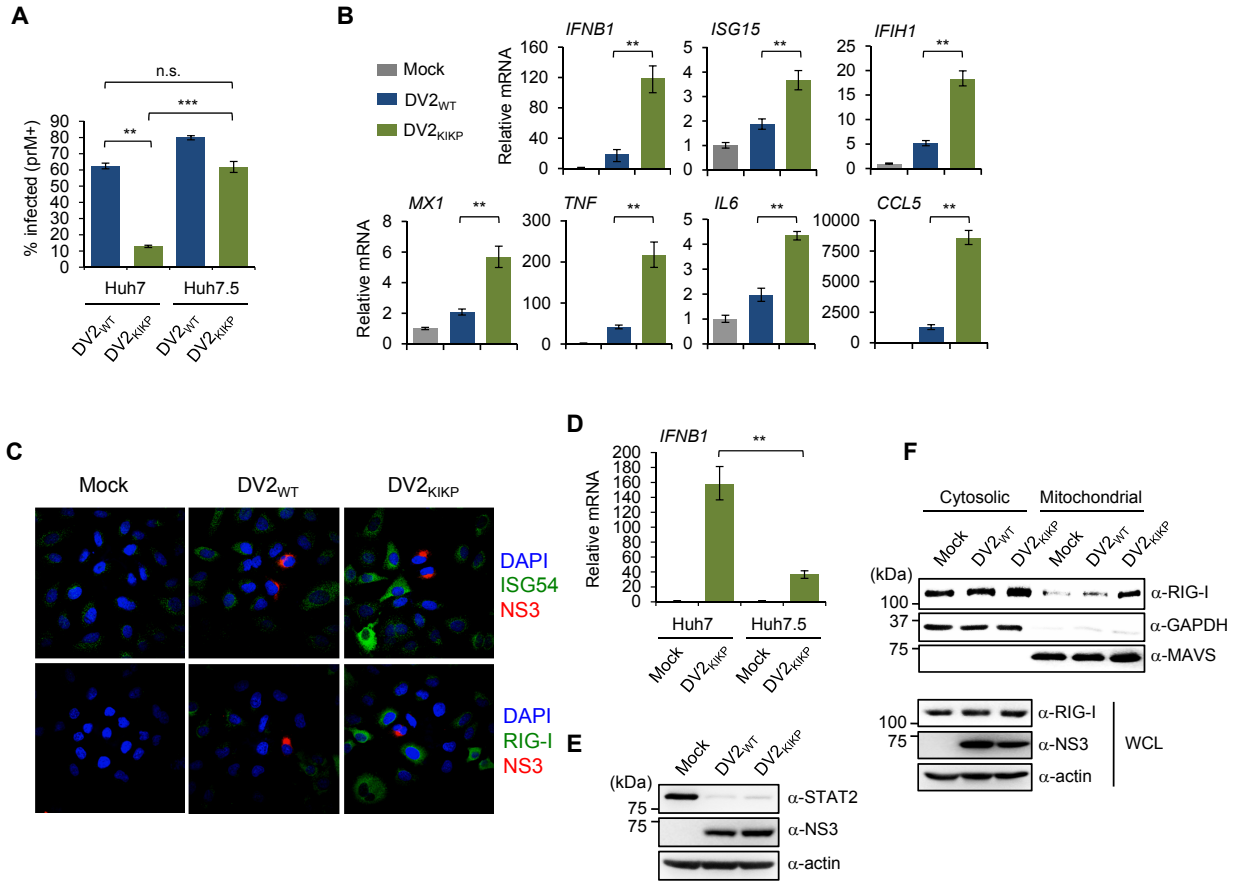


**Figure 2.11. $DV2_{KIKP}$ replication is strongly suppressed by RIG-I signaling and elicits an enhanced antiviral immune response. (A)** Huh7 or Huh7.5 cells were infected with $DV2_{WT}$ or $DV2_{KIKP}$ at MOI 0.01, as determined by titration on Vero cells. 72 h later, cells were harvested for intracellular prM staining and flow cytometry analysis. The results are expressed as means ± SD (n = 3). **p<0.005. **(B)** Huh7 cells were infected with $DV2_{WT}$ (MOI 0.3) or $DV2_{KIKP}$ (MOI 1), resulting in ~75% infectivity for both as determined by intracellular prM staining (not shown). 48 h later, total RNA was extracted and transcript levels of indicated genes were determined by quantitative real-time PCR. Transcript levels were normalized against *GAPDH* and shown as fold levels compared to mock infected cells. The results are expressed as means ± SD (n = 3). *p<0.05; **p<0.005. **(C)** A549 cells were infected with $DV2_{WT}$ or $DV2_{KIKP}$ (both MOI 0.2) for 24 h and subjected to immunofluorescence staining of endogenous ISG54 or RIG-I (green), NS3 (red), and DAPI (nuclei, blue). **(D)** Huh7 or Huh7.5 cells were infected with $DV2_{KIKP}$ at MOI 1 and harvested 48 h after infection for qRT-PCR as described in (B). The results are expressed as means ± SD (n = 3). **p<0.005. **(E)** Huh7 cells were infected with $DV2_{WT}$ or $DV2_{KIKP}$ as described in (B). 48 h later, WCLs were harvested and analyzed by IB with anti-STAT2 and anti-NS3 antibodies. **(F)** Huh7 cells were mock infected, or infected with $DV2_{WT}$ or $DV2_{KIKP}$ at MOI 0.8. 20 h later, cells were harvested for WCLs, or subjected to mitochondria fractionation, followed by IB analysis.

While the liver is commonly involved during DV infection *in vivo*, mononuclear phagocytes are thought to be the primary *in vivo* cell targets for DV replication [36]. Therefore, we infected primary human $CD14^+$ monocytes with $DV2_{WT}$ or $DV2_{KIKP}$ (both at an MOI of 1) and then measured *IFNB1* induction 24 h postinfection by qRT-PCR. *IFNB1* induction by both $DV2_{WT}$ and $DV2_{KIKP}$ was below the detection limit (data not shown), which in agreement with previous studies is likely due to the low infectivity of primary monocytes *in vitro* [37]. However, when we measured the gene expression of the proinflammatory cytokines *TNF, CCL5, IL8* and *IL6*, all of which are strongly induced in monocytes upon viral infection, we detected a robust induction of these cytokines by $DV2_{KIKP}$, but not $DV2_{WT}$ (Figure 2.12A). Consistent with this, $CD14^+$ monocytes infected with $DV_{KIKP}$ exhibited enhanced IL-6 protein secretion as compared to cells infected with $DV2_{WT}$ (Figure 2.12B). To detect *IFNB1* induction with a more sensitive assay, we performed intracellular staining of IFN-β in $DV2_{WT}$- or $DV2_{KIKP}$-infected monocytes. Flow cytometry analysis revealed that $DV2_{KIKP}$-infected prM+ monocytes produced significantly more IFN-β than $DV2_{WT}$-infected cells (Figure 2.12C). Collectively, these results show that a mutant DV encoding a 14-3-3ε-binding-deficient NS3 protein is impaired in its ability to antagonize RIG-I and thus elicits an augmented innate immune response in human hepatocytes and primary human monocytes.

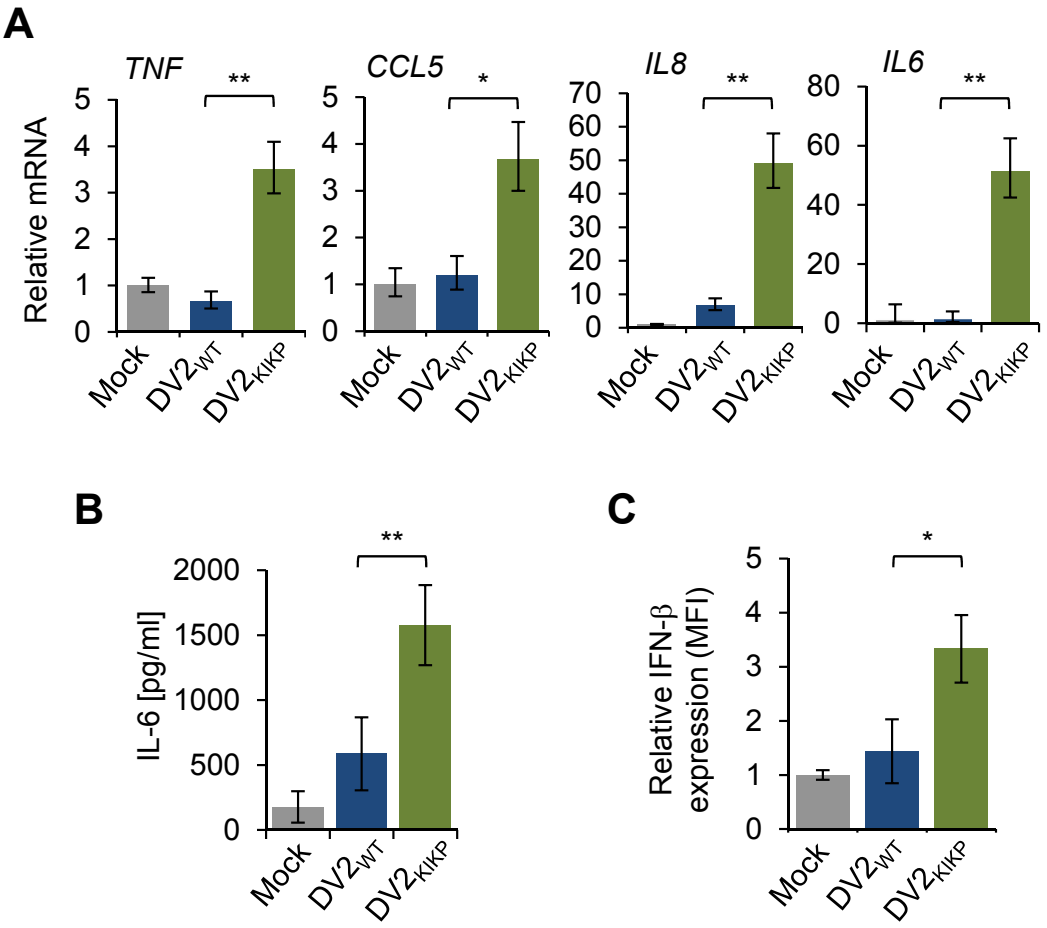


**Figure 2.12. $DV2_{KIKP}$ is defective in antagonizing the innate immune response in primary human monocytes. (A)** Primary $CD14^+$ monocytes were infected with $DV2_{WT}$ or $DV2_{KIKP}$ at MOI 1 for 24 h. RNA transcript levels were determined by qRT-PCR. The results are expressed as means ± SD (n = 3). *p<0.05; **p<0.005. **(B)** Primary $CD14^+$ monocytes were infected as in (A). Supernatants were harvested and analyzed by ELISA for IL-6. The results are expressed as means ± SD (n = 4). **p<0.005. **(C)** Primary PBMCs were infected similar to (A). 24 h after infection, cells were treated with brefeldin A for 6 h to block protein transport. Subsequently, cells were harvested for intracellular IFN-β and prM staining and analyzed by flow cytometry. prM+ monocytes were analyzed for mean fluorescence intensity (MFI) of IFN-β staining. The results are expressed as means ± SD (n = 3). *p<0.05.

## DISCUSSION

A key feature of eukaryotic cells is the compartmentalization of diverse biological activities by membrane-bound organelles. Among them, mitochondria, the endoplasmic reticulum (ER), and peroxisomes play important roles in the orchestration of antimicrobial immunity by serving as platforms for the assembly of multi-protein complexes, which induce innate immune signaling. Hence, upon PAMP recognition, cytosolic PRRs must relocate from the sites of PAMP detection to signaling-competent organelles — a highly regulated process that requires specific trafficking factors [38]. A major class of intracellular trafficking molecules are 14-3-3 proteins [39]. With regards to innate immune signaling, 14-3-3ε binds to RIG-I upon viral infection to translocate RIG-I to mitochondria and MAMs, which promotes MAVS activation and the induction of antiviral IFNs [40]. However, it has previously been unknown whether viral pathogens target specific trafficking proteins to perturb PRR translocation and innate immune signal transduction. Our findings show that the NS3 protein of DV inhibits the translocation of RIG-I to mitochondrion/MAM-localized MAVS by disrupting the interaction of RIG-I with 14-3-3ε. NS3 specifically inhibited 14-3-3ε-mediated trafficking of RIG-I, but did not interfere with two upstream activation steps of RIG-I, the binding of RIG-I to the E3 ligase TRIM25 and TRIM25-mediated RIG-I ubiquitination. Together, our results indicate that during DV infection RIG-I is initially activated via K63-linked ubiquitination by TRIM25. However, RIG-I fails to induce an antiviral response as NS3 prevents 14-3-3ε-mediated trafficking of RIG-I to membrane-bound MAVS.

The NS3 protease of DV, in complex with its cofactor NS2B, is critical for viral polyprotein processing and thus DV replication. In addition to their role in viral replication, NS2B/3 and the proteases of other flaviviruses also subvert innate immune responses — an

ability which is believed to primarily depend on their proteolytic activities. For example, DV NS2B/3 cleaves the adaptor protein STING, while HCV NS3/4A cleaves MAVS to directly suppress RIG-I signaling [20,21,24]. However, unlike HCV, DV does not cleave MAVS and therefore it has been unclear how DV inhibits signaling by RIG-I, a key sensor of DV infection. Our functional studies comparing the inhibitory effects of the active and inactive DV NS2B/3 protease complex revealed that NS2B/3 inhibits RIG-I-triggered IFN induction in a proteolysis-independent manner. Furthermore, overexpressed NS3 alone, which has no protease activity, also effectively blocked the RIG-I signaling pathway. Combined with previous studies, our data indicate that DV NS2B/3 utilizes both proteolysis-dependent and -independent mechanisms to block the type I IFN system. Our finding therefore provides a mandate to reconsider how viral proteases antagonize immunity, and we postulate that more examples of proteolysis-independent viral antagonism of host immunity will likely be uncovered.

As most cellular proteins interact with 14-3-3 family members via conserved pS/pT-containing motifs, we searched for similar motifs in DV NS3. The NS3-Pro domain harbors a highly conserved $^{64}$RxEP$^{67}$ motif that bears strong resemblance to the canonical Rxx(pS/pT)xP motif found in cellular 14-3-3-interacting proteins. Intriguingly, instead of harboring a central pS or pT residue, DV NS3 possesses a phosphomimetic residue, E$^{66}$. The chemical similarity of phosphomimetic residues (E and D) and pS/pT is well established, leading investigators to commonly utilize E/D substitutions to mimic site-specific phosphorylation in molecular biology experiments. Mutational analysis showed that the phosphomimetic residue E$^{66}$ is critical for 14-3-3ε binding, and that R$^{64}$ also contributes to NS3-14-3-3ε interaction. Our work thus provides the first example of a naturally occurring phosphomimetic utilized in an infectious disease mechanism, specifically the evasion of antiviral innate immunity by DV. While it is unclear why

DV has not evolved a classical pS/pT-containing 14-3-3ε-binding motif, it is possible that using a phosphomimetic residue for 14-3-3ε-binding may provide advantages to the virus such as the lack of requirement for a kinase, be it viral or cellular, and the uniform "phosphorylation state" of all NS3 molecules.

Other pathogens are known to hijack 14-3-3 proteins. For example, the bacterial pathogen *Pseudomonas aeruginosa* encodes the ADP-ribosyltransferase toxin Exoenzyme S (ExoS), which interacts with 14-3-3 proteins to drive cytotoxicity. However, ExoS binds to 14-3-3 proteins using a DALDL motif, which is not related to known cellular binding motifs [41], indicating that ExoS has evolved a completely different way to bind 14-3-3. In particular, the L residues, but not the negatively-charged D residues, are important for 14-3-3 binding, demonstrating that hydrophobic interaction forces mediate binding [42,43]. Furthermore, the synthetic peptide R18, which was discovered through phage display screen and is not derived from pathogens, is frequently used as a tool to block the binding of cellular proteins to 14-3-3 proteins [44]. Interestingly, R18 also harbors a phosphomimetic motif (WLDLE) containing two negatively charged residues (D and E), which mediate 14-3-3 binding by engaging residues in 14-3-3 proteins that are similar to those engaged by the pS/pT motif found in cellular binding partners of 14-3-3 proteins [45]. These studies, along with our findings, indicate that in addition to canonical pS/pT-containing motifs, unphosphorylated motifs containing hydrophobic residues and short phosphomimetic sequences – either synthetic or naturally-occurring in a viral pathogen – mediate efficient 14-3-3 binding. The observation that both DV NS3 and R18 can displace cellular proteins from engaging 14-3-3 suggests that phosphomimetic motifs may have higher 14-3-3-binding affinities than canonical cellular motifs. Additional studies are necessary to determine if DV NS3 also binds to and antagonizes other 14-3-3 family members, thereby

manipulating other signaling pathways.

To determine the physiological relevance of the NS3-14-3-3ε interaction, we engineered a recombinant DV that encodes a mutant NS3 protein deficient in 14-3-3ε binding ($DV2_{KIKP}$). The mutant virus was viable, consistent with our data that the introduced mutations did not affect the proteolytic activity of NS3 (as part of the protease complex), but displayed a mild replication defect compared to WT virus independent of the type I IFN system. However, in cells with an intact immune response, this virus was strongly attenuated compared to WT virus. The mutant virus induced significantly higher levels of IFN, ISGs, and proinflammatory cytokines both in human liver cells and primary monocytes, due to its inability to inhibit the translocation of RIG-I to mitochondria/MAMs, and hence RIG-I-dependent signaling. These results indicate that antagonism of RIG-I translocation is an effective mechanism for suppressing the type I IFN response, and also emphasize the important role of mitochondria/MAMs as a signaling compartment during DV infection. As the molecular details of how RIG-I translocates to other organelles such as peroxisomes are currently unknown, future studies will need to address the role of peroxisomal-MAVS signaling during DV infection, and whether DV has evolved means to block the translocation of RIG-I to peroxisomes. Furthermore, we hypothesize that other viral pathogens may also bind to and antagonize the 14-3-3ε translocon to inhibit innate immune signaling.

Dengue virus is known to potently suppress the innate immune system, a prerequisite for successful virus replication and pathogenesis. Our studies using a mutant DV that is deficient in 14-3-3ε binding and RIG-I antagonism showed that disabling a specific viral IFN-antagonistic mechanism leads to viral growth attenuation and robust activation of the innate immune response. We propose that systematically disabling immune evasion mechanisms while

preserving viral function may allow for the rational design of live-attenuated dengue vaccines. In particular, elimination of multiple immune evasion mechanisms (such as viral targeting of 14-3-3ε and STAT2) from a virus may dramatically improve its safety profile and potently induce antiviral responses for long-lasting immunity. Furthermore, our detailed characterization of the NS3-14-3-3ε interaction may also guide the design of small molecule inhibitors for antiviral therapy. In summary, our work unveils a key immune evasion mechanism of DV, which provides a framework for rational vaccine design and antiviral development.

## MATERIALS AND METHODS

### Cell Culture and Viruses

HEK293T, Huh7, Huh7.5, Vero and A549 cells were cultured in Dulbecco's Modified Eagle's Medium (DMEM) supplemented with 10% fetal bovine serum (FBS), 10 mM HEPES and 1% penicillin-streptomycin (Gibco). BHK-21 cells were propagated in Minimum Essential Medium Alpha (MEM-α) supplemented with 10% FBS, 10 mM HEPES and 1% penicillin-streptomycin. C6/36 cells were cultured in Eagle's Minimum Essential Medium (EMEM) supplemented with 10% FBS and 1% penicillin-streptomycin, and grown at 28°C. K562 cells and primary $CD14^+$ monocytes were maintained in Roswell Park Memorial Institute (RPMI) 1640 medium supplemented with 10% FBS, 1% non-essential amino acid solution (Gibco) and 1% penicillin-streptomycin. DV2 NGC, DV1 276 RK1, DV2 16681, DV3 BC188/97 and DV4 814699 were propagated in C6/36 cells. SeV (Cantell) was purchased from Charles River Laboratories. HSV-1 was a kind gift from David Knipe (Harvard).

### Plasmids and Transfections

pQCXIP-NS2B/3-HA and pQCXIP-NS3-HA were generated by subcloning NS2B/3 (containing NS2B and NS3) or NS3 of DV2 (strain NGC) into pQCXIP vector using NotI and BamHI sites. GST-NS3 and GST-NS5 were generated by subcloning NS3 or NS5 of DV2 (strain NGC) into pEBG vector between BamHI and ClaI. Similarly, NS3 of YFV (kindly provided by Richard Kuhn, Purdue University) and NS3 of HCV (kindly provided by Zhijian Chen, UT Southwestern) were subcloned into the pEBG vector. pEF-BOS-FLAG-NS3-Pro (aa 1-179), pEF-BOS-FLAG-NS3-Hel (aa 169-618), pEF-BOS-FLAG-NS5-MTase (aa 1-319) and pEF-BOS-FLAG-NS5-Pol (aa 297-901) were generated by subcloning into pEF-BOS-FLAG vector using NotI and SalI sites. 14-3-3ε (Uniprot: P62258-1) was purchased as a cDNA clone and

subcloned into pEF-BOS and pCAGGS vectors with an N-terminal FLAG and c-myc tag, respectively. HA-tagged 14-3-3σ was provided by Satoshi Inoue (University of Tokyo) and has been described [46]. pQCXIP-STING-HA was generated by subcloning STING (clone ID 5762441, Thermo Scientific) into pQCXIP vector using NotI and BamHI sites. The plasmids encoding the HCV NS3/4A protease complex (pcDNA3-FLAG-NS3/4A) and its S139A catalytically-inactive mutant were a kind gift of Zhijian Chen [24]. Plasmids encoding GST-RIG-I(2CARD), RIG-I-FLAG and TRIM25-FLAG have been described previously [7,47]. The DV NS3 truncation mutants GST-NS3(1-92), GST-NS3(93-168), GST-NS3(43-92), GST-NS3(82-168), GST-NS3(63-168), and GST-NS3(43-168) were generated by PCR using GST-NS3 full-length as template. All constructs were sequenced to verify 100% agreement with the original sequence. Transfections were performed using the calcium phosphate method, or with TurboFectin 8.0 (Origene), Lipofectamine and Plus reagent, or Lipofectamine 2000 (all Life Technologies) according to the manufacturer's instructions.

**14-3-3ε Knockdown Experiments**

siRNAs targeting 14-3-3ε (siGENOME SMARTpool M-017302-03-0005) as well as a non-targeting control siRNA were purchased from Dharmacon. K562 cells were seeded into 12-well plates and transfected with 300 nM siRNA using Lipofectamine RNAiMAX (Life Technologies) according to the manufacturer's instructions. Knockdown of endogenous 14-3-3ε was determined by western blot analysis.

**Antibodies and Reagents**

For western blot analysis, the following antibodies were used: anti-FLAG (M2, Sigma), anti-HA (HA-7, Sigma), anti-GST (Sigma), anti-c-myc (9E10), anti-β-actin (Abcam), anti-RIG-I (Alme-

1, Adipogen), anti-TRIM25 (BD Biosciences), anti-ubiquitin (P4D1, Santa Cruz), anti-PP1γ (Bethyl Laboratories), anti-ISG15 (F-9, Santa Cruz), anti-ISG54 (ProSci), anti-STAT2 (Santa Cruz), anti-14-3-3ε (8C3, Santa Cruz), anti-NS3 (E1D8, kindly provided by Eva Harris), anti-NS3 (GT2811, Genetex), anti-MAVS (AT107, Enzo), anti-GAPDH (CS204254, Millipore), anti-IRF3 (sc-9082, Santa Cruz). For immunoprecipitation of 14-3-3ε, anti-14-3-3ε (11648-2-AP, Proteintech) was used. For flow cytometry analysis, anti-prM (2H2, Merck Millipore) was conjugated to DyLight 633 using a commercial kit (Thermo Scientific) and used to detect DV-infected cells. Anti-CD14-FITC (M5E2, BD Biosciences) was used to determine purity of $CD14^+$ monocytes. Anti-IFN-β-FITC (MMHB-3, PBL Assay Science) was used to detect IFN-β+ monocytes upon DV infection. Isotype control antibodies were purchased from BD Biosciences.

**Luciferase Reporter Assay**

HEK293T cells were seeded into 12-well plates. The following day, cells were transfected with 200 ng IFN-β luciferase construct, 300 ng β-gal-expressing pGK-β-gal, and 100 ng - 1 μg of plasmid encoding effector protein. To stimulate IFN-β promoter activity, 2 ng of GST-RIG-I-2CARD was co-transfected, or cells were infected with SeV (50 HAU/ml) 48 hours after transfection. Cells were harvested and assayed for luciferase activity (Promega). Luciferase values were normalized to β-galactosidase activity to control for transfection efficiency.

**Pull-down Assay, Co-Immunoprecipitation, and Immunoblot Analysis**

HEK293T or Huh7 cells were lysed in NP-40 buffer (50 mM HEPES pH 7.4, 150 nM NaCl, 1% [vol/vol] NP-40, protease inhibitor cocktail [Sigma]) and centrifuged at 13,000 rpm for 20 min. GST or FLAG pull-down, Co-IP, and western blot analyses were performed as previously

described [7,48].

**Large-scale Protein Purification and Mass Spectrometry**

HEK239T cells were transfected with pEF-BOS-FLAG-NS3-Pro, pEF-BOS-FLAG-NS3-Hel, pEF-BOS-FLAG-NS5-MTase or pEF-BOS-FLAG-NS5-Pol. Two days later, cells were lysed with NP-40 buffer supplemented with protease inhibitor cocktail (Sigma). Clarified lysates were mixed with a ~50% slurry of anti-FLAG-conjugated sepharose beads (Sigma) and incubated for 4 h at 4°C. After extensive washing of the beads, bound proteins were eluted and separated on a NuPAGE 4-12% Bis-Tris gradient gel (Life Technologies). Coomassie staining was performed and a ~30kDa band specifically present in the FLAG-NS3-Pro sample was excised and analyzed by ion-trap mass spectrometry at the Harvard Taplin Biological Mass Spectrometry facility.

**Confocal Microscopy**

Huh7 cells were grown on chamber slides or on cover slips in 24-well plates, and then infected with DV2 or SeV at indicated titers, or mock infected. Cells were harvested at indicated time points and fixed with 4% (w/v) paraformaldehyde for 20 min, permeabilized with 0.2% (v/v) Triton-X-100 in PBS, and blocked with 10% (v/v) goat serum or FBS in PBS for 1 h. For immunostaining, anti-14-3-3ε (Proteintech), anti-NS3 (GT2811 or GTX 124252, Genetex), anti-NS4A (GTX 124249, Genetex), anti-ISG54 (12604-1-AP, Proteintech), anti-RIG-I (Alme-1, Adipogen), and anti-FLAG (Sigma, Abcam and Bethyl) were used, followed by incubation with secondary antibodies conjugated to Alexa Fluor 488, Alexa Fluor 594, or Alexa Fluor 647 (Life Technologies or Abcam). Cells were mounted in DAPI-containing Vectashield (Vector Labs) to co-stain nuclei. All laser scanning images were acquired on an Olympus IX8I confocal microscope.

**Direct Protein Interaction Assay**

Bacterially-purified recombinant human 14-3-3ε protein (NP_006752.1) was purchased from Sino Biological. GST or GST-NS3 (DV2, strain NGC) expressed in HEK293T cells was immobilized on glutathione-conjugated sepharose beads in NP-40 buffer and incubated with recombinant 14-3-3ε protein (final concentration of 10 μg/ml) for 2 h at 4°C. After extensive washing with NP-40 buffer, bound proteins were eluted from the beads with 2x Laemmli buffer and heated at 95°C for 5 min, followed by SDS-PAGE and western blot analysis. Similarly, TRIM25-FLAG and RIG-I-FLAG were purified from transfected HEK293T cells using anti-FLAG-conjugated sepharose beads and tested for binding to recombinant 14-3-3ε.

**Mitochondria Fractionation Assay**

HEK293T or Huh7 cells were infected with DV or SeV at indicated titers, or mock infected. 20 - 24 hours later, a portion of cells was harvested for WCLs, and another portion for fractionation assay using a commercial mitochondria/cytosol fractionation kit (MIT1000, Merck Millipore) according to the manufacturer's instructions. Briefly, cells were disrupted in Isotonic Mitochondrial Buffer using a Dounce homogenizer. Lysates were subjected to low-speed centrifugation to pellet nuclei and unbroken cells. Supernatant was subsequently centrifuged at 10,000 x g for 30 min at 4°C. The supernatant containing the cytosol and microsome fraction ('cytosolic fraction') as well as the pellet containing the enriched mitochondrial fraction were subjected to a bicinchoninic acid (BCA) assay. Equal amounts of protein were loaded for SDS-PAGE and analyzed by western blot. Anti-GAPDH and anti-MAVS western blot analyses served as controls.

**Dengue Virus Infection and Flow Cytometry Analysis**

Infection was performed based on a published protocol [49]. Briefly, ~1.5 x $10^5$ Huh7 cells per well were seeded into 24-well plates and allowed to adhere for 4 h. Virus diluted in 250 µl DMEM containing 2% FBS was incubated at 37°C for 1.5 h. At the indicated time points after infection, cells and/or supernatants were harvested. For K562 suspension cells, the infection was performed similarly except growth media was directly added to cells after infection. To detect DV-infected cells, cells were washed once in PBS, fixed in 1% (w/v) paraformaldehyde, permeabilized with 0.1% saponin (Sigma), and then stained with anti-prM-DyLight 633 in permeabilization buffer for ~40 min at 4°C. Subsequently, cells were washed with PBS and resuspended in 1% (w/v) paraformaldehyde before flow cytometry analysis on a FACS Calibur (BD Biosciences). Analysis was performed using FlowJo software (Tree Star).

**Bioinformatics analysis**

NS3 protein sequences from full genome DV sequences were analyzed with NIAID Virus Pathogen Database and Analysis Resource (ViPR) online through the website at http://www.viprbrc.org.

**Quantitative Real Time-PCR (qRT-PCR)**

Total RNA was extracted from cells using an RNA extraction kit (OMEGA Bio-Tek). Equal amounts of RNA (typically 10 - 100 ng) were used in an one-step qRT-PCR reaction (SuperScript III Platinum One-Step qRT-PCR kit with ROX, Life Technologies) with commercially available primers with FAM reporter dye for the indicated target genes (IDT). Expression level for each target gene was calculated by normalizing against GAPDH using the ΔΔCT method and expressed as fold levels compared to mock-infected cells. All qRT-PCR

reactions were run on a 7300 RT-PCR System or 7500 FAST RT-PCR System (both ABI).

**Generation of a $NS3_{KIKP}$ Mutant Dengue Virus**

$DV2_{KIKP}$ was generated based on an infectious clone of DV2 16681, pD2/IC-30P, kindly provided by Claire Huang (CDC) and described previously [31,32]. PCR was used to generate mutant pD2/IC-30P harboring R64K and E66K mutations in the NS3 gene. The wild-type and mutant infectious clone plasmids were linearized by XbaI digestion and *in vitro* transcribed using the T7 promoter (RiboMAX Large Scale RNA Production System, Promega) with the addition of a $m^7$G(5')ppp(5')A RNA cap structure analog (New England Biolabs). The *in vitro* transcribed RNA was purified using Micro Bio-Spin columns (Bio Rad) and transfected into Vero cells using Lipofectamine 2000. Viral supernatants were harvested and used to propagate the wild-type and mutant virus in Vero cells. Vero cells were further used to titer the recombinant viruses using a FACS-based assay [50] with anti-prM antibody.

**DV infection studies in Primary Human Monocytes**

Human peripheral blood or peripheral blood mononuclear cells (PBMCs) from unidentified healthy donors was purchased (HemaCare). In the case of human peripheral blood, PBMCs were isolated using Ficoll-Hypaque (GE Healthcare) density gradient centrifugation. $CD14^+$ monocytes were positively selected from PBMCs using anti-CD14 magnetic microbeads according to the manufacturer's instructions (Miltenyi Biotec). $CD14^+$ monocytes were rested overnight in growth media before use, or cryopreserved for use in future experiments. The purity of $CD14^+$ cells was routinely ~90%, as determined by anti-CD14-FITC staining (BD Biosciences) and flow cytometry analysis. For infection experiments, ~1.5 x $10^5$ $CD14^+$ monocytes or PBMCs per well were infected with DV in a 96-well plate in 250 µl DMEM containing 2% FBS for 5 h, with occasional agitation. For flow cytometry analysis of

intracellular IFN-β-FITC staining, cells were treated for 5-6 h with 5 μg/ml Brefeldin A (BioLegend) to block protein transport before fixing and staining for flow cytometry analysis.

**Statistical analysis**

Unpaired two-tailed Student's t tests were used. $P<0.05$ was defined as statistically significant.

## REFERENCES


1. Villar L, Dayan GH, Arredondo-Garcia JL, Rivera DM, Cunha R, et al. (2014) Efficacy of a Tetravalent Dengue Vaccine in Children in Latin America. N Engl J Med.

2. Capeding MR, Tran NH, Hadinegoro SR, Ismail HI, Chotpitayasunondh T, et al. (2014) Clinical efficacy and safety of a novel tetravalent dengue vaccine in healthy children in Asia: a phase 3, randomised, observer-masked, placebo-controlled trial. Lancet 384: 1358-1365.

3. Takeuchi O, Akira S (2010) Pattern recognition receptors and inflammation. Cell 140: 805-820.

4. Goubau D, Deddouche S, Reis e Sousa C (2013) Cytosolic sensing of viruses. Immunity 38: 855-869.

5. Loo YM, Gale M, Jr. (2011) Immune signaling by RIG-I-like receptors. Immunity 34: 680-692.

6. Goubau D, Schlee M, Deddouche S, Pruijssers AJ, Zillinger T, et al. (2014) Antiviral immunity via RIG-I-mediated recognition of RNA bearing 5'-diphosphates. Nature 514: 372-375.

7. Gack MU, Shin YC, Joo CH, Urano T, Liang C, et al. (2007) TRIM25 RING-finger E3 ubiquitin ligase is essential for RIG-I-mediated antiviral activity. Nature 446: 916-920.

8. Peisley A, Wu B, Xu H, Chen ZJ, Hur S (2014) Structural basis for ubiquitin-mediated antiviral signal activation by RIG-I. Nature 509: 110-114.

9. Zeng W, Sun L, Jiang X, Chen X, Hou F, et al. (2010) Reconstitution of the RIG-I pathway reveals a signaling role of unanchored polyubiquitin chains in innate immunity. Cell 141: 315-330.

10. Dixit E, Boulant S, Zhang Y, Lee AS, Odendall C, et al. (2010) Peroxisomes are signaling platforms for antiviral innate immunity. Cell 141: 668-681.

11. Horner SM, Liu HM, Park HS, Briley J, Gale M, Jr. (2011) Mitochondrial-associated endoplasmic reticulum membranes (MAM) form innate immune synapses and are targeted by hepatitis C virus. Proc Natl Acad Sci U S A 108: 14590-14595.

12. Seth RB, Sun L, Ea CK, Chen ZJ (2005) Identification and characterization of MAVS, a mitochondrial antiviral signaling protein that activates NF-kappaB and IRF 3. Cell 122: 669-682.

13. Belgnaoui SM, Paz S, Hiscott J (2011) Orchestrating the interferon antiviral response through the mitochondrial antiviral signaling (MAVS) adapter. Curr Opin Immunol 23:

564-572.

14. Goswami R, Majumdar T, Dhar J, Chattopadhyay S, Bandyopadhyay SK, et al. (2013) Viral degradasome hijacks mitochondria to suppress innate immunity. Cell Res 23: 1025-1042.

15. Liu HM, Loo YM, Horner SM, Zornetzer GA, Katze MG, et al. (2012) The mitochondrial targeting chaperone 14-3-3epsilon regulates a RIG-I translocon that mediates membrane association and innate antiviral immunity. Cell Host Microbe 11: 528-537.

16. Schmid MA, Diamond MS, Harris E (2014) Dendritic cells in dengue virus infection: targets of virus replication and mediators of immunity. Front Immunol 5: 647.

17. Green AM, Beatty PR, Hadjilaou A, Harris E (2014) Innate immunity to dengue virus infection and subversion of antiviral responses. J Mol Biol 426: 1148-1160.

18. Ashour J, Laurent-Rolle M, Shi PY, Garcia-Sastre A (2009) NS5 of dengue virus mediates STAT2 binding and degradation. J Virol 83: 5408-5418.

19. Rodriguez-Madoz JR, Belicha-Villanueva A, Bernal-Rubio D, Ashour J, Ayllon J, et al. (2010) Inhibition of the type I interferon response in human dendritic cells by dengue virus infection requires a catalytically active NS2B3 complex. J Virol 84: 9760-9774.

20. Aguirre S, Maestre AM, Pagni S, Patel JR, Savage T, et al. (2012) DENV inhibits type I IFN production in infected cells by cleaving human STING. PLoS Pathog 8: e1002934.

21. Yu CY, Chang TH, Liang JJ, Chiang RL, Lee YL, et al. (2012) Dengue virus targets the adaptor protein MITA to subvert host innate immunity. PLoS Pathog 8: e1002780.

22. Apte-Sengupta S, Sirohi D, Kuhn RJ (2014) Coupling of replication and assembly in flaviviruses. Curr Opin Virol 9C: 134-142.

23. Miller S, Kastner S, Krijnse-Locker J, Buhler S, Bartenschlager R (2007) The non-structural protein 4A of dengue virus is an integral membrane protein inducing membrane alterations in a 2K-regulated manner. J Biol Chem 282: 8873-8882.

24. Li XD, Sun L, Seth RB, Pineda G, Chen ZJ (2005) Hepatitis C virus protease NS3/4A cleaves mitochondrial antiviral signaling protein off the mitochondria to evade innate immunity. Proc Natl Acad Sci U S A 102: 17717-17722.

25. Meylan E, Curran J, Hofmann K, Moradpour D, Binder M, et al. (2005) Cardif is an adaptor protein in the RIG-I antiviral pathway and is targeted by hepatitis C virus. Nature 437: 1167-1172.

26. Khumthong R, Angsuthanasombat C, Panyim S, Katzenmeier G (2002) In vitro determination of dengue virus type 2 NS2B-NS3 protease activity with fluorescent peptide substrates. J Biochem Mol Biol 35: 206-212.

27. Falgout B, Pethel M, Zhang YM, Lai CJ (1991) Both nonstructural proteins NS2B and NS3 are required for the proteolytic processing of dengue virus nonstructural proteins. J Virol 65: 2467-2475.

28. Mhawech P (2005) 14-3-3 proteins--an update. Cell Res 15: 228-236.

29. Yaffe MB, Rittinger K, Volinia S, Caron PR, Aitken A, et al. (1997) The structural basis for 14-3-3:phosphopeptide binding specificity. Cell 91: 961-971.

30. Luo D, Xu T, Hunke C, Gruber G, Vasudevan SG, et al. (2008) Crystal structure of the NS3 protease-helicase from dengue virus. J Virol 82: 173-183.

31. Kinney RM, Butrapet S, Chang GJ, Tsuchiya KR, Roehrig JT, et al. (1997) Construction of infectious cDNA clones for dengue 2 virus: strain 16681 and its attenuated vaccine derivative, strain PDK-53. Virology 230: 300-308.

32. Butrapet S, Huang CY, Pierro DJ, Bhamarapravati N, Gubler DJ, et al. (2000) Attenuation markers of a candidate dengue type 2 vaccine virus, strain 16681 (PDK-53), are defined by mutations in the 5' noncoding region and nonstructural proteins 1 and 3. J Virol 74: 3011-3019.

33. Desmyter J, Melnick JL, Rawls WE (1968) Defectiveness of interferon production and of rubella virus interference in a line of African green monkey kidney cells (Vero). J Virol 2: 955-961.

34. Gack MU, Kirchhofer A, Shin YC, Inn KS, Liang C, et al. (2008) Roles of RIG-I N-terminal tandem CARD and splice variant in TRIM25-mediated antiviral signal transduction. Proc Natl Acad Sci U S A 105: 16743-16748.

35. Sumpter R, Jr., Loo YM, Foy E, Li K, Yoneyama M, et al. (2005) Regulating intracellular antiviral defense and permissiveness to hepatitis C virus RNA replication through a cellular RNA helicase, RIG-I. J Virol 79: 2689-2699.

36. Jessie K, Fong MY, Devi S, Lam SK, Wong KT (2004) Localization of dengue virus in naturally infected human tissues, by immunohistochemistry and in situ hybridization. J Infect Dis 189: 1411-1418.

37. Kou Z, Lim JY, Beltramello M, Quinn M, Chen H, et al. (2011) Human antibodies against dengue enhance dengue viral infectivity without suppressing type I interferon secretion in primary human monocytes. Virology 410: 240-247.

38. Kagan JC (2012) Signaling organelles of the innate immune system. Cell 151: 1168-1178.

39. Dougherty MK, Morrison DK (2004) Unlocking the code of 14-3-3. J Cell Sci 117: 1875-1884.

40. Hou F, Sun L, Zheng H, Skaug B, Jiang QX, et al. (2011) MAVS forms functional prion-like aggregates to activate and propagate antiviral innate immune response. Cell 146: 448-461.

41. Henriksson ML, Francis MS, Peden A, Aili M, Stefansson K, et al. (2002) A nonphosphorylated 14-3-3 binding motif on exoenzyme S that is functional in vivo. Eur J Biochem 269: 4921-4929.

42. Yasmin L, Veesenmeyer JL, Diaz MH, Francis MS, Ottmann C, et al. (2010) Electrostatic interactions play a minor role in the binding of ExoS to 14-3-3 proteins. Biochem J 427: 217-224.

43. Yang X, Lee WH, Sobott F, Papagrigoriou E, Robinson CV, et al. (2006) Structural basis for protein-protein interactions in the 14-3-3 protein family. Proc Natl Acad Sci U S A 103: 17237-17242.

44. Wang B, Yang H, Liu YC, Jelinek T, Zhang L, et al. (1999) Isolation of high-affinity peptide antagonists of 14-3-3 proteins by phage display. Biochemistry 38: 12499-12504.

45. Petosa C, Masters SC, Bankston LA, Pohl J, Wang B, et al. (1998) 14-3-3zeta binds a phosphorylated Raf peptide and an unphosphorylated peptide via its conserved amphipathic groove. J Biol Chem 273: 16305-16310.

46. Urano T, Saito T, Tsukui T, Fujita M, Hosoi T, et al. (2002) Efp targets 14-3-3 sigma for proteolysis and promotes breast tumour growth. Nature 417: 871-875.

47. Wies E, Wang MK, Maharaj NP, Chen K, Zhou S, et al. (2013) Dephosphorylation of the RNA sensors RIG-I and MDA5 by the phosphatase PP1 is essential for innate immune signaling. Immunity 38: 437-449.

48. Chan YK, Huang IC, Farzan M (2012) IFITM proteins restrict antibody-dependent enhancement of dengue virus infection. PLoS One 7: e34508.

49. Diamond MS, Edgil D, Roberts TG, Lu B, Harris E (2000) Infection of human cells by dengue virus is modulated by different cell types and viral strains. J Virol 74: 7814-7823.

50. Lambeth CR, White LJ, Johnston RE, de Silva AM (2005) Flow cytometry-based assay for titrating dengue virus. J Clin Microbiol 43: 3267-3272.

# Chapter 3

## NS3-mediated Degradation of RIG-I during Dengue Virus Infection

Ying Kai Chan and Michaela U. Gack

Department of Microbiology and Immunobiology, Harvard Medical School, Boston, MA 02115, USA

**ABSTRACT**

RIG-I is a key cytosolic sensor of numerous RNA viruses, including dengue virus (DV). In order to replicate, pathogenic RNA viruses have evolved mechanisms to evade RIG-I-mediated immunity. Here, we show that RIG-I is degraded in DV-infected cells. Furthermore, the NS3 protein of DV is sufficient to degrade RIG-I, but not the related helicase MDA5. In contrast to the previously described NS5-mediated proteasomal degradation of STAT2, NS3 degrades RIG-I via lysosomes. In agreement, RIG-I co-localizes with LAMP1+ compartments during DV infection. A mutant NS3 protein that is deficient in 14-3-3ε binding ($NS3_{KIKP}$) is impaired in RIG-I degradation. Importantly, infection with a recombinant DV encoding $NS3_{KIKP}$ ($DV2_{KIKP}$) fails to degrade RIG-I and further elicits RIG-I induction. Our data support a model where RIG-I fails to bind 14-3-3ε for translocation to mitochondria during DV infection and is subsequently degraded by lysosomes, thereby highlighting the multifaceted antagonism of RIG-I by NS3.

**INTRODUCTION**

The two essential enzymes of DV, NS5 and NS3, play important roles in both viral replication and immune evasion (reviewed in [1].) NS5 is an RNA-dependent RNA polymerase and is responsible for replicating and capping the viral RNA genome. In addition, NS5 antagonizes type I IFN-receptor (IFNAR) signaling by inducing the proteasomal degradation of STAT2 [2]. NS3, which forms the protease complex with its small co-factor NS2B, is critical for proteolytic processing of the DV polyprotein and also potently inhibits type I IFN induction [1,3]. Previously, NS2B/3 has been shown to cleave stimulator of interferon genes (STING)

[4,5], an adaptor protein downstream of cytosolic DNA sensors. Other work has suggested that NS2B/3 may target IκB kinase ε (IKKε) to prevent phosphorylation of IRF3 [6]. Furthermore, in Chapter 2, we demonstrated that NS3 binds to 14-3-3ε and blocks RIG-I translocation to mitochondria, thereby inhibiting MAVS interaction and antiviral signaling. These results provide a key mechanism for NS3-mediated inhibition of type I IFN induction.

RIG-I is a key cytosolic sensor of numerous RNA viruses, and is extensively targeted by viral pathogens for immune evasion (reviewed in [7]). Viruses have evolved to i) manipulate the posttranslational modification program and hence activation state of RIG-I, ii) bind and sequester RIG-I from signaling, iii) or cleave and inactivate RIG-I. Interestingly, recent work has shown that the NS1 and NS2 proteins of respiratory syncytial virus (RSV) assemble a large multi-protein complex on mitochondria, termed "degradasome", which leads to the degradation of several innate immune signaling molecules including RIG-I by host proteases [8]. This finding suggests that apart from encoding viral proteins that directly target RIG-I, viruses can also usurp cellular processes to degrade RIG-I, thereby antagonizing innate immunity.

Here, we extend our earlier findings to show that DV NS3 NS3 – upon inhibiting the mitochondrial translocation of K63-ubiquitin-activated RIG-I – mediates lysosomal degradation of RIG-I, thereby bolstering inhibition of IFN induction.

## RESULTS AND DISCUSSION

### NS3 triggers lysosomal degradation of RIG-I

We have previously shown that the NS3 protein of DV binds directly to 14-3-3ε to prevent RIG-I binding and translocation to mitochondria for MAVS interaction and antiviral

signaling. During the course of these studies, we fortuitously observed that RIG-I protein levels in DV2-infected Huh7 cells were markedly diminished in a MOI-dependent manner, and that this loss was evident at 20 h postinfection (Figures 3.1A and 3.1B). In contrast, 14-3-3ε and actin protein levels were unaffected. It has been previously demonstrated that DV NS5 targets STAT2 for proteasomal degradation and that this degradation occurs very early (~3 h) after DV infection (also seen in Figure 3.1B) [2]. As STAT2 degradation by the proteasome occurs significantly earlier than RIG-I degradation, we hypothesized that a distinct mechanism is responsible for RIG-I degradation during DV infection.

Since NS3 is the DV protein responsible for inhibition of RIG-I-mediated IFN induction ([3] and also described in Chapter 2), we first tested if ectopic expression of NS3 degrades RIG-I. Previous studies have shown that RIG-I is an interferon-stimulated gene (ISG). To separate the degradation of RIG-I protein from the block in its induction by NS3, we expressed exogenous tagged RIG-I, which as expected was not upregulated by infection with Sendai virus (SeV) (Figure 3.1C), a potent inducer of IFN. We observed that GST-NS3, but not GST-NS5, degraded exogenous RIG-I in a dose-dependent manner (Figure 3.1C). Similar to DV infection, 14-3-3ε protein levels were not affected by NS3 overexpression. Furthermore, ectopic expression of GST-NS3, but not GST alone, strongly diminished the protein levels of tagged RIG-I, but not the related helicase MDA5, demonstrating that NS3 specifically degrades RIG-I (Figure 3.1D). These data show that NS3 is able to degrade RIG-I independent of blocking its gene induction.

We have previously shown that the DV NS2B/3 protease complex does not cleave RIG-I (Figure 2.3). To gain mechanistic insights into the observed degradation of RIG-I during DV infection, we infected Huh7 cells with DV2, incubated the cells to allow viral replication, and then treated them with a proteasomal inhibitor (MG132) or two different lysosomal inhibitors

($NH_4Cl$ and chloroquine). Both lysosomal inhibitors were able to rescue the loss of endogenous RIG-I, while MG132 failed to do so (Figure 3.1E). Furthermore, confocal fluorescence microscopy showed that FLAG-RIG-I co-localized with LAMP1+ compartments during DV2 infection, supporting that RIG-I is targeted for degradation via lysosomes (Figure 3.1F). Together, our data demonstrate that RIG-I is degraded in a lysosome-dependent manner during DV infection and that this activity is dependent on the NS3 protein.

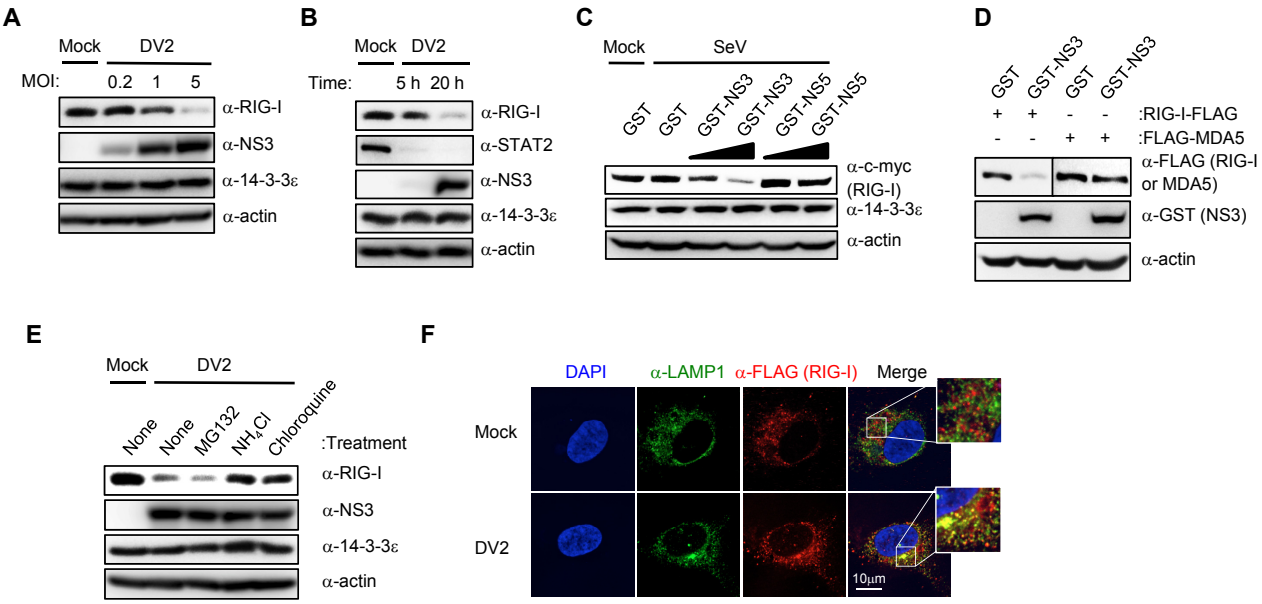


**Figure 3.1. NS3 triggers lysosomal degradation of RIG-I. (A)** Huh7 cells were mock-infected or infected with increasing MOIs (0.2, 1, and 5) of DV2 (NGC) for 20 h. WCLs were analyzed by IB with anti-RIG-I, anti-NS3 and anti-14-3-3ε antibodies. **(B)** Huh7 cells were infected with DV2 (NGC) at MOI 5. WCLs were harvested at the indicated time points after infection, followed by IB analysis as in (A). Endogenous STAT2 expression was also determined. **(C)** HEK293T cells were transfected with GST, GST-NS3 or GST-NS5, together with c-myc-tagged RIG-I. 24 h later, cells were infected with SeV (50 HAU/ml) for 22 h. WCLs were analyzed by IB with anti-c-myc, anti-14-3-3ε and anti-actin antibodies. **(D)** HEK293T cells were transfected with GST or GST-NS3, and either FLAG-tagged RIG-I or MDA5. 48 h later, WCLs were analyzed by IB with anti-FLAG or anti-GST antibodies. **(E)** Huh7 cells were infected with DV2 (NGC) at MOI 5 for 16 h, and then treated with the indicated inhibitors for 7 h. WCLs were analyzed by IB as in (A). **(F)** Huh7 cells were transfected with FLAG-RIG-I. 24 h later, cells were infected with DV2 (NGC) at MOI 5 or mock infected for 13 h. Cells were stained for FLAG (RIG-I; red) and LAMP1 (green) and imaged by confocal microscopy. Nuclei were stained with DAPI (blue).

**$DV2_{KIKP}$ is deficient in RIG-I degradation**

We have previously characterized the binding of NS3 and 14-3-3ε, and found that NS3 possesses a highly conserved phosphomimetic motif, $^{64}$RxEP$^{67}$, that closely resembles a canonical phospho-serine/threonine motif found in cellular proteins that interact with 14-3-3. By mutating this phosphomimetic motif, we generated a NS3 protein that is deficient in 14-3-3ε binding ($NS3_{KIKP}$) and therefore allows RIG-I to bind 14-3-3ε. While wild-type (WT) NS3 efficiently degraded RIG-I, $NS3_{KIKP}$ failed to do so, demonstrating that NS3-mediated degradation of RIG-I is dependent on its ability to inhibit RIG-I-14-3-3ε interaction (Figure 3.2A). Furthermore, infection of Huh7 cells with WT DV2 ($DV2_{WT}$) led to robust degradation of endogenous RIG-I, while $DV2_{KIKP}$, which encodes $NS3_{KIKP}$, did not degrade RIG-I. Instead, $DV2_{KIKP}$ infection induced RIG-I protein levels, which is consistent with $DV2_{KIKP}$ eliciting an augmented immune response (Figure 3.2B). In contrast, both $DV2_{WT}$ and $DV2_{KIKP}$ were able to induce STAT2 degradation (Figure 3.2B). These results indicate that $NS3_{KIKP}$ expression and $DV2_{KIKP}$ infection fail to induce RIG-I degradation, indicating that RIG-I degradation is a direct consequence of the NS3-mediated inhibition of RIG-I-14-3-3ε complex formation. These data reinforce the importance of 14-3-3ε targeting by NS3 for evasion of RIG-I-mediated immunity.

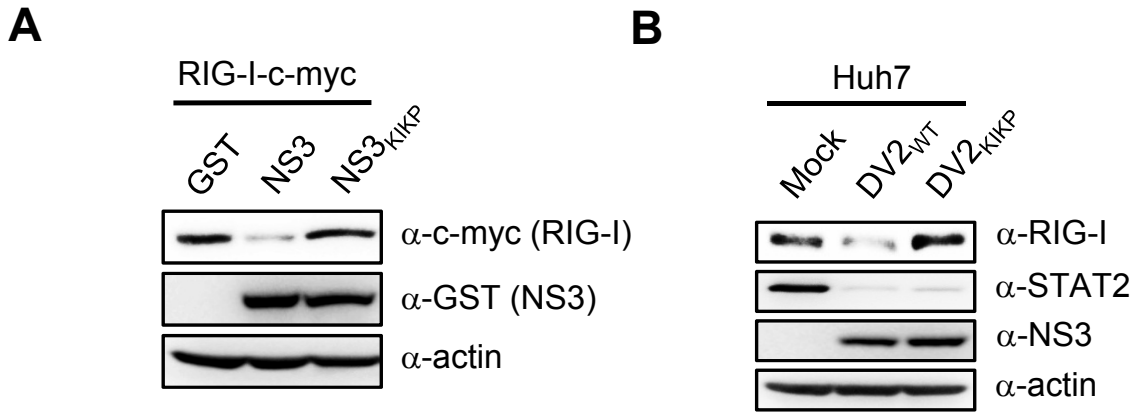


**Figure 3.2. $DV2_{KIKP}$ is deficient in RIG-I degradation. (A)** HEK293T cells were transfected with GST, GST-NS3 or GST-$NS3_{KIKP}$, together with RIG-I-c-myc. 48 h later, WCLs were analyzed by IB with anti-c-myc or anti-GST antibody. **(B)** Huh7 cells were infected with $DV2_{WT}$ (MOI 0.3) or $DV2_{KIKP}$ (MOI 1), resulting in ~75% infectivity for both as determined by intracellular prM staining (not shown). 48 h later, WCLs were analyzed by IB with anti-RIG-I, anti-STAT2 and anti-NS3 antibodies.

In this study, we uncover the lysosome-mediated degradation of RIG-I during DV infection, and found that NS3 is able to degrade specifically RIG-I, but not MDA5. Importantly, ectopic expression of $NS3_{KIKP}$ or infection with $DV2_{KIKP}$ does not induce RIG-I degradation, demonstrating that inhibition of RIG-I-14-3-3ε interaction is critical for RIG-I degradation. Together with our previous findings, our data indicate that NS3 binding to 14-3-3ε blocks RIG-I signaling via two distinct mechanisms. First, RIG-I is initially activated by TRIM25-mediated K63-linked ubiquitination upon DV infection, but is unable to bind 14-3-3ε to translocate to mitochondria for MAVS interaction and antiviral signaling. Second, during DV replication, K63-ubiquitin-activated RIG-I that fails to translocate to mitochondria is degraded in a lysosome-dependent manner, hence blocking antiviral signaling that may occur later during infection.

Among pathogenic viruses, there are several examples of viral proteins that bind and sequester RIG-I from signaling, or cleave and inactivate RIG-I [9-13]. In contrast, DV targets 14-3-3ε, the trafficking molecule required for RIG-I translocation to mitochondria. We propose that by binding 14-3-3ε, NS3 is able to indirectly sequester initially activated RIG-I from mitochondrial MAVS, which subsequently leads to host-mediated degradation of RIG-I via lysosomes. While the molecular mechanism of RIG-I degradation by DV NS3 is unique, the outcome is fundamentally akin to the direct sequestration *and* cleavage of RIG-I shown for other viral pathogens.

We do not fully understand how RIG-I is targeted for lysosome-mediated degradation. One possibility is that after sensing DV RNA, K63-ubiquitinated RIG-I that fails to translocate is somehow destined for degradation in lysosomes. In support of this, K63-linked ubiquitination of some membrane proteins is known to target them for endocytosis and lysosome-mediated degradation [14-16]. Furthermore, DV is known to induce autophagy to promote its replication

[17] Therefore, it is also possible that activated RIG-I tetramers that fail to translocate to mitochondria may be engulfed in autophagosomes that eventually fuse with lysosomes. In support of this, key autophagy molecules atg5 and atg12 are known to interact with RIG-I via its CARDs to downregulate activation [18]. These two possibilities are not mutually exclusive, as K63-linked ubiquitination has also been implicated in autophagy [19,20]. Future work is required to determine the mechanistic details of RIG-I degradation during DV infection, which may also shed light on mechanisms of homeostatic regulation of RIG-I in the cell.

We have previously described how NS3 antagonizes RIG-I translocation to mitochondria by binding to 14-3-3ε. Here, we further show that NS3 mediates lysosomal degradation of RIG-I during DV infection. Our work highlights the importance of viral targeting of 14-3-3ε for immune evasion, which may have implications for vaccine and antiviral design.

## MATERIALS AND METHODS

### Cell Culture and Viruses

HEK293T and Huh7 cells were cultured in Dulbecco's Modified Eagle's Medium (DMEM) supplemented with 10% fetal bovine serum (FBS), 10 mM HEPES and 1% penicillin-streptomycin (Gibco). DV2 New Guinea C (NGC) was propagated in C6/36 cells. SeV (Cantell) was purchased from Charles River Laboratories.

### Plasmids and Transfections

GST-NS3 and GST-NS5 were generated by subcloning NS3 or NS5 of DV2 (strain NGC) into pEBG vector between BamHI and ClaI. Plasmids encoding RIG-I-c-myc, RIG-I-FLAG and FLAG-MDA5 have been described previously [21,22]. Transfections were performed using the calcium phosphate method, or with TurboFectin 8.0 (Origene), Lipofectamine and Plus reagent, or Lipofectamine 2000 (all Life Technologies) according to the manufacturer's instructions.

### Antibodies and Reagents

For western blot analysis, the following antibodies were used: anti-FLAG (M2, Sigma), anti-GST (Sigma), anti-c-myc (9E10), anti-β-actin (Abcam), anti-RIG-I (Alme-1, Adipogen), anti-STAT2 (Santa Cruz), anti-14-3-3ε (8C3, Santa Cruz), anti-NS3 (GT2811, Genetex). MG132, ammonium chloride and chloroquine diphosphate were purchased from Sigma.

### Immunoblot Analysis

HEK293T or Huh7 cells were lysed in NP-40 buffer (50 mM HEPES pH 7.4, 150 nM NaCl, 1% [vol/vol] NP-40, protease inhibitor cocktail [Sigma]) and centrifuged at 13,000 rpm for 20 min. Western blot analyses were performed as previously described [21,23].

**Confocal Microscopy**

Huh7 cells were grown on chamber slides or on cover slips in 24-well plates, and then infected with DV2 at indicated titers, or mock infected. Cells were harvested at indicated time points and fixed with 4% (w/v) paraformaldehyde for 20 min, permeabilized with 0.2% (v/v) Triton-X-100 in PBS, and blocked with 10% (v/v) goat serum or FBS in PBS for 1 h. For immunostaining, anti-LAMP1 (Abcam) and anti-FLAG (Sigma) were used, followed by incubation with secondary antibodies conjugated to Alexa Fluor 488 or Alexa Fluor 594 (Life Technologies). Cells were mounted in DAPI-containing Vectashield (Vector Labs) to co-stain nuclei. All laser scanning images were acquired on an Olympus IX8I confocal microscope.

## REFERENCES


1. Clyde K, Kyle JL, Harris E (2006) Recent advances in deciphering viral and host determinants of dengue virus replication and pathogenesis. J Virol 80: 11418-11431.

2. Ashour J, Laurent-Rolle M, Shi PY, Garcia-Sastre A (2009) NS5 of dengue virus mediates STAT2 binding and degradation. J Virol 83: 5408-5418.

3. Rodriguez-Madoz JR, Belicha-Villanueva A, Bernal-Rubio D, Ashour J, Ayllon J, et al. (2010) Inhibition of the type I interferon response in human dendritic cells by dengue virus infection requires a catalytically active NS2B3 complex. J Virol 84: 9760-9774.

4. Aguirre S, Maestre AM, Pagni S, Patel JR, Savage T, et al. (2012) DENV inhibits type I IFN production in infected cells by cleaving human STING. PLoS Pathog 8: e1002934.

5. Yu CY, Chang TH, Liang JJ, Chiang RL, Lee YL, et al. (2012) Dengue virus targets the adaptor protein MITA to subvert host innate immunity. PLoS Pathog 8: e1002780.

6. Anglero-Rodriguez YI, Pantoja P, Sariol CA (2014) Dengue virus subverts the interferon induction pathway via NS2B/3 protease-IkappaB kinase epsilon interaction. Clin Vaccine Immunol 21: 29-38.

7. Chan YK, Gack MU (2015) RIG-I-like receptor regulation in virus infection and immunity. Curr Opin Virol 12C: 7-14.

8. Goswami R, Majumdar T, Dhar J, Chattopadhyay S, Bandyopadhyay SK, et al. (2013) Viral degradasome hijacks mitochondria to suppress innate immunity. Cell Res 23: 1025-1042.

9. Siu KL, Kok KH, Ng MH, Poon VK, Yuen KY, et al. (2009) Severe acute respiratory syndrome coronavirus M protein inhibits type I interferon production by impeding the formation of TRAF3.TANK.TBK1/IKKepsilon complex. J Biol Chem 284: 16202-16209.

10. Fan L, Briese T, Lipkin WI (2010) Z proteins of New World arenaviruses bind RIG-I and interfere with type I interferon induction. J Virol 84: 1785-1791.

11. Bao X, Kolli D, Ren J, Liu T, Garofalo RP, et al. (2013) Human metapneumovirus glycoprotein G disrupts mitochondrial signaling in airway epithelial cells. PLoS One 8: e62568.

12. Bao X, Liu T, Shan Y, Li K, Garofalo RP, et al. (2008) Human metapneumovirus glycoprotein G inhibits innate immune responses. PLoS Pathog 4: e1000077.

13. Barral PM, Sarkar D, Fisher PB, Racaniello VR (2009) RIG-I is cleaved during picornavirus infection. Virology 391: 171-176.

14. Barriere H, Nemes C, Lechardeur D, Khan-Mohammad M, Fruh K, et al. (2006) Molecular

basis of oligoubiquitin-dependent internalization of membrane proteins in Mammalian cells. Traffic 7: 282-297.

15. Lauwers E, Jacob C, Andre B (2009) K63-linked ubiquitin chains as a specific signal for protein sorting into the multivesicular body pathway. J Cell Biol 185: 493-502.

16. Huang F, Zeng X, Kim W, Balasubramani M, Fortian A, et al. (2013) Lysine 63-linked polyubiquitination is required for EGF receptor degradation. Proc Natl Acad Sci U S A 110: 15722-15727.

17. Lee YR, Lei HY, Liu MT, Wang JR, Chen SH, et al. (2008) Autophagic machinery activated by dengue virus enhances virus replication. Virology 374: 240-248.

18. Jounai N, Takeshita F, Kobiyama K, Sawano A, Miyawaki A, et al. (2007) The Atg5 Atg12 conjugate associates with innate antiviral immune responses. Proc Natl Acad Sci U S A 104: 14050-14055.

19. Olzmann JA, Chin LS (2008) Parkin-mediated K63-linked polyubiquitination: a signal for targeting misfolded proteins to the aggresome-autophagy pathway. Autophagy 4: 85-87.

20. Shi CS, Kehrl JH (2010) TRAF6 and A20 regulate lysine 63-linked ubiquitination of Beclin-1 to control TLR4-induced autophagy. Sci Signal 3: ra42.

21. Gack MU, Shin YC, Joo CH, Urano T, Liang C, et al. (2007) TRIM25 RING-finger E3 ubiquitin ligase is essential for RIG-I-mediated antiviral activity. Nature 446: 916-920.

22. Wies E, Wang MK, Maharaj NP, Chen K, Zhou S, et al. (2013) Dephosphorylation of the RNA sensors RIG-I and MDA5 by the phosphatase PP1 is essential for innate immune signaling. Immunity 38: 437-449.

23. Chan YK, Huang IC, Farzan M (2012) IFITM proteins restrict antibody-dependent enhancement of dengue virus infection. PLoS One 7: e34508.

# Chapter 4

## IFITM Proteins Restrict Antibody-Dependent Enhancement of Dengue Virus Infection

Ying Kai Chan, I-Chueh Huang, Michael Farzan

New England Primate Research Center, Department of Microbiology and Immunobiology, Harvard Medical School, Southborough, MA, USA

Originally published as:

Chan YK, Huang I-C, Farzan M (2012) IFITM Proteins Restrict Antibody-Dependent Enhancement of Dengue Virus Infection. PLoS ONE 7(3): e34508. doi:10.1371/journal.pone.0034508

**ABSTRACT**

Interferon-inducible transmembrane (IFITM) proteins restrict the entry processes of several pathogenic viruses, including the flaviviruses West Nile virus and dengue virus (DENV). DENV infects cells directly or via antibody-dependent enhancement (ADE) in Fc-receptor-bearing cells, a process thought to contribute to severe disease in a secondary infection. Here we investigated whether ADE-mediated DENV infection bypasses IFITM-mediated restriction or whether IFITM proteins can be protective in a secondary infection. We observed that IFITM proteins restricted ADE-mediated and direct infection with comparable efficiencies in a myelogenous leukemia cell line. Our data suggest that IFITM proteins can contribute to control of secondary DENV infections.

**INTRODUCTION**

The four serotypes of dengue virus (DENV1–4) are responsible for approximately 50 to 100 million infections annually, and 2.5 billion people are at risk of infection, making DENV the most widespread arboviral disease [1,2]. Most symptomatic DENV infections present as a debilitating, febrile disease known as dengue fever (DF), but serious cases can progress to dengue hemorrhagic fever (DHF) and dengue shock syndrome (DSS). These can be fatal if patients do not receive fluid replacement. Currently, there are no approved therapies for DENV infections.

Clinical and autopsy studies indicate that cells of the mononuclear phagocyte lineage, including monocytes/macrophages and dendritic cells, are primary targets of DENV in vivo [3]. In addition, epidemiological studies show that DHF/DSS often occurs in patients with secondary

heterotypic DENV infections or in infants with maternally transferred dengue immunity [4,5]. Antibody-dependent enhancement (ADE) is thought to be a major contributor to severe disease following secondary infection [4]. In a secondary infection with a heterologous serotype, the virus forms immune complexes with pre-existing sub-neutralizing antibodies and bind to Fc-receptor-bearing cells, leading to increased infection and viral replication [5]. The cell biology of ADE is not fully understood, but some proposed mechanisms include: increased virus attachment to the cell surface, increased efficiency in post-attachment steps due to Fc-receptor-mediated signaling, delivery of antibody-virus complexes to more favorable locations in the endocytic compartment, and direct alterations in the fusion process (reviewed in [6,7]).

We have recently shown that interferon-inducible transmembrane (IFITM) proteins restrict replication of multiple viruses, including influenza A (IAV), SARS coronavirus, filoviruses (Ebola and Marburg viruses) and flaviviruses (including dengue and West Nile viruses), whereas vesicular stomatitis virus is less efficiently restricted [8,9]. Other groups have also demonstrated that IFITM proteins restrict HIV-1 [10,11]. In addition, IFITM-mediated restriction of flaviviruses has been confirmed in two subsequent studies [11,12]. The IFITM proteins are relatively small (~130 amino acids) and share a common topology, with two conserved transmembrane domains, a short highly conserved cytoplasmic region, and luminal amino- and carboxy-termini [13]. In humans, IFITM1, 2, and 3 are expressed in a wide range of tissues, while IFITM5 expression is limited to bone [14]. As their names suggest, IFITM proteins are strongly upregulated by type I and II interferons [8,9,15], and most cells express basal levels of one or more of these proteins [16]. Currently, IFITM proteins are the only known mediators of innate immunity that inhibit viral infection by blocking viral entry [17].

We have demonstrated that IFITM1, 2, and 3 restrict entry mediated by IAV, SARS

coronavirus and filovirus entry proteins *in vitro*, and abrogate infection by three flavivirus virus-like particles (VLPs), suggesting that IFITM proteins also restrict flavivirus infections by blocking virus entry [8]. In agreement with this, Jiang et al. [12] have shown that IFITM proteins restrict infection by flavivirus VLPs, but do not inhibit replication of flavivirus replicons. In contrast, IFITMs do not inhibit the entry processes of amphotropic mouse leukemia virus (MLV), Machupo virus (MACV), Lassa virus (LASV) or lymphocytic choriomeningitis virus (LCMV) [8].

Currently it is not clear what distinguishes the entry mechanisms of IFITM-restricted and IFITM-insensitive viruses or how IFITM proteins suppress viral entry. In addition, IFITM-mediated restriction can be bypassed by inducing viral fusion at the plasma membrane, suggesting that the site or mechanism of viral entry can affect the sensitivity to IFITM-mediated restriction [9]. Given the potential importance of ADE to severe dengue disease and the lack of full understanding of the biology of ADE, an attractive hypothesis is that, unlike direct DENV infection, ADE-mediated DENV infection bypasses IFITM-mediated restriction, thereby increasing viral replication and disease severity in a secondary infection.

In this study, we sought to determine if ADE could bypass IFITM-mediated restriction, or, alternatively, if IFITM proteins could contribute to the control of DENV in secondary infections as well. Previous studies of IFITM-mediated restriction of flaviviruses used cell lines lacking Fc receptors [8,11,12]. Here, we infected human myelogenous leukemia K562 cells, which bear FcγRIIa, with DENV (direct infection) or antibody-opsonized DENV (ADE-mediated infection). We show that IFITM proteins are able to restrict both direct and ADE-mediated infection, and that both infection modes appear equally sensitive to IFITM-mediated restriction.

## RESULTS AND DISCUSSION

### IFITM proteins restrict both direct and ADE-mediated DENV infection of K562 cells

We first investigated the basal and interferon-induced expression of IFITM proteins in K562 cells, using an antibody that recognizes IFITM1 alone, or one that recognizes both IFITM2 and IFITM3 [8,9]. Western blot analysis showed that resting K562 cells express a basal level of IFITM1 and IFITM2 and/or 3, and that treatment with human IFN-α for 48 h strongly upregulated expression of both IFITM1 and IFITM2/3 (Figure 4.1A).

To study the restriction activity of each IFITM protein, we transduced K562 cells to stably express myc-tagged IFITM1, 2 or 3, or with vector alone, and selected transduced cells with puromycin. Western blot analysis using an antibody against c-myc showed robust expression of each IFITM protein (Figure 4.1B). To verify their activities, we infected transduced cells with viral pseudoparticles that contain an MLV genome encoding the enhanced green fluorescence protein (EGFP), and pseudotyped with entry proteins of IAV (A/Thailand/2(SP-33)/2004 (H5N1)) or MACV [18,19]. Pseudovirus infection was measured two days later by flow cytometry. As expected, overexpression of IFITM1, 2 or 3 potently restricted infection by MLV-EGFP virus pseudotyped with IAV but not MACV entry proteins (Figure 4.1C).

We next infected these cells with infectious DENV2 New Guinea C strain (NGC) propagated in mosquito C6/36 cells. DENV2 was incubated in media alone, or with enhancing titers of monoclonal antibodies against dengue prM or envelope (E). We used two commercially available antibodies, 2H2 and 4G2, which bind dengue virus structural proteins prM and E respectively. Anti-prM antibodies opsonize virions that are not fully mature while antibodies

against E can opsonize most virions (reviewed in [20]). As previously described [21], dengue virions were incubated with each antibody or with media alone, and subsequently incubated with K562 cells. Previous studies have shown that intracellular staining of DENV antigen less than 43 h post-infection of K562 cells indicates a single round of infection [22]. Accordingly, to evaluate viral entry, we assessed productive infection by intracellular prM-staining 24 h post-infection [23]. As expected, with direct (antibody-independent) infection at a multiplicity of infection (MOI) 1, expression of IFITM1, 2, or 3 potently inhibited infection by ~80% when compared to vector-transduced cells. With ADE-mediated infection at MOI 1, baseline infectivity increased roughly three-fold indicating successful ADE, but expression of IFITM1, 2 or 3 continued to potently inhibit infection by ~70–90% (n = 3 or 4 per condition; $p<0.05$). Similarly, at MOI 10, we observed less efficient restriction, but comparable restriction levels in direct and ADE-mediated infection (Figure 4.1D). Consistent with our previous studies, IFITM2 restricted DENV infection less efficiently than either IFITM1 or IFITM3 [8]. We further quantified viral loads in the supernatant by standard plaque assays with BHK cells [21]. Again, overexpression of IFITM1 or IFITM3 effectively restricted ADE-mediated infection, and suppressed viral production by more than 10-fold (Figure 4.1E; n = 3; $p<0.05$). Finally, we verified the generality of our observations by confirming them in J774A.1 murine macrophages [24] stably expressing murine orthologs of IFITM1, 2 or 3 (Figure 4.1F; n = 4; asterisks indicate $p<0.05$). We conclude that IFITM1, 2 or 3 can restrict ADE-mediated DENV infection of K562 cells.

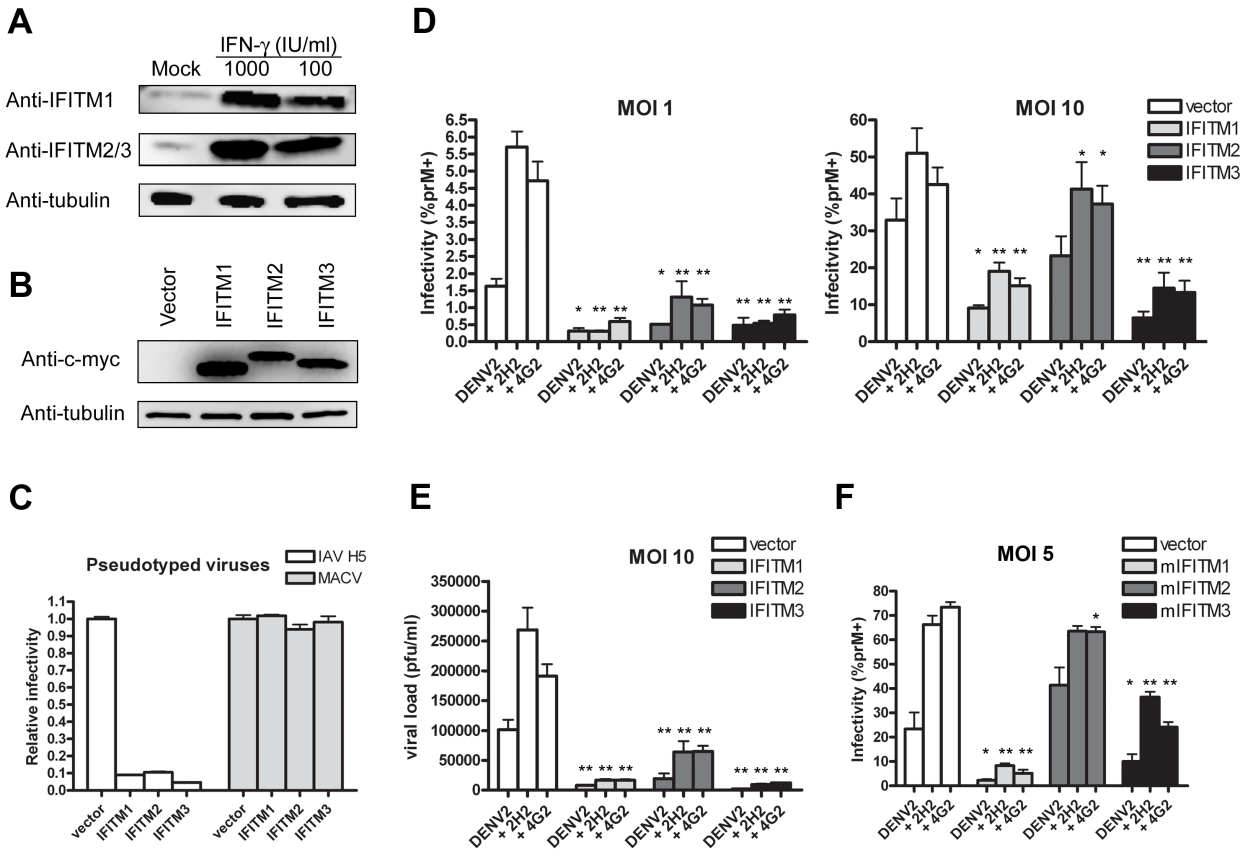


**Figure 4.1. IFITM proteins restrict both direct and ADE-mediated DENV infection of K562 cells.** **(A)** K562 cells were treated with the indicated concentrations of human interferon-α or mock treated, and lysed for Western blot analysis 48 h later, using an antibody that recognizes IFITM1 alone, or one that recognizes both IFITM2 and IFITM3. **(B)** K562 cells were stably transduced to express human IFITM1, 2, or 3 or with the control vector pQCXIP. IFITM protein expression was measured by Western blot using an anti-c-myc antibody. **(C)** Stably transduced K562 cells characterized in panel B were infected with an MLV-based retrovirus expressing EGFP and pseudotyped with MACV or IAV H5 entry proteins, as previously described [9]. Infection was determined by flow cytometry, and normalized to K562 cells transduced with vector alone. **(D)** K562 cells characterized in panel B were infected with infectious DENV2 NGC strain (labeled ‘‘DENV2’’ for virus only) at the indicated MOI, or the same amount of infectious DENV2 pre-opsonized with enhancing titers of antibodies against DENV structural proteins prM or E (‘‘+2H2’’ and ‘‘+4G2’’ respectively) [8,21]. Cells were washed after 1.5 h and incubated for ~24 h. Intracellular staining of DENV antigen was performed with a DyLight-649-conjugated antibody against prM and infection was determined by flow cytometry. Experiment is representative of three with similar results. **(E)** An experiment similar to that shown in panel D was performed except that infection was assayed by measuring viral loads in the supernatant by plaque assays using BHK cells. **(F)** An experiment similar to that in panel D was performed, except that J774A.1 murine macrophage cells were stably transduced to express murine orthologs of IFITM1, 2, or 3 or with the control vector pQCXIP. Stably transduced cells were infected with infectious DENV2 NGC strain at ~MOI 5 and incubated for ~2 days before harvesting for flow cytometry. Error bars indicate standard error. Single and double asterisks indicate statistically significant ($p<0.05$ and $p<0.005$, respectively) differences between IFITM protein expressing and control cells for corresponding infection conditions.

**Endogenous IFITM1 restricts both direct and ADE-mediated DENV infection of K562 cells**

We subsequently investigated whether endogenous IFITM proteins contributed to DENV restriction. We stably transduced K562 cells to express previously characterized shRNAs against IFITM1, 2, or 3 [8,9], or with a control non-targeting shRNA (scrambled), and selected transduced cells with puromycin. IFITM1 expression was nearly undetectable in cells expressing shRNA targeting IFITM1, whereas IFITM2 and 3 levels were unaffected. shRNA targeting IFITM2 reduced IFITM2/3 expression slightly, while shRNA targeting IFITM3 substantially reduced IFITM2/3 expression (Figure 4.2A). As we have previously observed [9], IFITM1 depletion increased infection by IAV pseudoviruses by almost 2-fold, whereas little or no increase in infection was observed with shRNA targeting IFITM2 or IFITM3 (Figure 4.2B). Similarly, with DENV2 infection at MOI 1, knockdown of IFITM1 roughly doubled infection rates with both direct and ADE-mediated infections (Figure 4.2C; $n = 3$ or 4; $p<0.05$). This increase was less pronounced at a higher MOI of 10, but remained statistically significant. These data show that endogenous IFITM1 in K562 cells restricts ADE-mediated DENV infection.

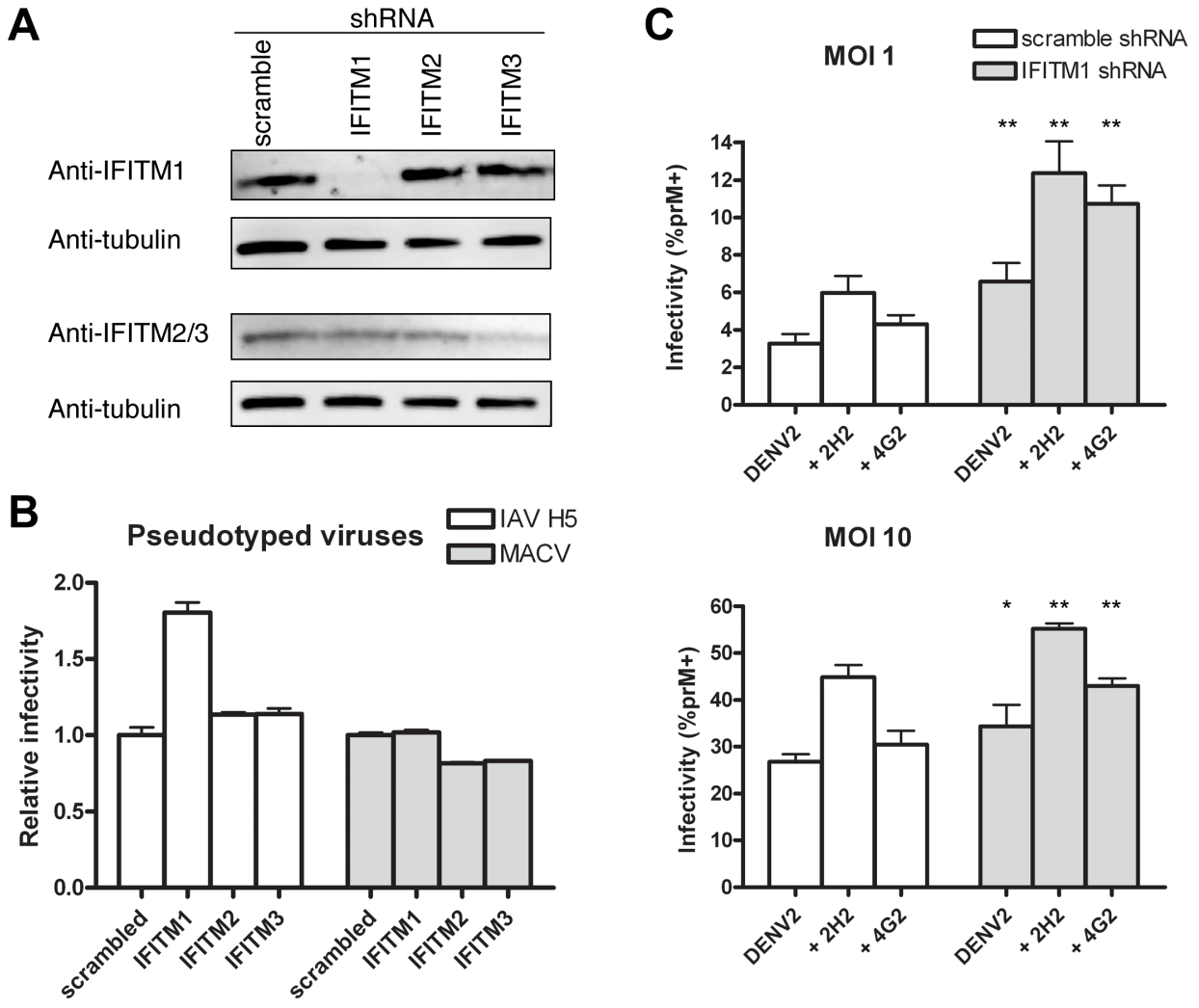


**Figure 4.2. Endogenous IFITM1 restricts both direct and ADE-mediated DENV infection of K562 cells. (A)** K562 cells were stably transduced to express shRNA targeting IFITM1, 2, or 3 or non-targeting control shRNA (scrambled). IFITM protein expression was measured by Western blot, as in Figure 4.1A. **(B)** shRNA-transduced K562 cells characterized in panel A were infected with the indicated pseudoviruses as described in Figure 4.1C. **(C)** shRNA-transduced K562 cells characterized in panel A were infected with infectious DENV2 NGC strain as described in Figure 4.1D. Error bars indicate standard error. Single and double asterisks indicate statistically significant ($p<0.05$ and $p<0.005$, respectively) differences between cells expressing IFITM1 and control shRNA for corresponding infection conditions. Experiment is representative of three with similar results.

**IFITM proteins restrict direct and ADE-mediated infection with similar efficiencies**

Figures 4.1 and 4.2 show that ADE cannot bypass IFITM-mediated restriction, but leave open the possibility that ADE-mediated infection is quantitatively less sensitive to restriction than direct infection. To determine if IFITM proteins restrict ADE-mediated infection to the same extent as direct infection, we identified in pilot studies virus titers for direct and ADE-mediated infection that resulted in comparable infectivity, and used these titers to investigate the effect of IFITM overexpression or IFITM1 depletion as in Figures 4.1D and 4.2C. When IFITM1, 2 or 3 were over-expressed in K562 cells under these conditions, nearly identical restriction was observed in direct and ADE-mediated infection (Figure 4.3A). Similarly when IFITM1 was depleted in the same cells, a comparable increase in infection was observed (Figure 4.3B). We conclude that IFITM proteins restrict ADE- mediated infection and direct infection with similar efficiencies.

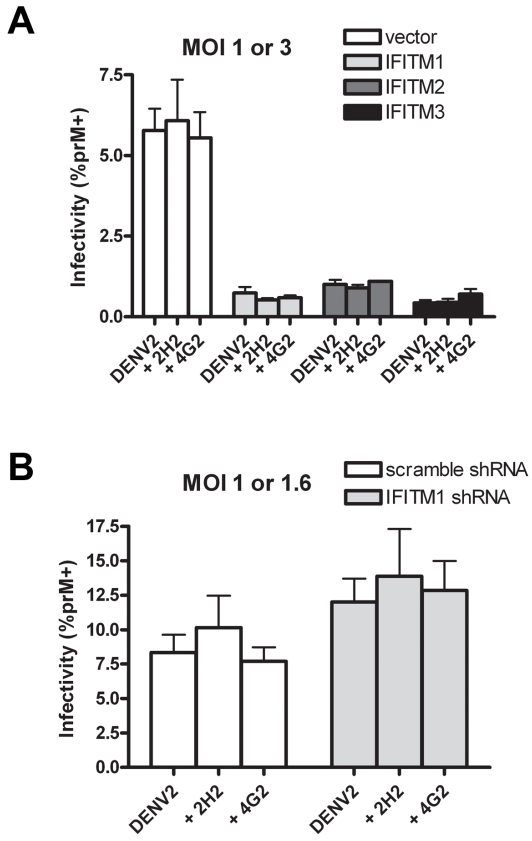


**Figure 4.3. IFITM proteins restrict direct and ADE-mediated infection with similar efficiencies. (A)** K562 cells stably transduced to express human IFITM1, 2, or 3 or with control vector were infected as in Figure 4.1D, except that an MOI of 3.0 was used for non-opsonized DENV, and an MOI of 1.0 was used for DENV pre-opsonized with the antibodies 2H2 or 4G2. Different MOIs were used to achieve comparable infection levels between direct and ADE-mediated infection. **(B)** K562 cells stably transduced to express control shRNA or shRNA targeting IFITM1 were infected as described in Figure 4.2C, except that an MOI of 1.6 was used for non-opsonized DENV, and an MOI of 1.0 was used for DENV pre-opsonized with the indicated antibodies. Standard error bars are shown. For each transduction condition, differences between direct infection and ADE-mediated infection were not statistically significant.

We have previously shown that IFITM-mediated restriction depends on the site or mechanism of viral entry [9]. This finding raised a key question: can ADE facilitate bypass of this restriction, or, instead, can IFITM proteins contribute to control of a secondary infection, including those resulting in DHF/DSS? Our data show clearly that in a human myelogenous leukemia cell line widely used in the study of ADE [22,25,26], IFITM proteins restrict ADE-mediated infection as efficiently as direct infection. Therefore, we find no evidence supporting the hypothesis that ADE-mediated DENV infection bypasses or is less sensitive to IFITM-mediated restriction. It is formally possible that differences in cell types, antibody properties, or viral strains could alter the sensitivity of ADE-mediated infection to IFITM restriction. However we show that our observations are consistent across two different cell lines from two species expressing their respective IFITM orthologs. In addition, it has been suggested that patients with DHF exhibit lower IFN-α levels than patients with DF (reviewed in [27]), which may lead to reduced IFITM-induction. *In vivo* studies may be necessary to clarify these possibilities. Nonetheless, our observation suggests that therapeutic strategies that specifically induce IFITM activity could control both primary and secondary dengue virus infections.

To date, the mechanisms of IFITM-mediated restriction remain elusive. We have previously demonstrated that IFITM proteins do not interfere with virion access to acidic cellular compartments [9]. Furthermore, inducing viral fusion at the plasma membrane bypasses IFITM-mediated restriction [9], supporting a mechanism which operates within the endocytic pathway. Our work in this study shows that IFITM proteins restrict ADE-mediated DENV infection as efficiently as direct infection, but does not distinguish between the possible mechanisms of ADE, including alterations in viral attachment, endocytosis and/or fusion. However, the similar sensitivity of direct and ADE-mediated infection to IFITM restriction indicates that these

infection modes share common features that render them both sensitive to IFITM proteins.

## MATERIALS AND METHODS

### Cells and plasmids

Human embryonic kidney 293T cells and murine macrophage J774A.1 cells were grown in Dulbecco's minimal essential medium (DMEM; Invitrogen) and human myelogenous leukemia K562 cells were grown in Roswell Park Memorial Institute (RPMI) 1640 medium (Invitrogen). Media were supplemented with 10% fetal bovine serum, 100 U/ml penicillin and 100 mg/ml streptomycin. Human interferon-α (NR-3077) was obtained from NIH Biodefense and Emerging Infectious Research Resources Depository, NIAID, NIH and used to stimulate K562 cells at indicated concentrations in growth media for 48 h. Plasmids encoding c-myc-tagged IFITM proteins in pQCXIP vector and plasmids encoding control shRNA or shRNA targeting IFITMs in pRS vector have been described [9]. Transduced K562 or J774A.1 cells were selected by supplementing media with 3 or 4 mg/ml puromycin(Invitrogen), respectively.

### Western blots

Cells were lysed with 1% NP-40 (Thermo Scientific) and Western blot analysis was performed as previously described [9]. C-myc-tagged IFITM proteins were detected by a murine monoclonal anti-c-myc antibody (9E10, Santa Cruz Biotechnology). Endogenous IFITM protein expression was detected by polyclonal rabbit anti-IFITM1 (FL-125, Santa Cruz Biotechnology) or rabbit anti-IFITM2 (12769-1-AP, Proteintech Group, cross reacts with IFITM3 protein). Anti-tubulin antibodies (Sigma) were used as a loading control.

**Pseudotyped murine leukemia viruses (MLVs) for transduction and infection assays**

Viral entry proteins, plasmids and procedures for generating pseudotyped MLV-EGFP have been described [9]. Entry proteins used are IAV HA proteins from A/Thailand/2(SP-33)/2004(H5N1) and glycoprotein (GP) from Machupo virus Carvallo. Similarly, transduction of K562 or J774A.1 cells and MLV-EGFP pseudovirus infection procedures have been described [9]. Relative infectivity was calculated by normalizing against infectivity in control cells.

**Infectious DENV infections**

DENV2 New Guinea C strain (NGC) was propagated in *Aedes albopictus* C6/36 cells, clarified by centrifugation and stored at -80°C. Virus titers were measured by standard plaque assays on BHK cells [21]. Direct and ADE-mediated infections were performed based on a published protocol with minor modifications [21]. Murine 2H2 and 4G2 antibodies were purchased from Millipore. Briefly, DENV2 was incubated in RPMI containing 2% FBS with or without enhancing titers of 2H2 (20 ng for MOI 1 and 200 ng for MOI 10) or 4G2 antibodies (~20 ng for both MOI 1 and 10) in a total volume of 250 μl for 30 min at 37°C. $2x10^5$ K562 cells in a similar volume of media in 24-well plates were then infected similarly to pseudovirus infection procedures. After incubation for 1.5 h at 37°C, cells were then washed in DPBS and incubated for ~24 h before harvesting cells for flow cytometry or supernatant for plaque assay. Cells were assayed for productive infection by intracellular prM staining [23] and analyzed by flow cytometry. The supernatant was clarified by centrifugation, frozen at -80°C, before plaque assays were performed with BHK cells. The infection protocol was slightly modified for adherent J774A.1 cells. $2x10^5$ cells were seeded overnight in 12-well plates and infected with a similar total volume (500 μl) of virus or virus-antibody complex in DMEM containing 2% FBS the next

day. After infection and washing, cells were incubated for ~2 days before harvesting for flow cytometry. Enhancing titers of 2H2 were based on a previous study [21] while enhancing titers of 4G2 were empirically determined in a pilot experiment using serial 10-fold dilutions of the antibody complexed with DENV2 at MOI 1 or MOI 10. The dilution that gave the best enhancement in infection of K562 cells was subsequently used in all experiments. All statistical analysis was performed using a one-tailed Student's t test. $P<0.05$ was considered statistically significant.

## REFERENCES


1. Gubler DJ (1998) Dengue and dengue hemorrhagic fever. Clin Microbiol Rev 11: 480-496.

2. Halstead SB (2007) Dengue. Lancet 370: 1644-1652.

3. Jessie K, Fong MY, Devi S, Lam SK, Wong KT (2004) Localization of dengue virus in naturally infected human tissues, by immunohistochemistry and in situ hybridization. J Infect Dis 189: 1411-1418.

4. Halstead SB (1970) Observations related to pathogensis of dengue hemorrhagic fever. VI. Hypotheses and discussion. Yale J Biol Med 42: 350-362.

5. Kliks SC, Nimmanitya S, Nisalak A, Burke DS (1988) Evidence that maternal dengue antibodies are important in the development of dengue hemorrhagic fever in infants. Am J Trop Med Hyg 38: 411-419.

6. Pierson TC, Diamond MS (2008) Molecular mechanisms of antibody-mediated neutralisation of flavivirus infection. Expert Rev Mol Med 10: e12.

7. Dowd KA, Pierson TC (2011) Antibody-mediated neutralization of flaviviruses: a reductionist view. Virology 411: 306-315.

8. Brass AL, Huang IC, Benita Y, John SP, Krishnan MN, et al. (2009) The IFITM proteins mediate cellular resistance to influenza A H1N1 virus, West Nile virus, and dengue virus. Cell 139: 1243-1254.

9. Huang IC, Bailey CC, Weyer JL, Radoshitzky SR, Becker MM, et al. (2011) Distinct patterns of IFITM-mediated restriction of filoviruses, SARS coronavirus, and influenza A virus. PLoS Pathog 7: e1001258.

10. Lu J, Pan Q, Rong L, He W, Liu SL, et al. (2011) The IFITM proteins inhibit HIV-1 infection. J Virol 85: 2126-2137.

11. Schoggins JW, Wilson SJ, Panis M, Murphy MY, Jones CT, et al. (2011) A diverse range of gene products are effectors of the type I interferon antiviral response. Nature 472: 481-485.

12. Jiang D, Weidner JM, Qing M, Pan XB, Guo H, et al. (2010) Identification of five interferon-induced cellular proteins that inhibit west nile virus and dengue virus infections. J Virol 84: 8332-8341.

13. Lewin AR, Reid LE, McMahon M, Stark GR, Kerr IM (1991) Molecular analysis of a human interferon-inducible gene family. Eur J Biochem 199: 417-423.

14. Moffatt P, Gaumond MH, Salois P, Sellin K, Bessette MC, et al. (2008) Bril: a novel bone-

specific modulator of mineralization. J Bone Miner Res 23: 1497-1508.

15. Samuel CE (2001) Antiviral actions of interferons. Clin Microbiol Rev 14: 778-809, table of contents.

16. Friedman RL, Manly SP, McMahon M, Kerr IM, Stark GR (1984) Transcriptional and posttranscriptional regulation of interferon-induced gene expression in human cells. Cell 38: 745-755.

17. Liu SY, Sanchez DJ, Cheng G (2011) New developments in the induction and antiviral effectors of type I interferon. Curr Opin Immunol 23: 57-64.

18. Huang IC, Bosch BJ, Li F, Li W, Lee KH, et al. (2006) SARS coronavirus, but not human coronavirus NL63, utilizes cathepsin L to infect ACE2-expressing cells. J Biol Chem 281: 3198-3203.

19. Huang IC, Li W, Sui J, Marasco W, Choe H, et al. (2008) Influenza A virus neuraminidase limits viral superinfection. J Virol 82: 4834-4843.

20. Rodenhuis-Zybert IA, Wilschut J, Smit JM (2011) Partial maturation: an immune-evasion strategy of dengue virus? Trends Microbiol 19: 248-254.

21. Diamond MS, Edgil D, Roberts TG, Lu B, Harris E (2000) Infection of human cells by dengue virus is modulated by different cell types and viral strains. J Virol 74: 7814-7823.

22. Rodenhuis-Zybert IA, van der Schaar HM, da Silva Voorham JM, van der Ende-Metselaar H, Lei HY, et al. (2010) Immature dengue virus: a veiled pathogen? PLoS Pathog 6: e1000718.

23. Tassaneetrithep B, Burgess TH, Granelli-Piperno A, Trumpfheller C, Finke J, et al. (2003) DC-SIGN (CD209) mediates dengue virus infection of human dendritic cells. J Exp Med 197: 823-829.

24. Moreno-Altamirano MM, Sanchez-Garcia FJ, Legorreta-Herrera M, Aguilar-Carmona I (2007) Susceptibility of mouse macrophage J774 to dengue virus infection. Intervirology 50: 237-239.

25. Guy B, Chanthavanich P, Gimenez S, Sirivichayakul C, Sabchareon A, et al. (2004) Evaluation by flow cytometry of antibody-dependent enhancement (ADE) of dengue infection by sera from Thai children immunized with a live-attenuated tetravalent dengue vaccine. Vaccine 22: 3563-3574.

26. Littaua R, Kurane I, Ennis FA (1990) Human IgG Fc receptor II mediates antibody-dependent enhancement of dengue virus infection. J Immunol 144: 3183-3186.

27. Ubol S, Halstead SB (2010) How innate immune mechanisms contribute to antibody-

enhanced viral infections. Clin Vaccine Immunol 17: 1829-1835.

# Chapter 5

## Concluding Remarks

## OVERVIEW

Research on dengue virus (DV) and its interplay with the host immune response has made remarkable advances in recent years. While work from the past few decades has largely focused on mechanisms of severe dengue disease during secondary infections, the discovery of pattern recognition receptors (PRRs) and pathogen-associated molecular patterns (PAMPs) has launched a new exciting field of dengue and innate immunity. An emerging consensus is that, while innate immune sensors are typically effective at detecting viral pathogens and triggering robust immune responses, DV has evolved to potently evade or subvert most of these responses. DV escapes immune detection by concealing double-stranded RNA in intracellular membrane structures [1]. Furthermore, it actively antagonizes type I IFN induction and type I IFN-receptor (IFNAR) signaling by targeting 14-3-3ε, STING, STAT1, STAT2 and RNA-binding proteins (Chapters 2 and 3, and reviewed in [2-5]). In addition, DV inhibits formation of antiviral stress granules (SGs), subverts autophagy for its replication, elicits the unfolded protein responses (UPR) to override inhibition of translation, and utilizes antibody-dependent enhancement (ADE) infection to increase infectivity and suppress production of antiviral and inflammatory cytokines [6-12]. This impressive list of mechanisms allows DV to defeat the host immune response and replicate unchecked for dissemination. Furthermore, new immune evasion strategies may emerge in virulent strains, which would have a profound impact on dengue transmission. Therefore, elucidating immune evasion mechanisms and systematically disabling them are critical for guiding the rational design of live-attenuated dengue vaccines.

While DV infection is able to overcome the human immune response, it has been described that pre-treatment of human cells with type I or II interferon (IFN) can potently restrict DV infection [13-15]. In line with this observation, several interferon-stimulated genes (ISGs)

have been demonstrated to inhibit DV replication (reviewed in [16]). Given the well-documented side effects of IFN treatment in patients, identification of ISGs that potently restrict DV infection and specifically inducing their activity may provide another avenue for therapeutic intervention.

In this dissertation, we explored these concepts and identified potential molecular targets for anti-dengue therapies.

## MAJOR FINDINGS AND IMPLICATIONS

In Chapter 2, we described a key mechanism for DV evasion of RIG-I-mediated immunity. The findings are:

- NS3 binds directly to 14-3-3ε to block RIG-I binding and RIG-I translocation to mitochondria.
- NS3 inhibits IFN induction in a proteolysis-independent manner.
- NS3 usurps 14-3-3ε binding by using a phosphomimetic motif that resembles a canonical phospho-serine/threonine motif found in cellular binding partners of 14-3-3.
- A recombinant DV that encodes a 14-3-3ε-binding deficient NS3 protein ($DV2_{KIKP}$) is deficient in RIG-I antagonism and elicits a markedly enhanced innate immune response.

It has been long described that DV infection poorly elicits IFN induction, but mechanistic details remained elusive. We uncover how DV NS3 blocks the translocation of RIG-I, a key sensor of DV, to inhibit IFN induction. Furthermore, most viral proteases that antagonize immunity do so by cleaving immune molecules. However, NS3 targets 14-3-3ε and RIG-I via a proteolysis-independent mechanism, which provides a mandate to reconsider how viral proteases subvert immunity. We speculate that other examples of proteolysis-independent antagonism of

immunity by viral proteases will be uncovered.

The phosphomimetic residue E has been used to emulate site-specific phosphorylation of S/T in molecular biology experiments for decades. Intriguingly, we find that NS3 usurps 14-3-3 binding by using a phosphomimetic motif. To the best of our knowledge, this is the first example of a naturally occurring phosphomimetic utilized in an infectious disease mechanism. Furthermore, we engineered a mutant virus $DV2_{KIKP}$ which elicits a markedly enhanced immune response. Given the poor efficacy against DV2 in recent vaccine trials [17,18], our work provides a framework for rational design of dengue vaccines In addition, our detailed characterization of NS3-14-3-3ε binding may aid the design of small molecule inhibitors. Finally, dysregulation of innate immune sensors has been implicated in autoimmune and inflammatory diseases. Therefore, NS3 or NS3-derived peptides might be useful for modulating aberrant RIG-I signaling.

In Chapter 3, we extended our findings from Chapter 2 and demonstrated another aspect of RIG-I antagonism by DV. The findings are:

- RIG-I is degraded in a lysosome-dependent manner in DV-infected cells.
- NS3 expression is sufficient to degrade RIG-I.
- $DV2_{KIKP}$ fails to degrade RIG-I and further induces RIG-I expression.

These findings support a model where NS3 binds to 14-3-3ε to block RIG-I binding and translocation to mitochondria, and RIG-I is subsequently targeted for degradation via lysosomes. These results uncover a novel strategy used by DV to drive host-mediated degradation of RIG-I. In addition, $DV2_{KIKP}$ fails to degrade RIG-I, which has implications for its use as a potential vaccine.

In Chapter 4, we tested if IFITM proteins could restrict the antibody-dependent enhancement (ADE) of DV infection. The findings are:

- IFITM1-3 restrict both direct and ADE DV infection.
- Both direct DV infection and ADE-mediated DV infection are equally susceptible to IFITM-mediated restriction.

These results show that IFITM proteins, which are ISGs that potently inhibit virus entry, are equally effective at restricting both direct and ADE DV infection. Since ADE is thought to be a principal mechanism underlying severe dengue disease during a secondary infection, our data suggest that upregulation of IFITM activity may be effective against secondary DV infections.

**FUTURE DIRECTIONS**

In this section, we discuss potential research directions that may further our understanding of dengue pathogenesis, with a focus on implications for therapeutic interventions. First, while we demonstrated NS3 inhibition of RIG-I translocation to mitochondrial MAVS to inhibit type I IFN induction, it has been described recently that peroxisomal MAVS mediates type III IFN induction [19]. Therefore, it would be interesting to determine if NS3 also inhibits RIG-I translocation to peroxisomes, and if DV infection inhibits type III IFN induction. Similarly, it is not known if the related sensor MDA5 requires 14-3-3ε to translocate to mitochondria. If NS3 also inhibits RIG-I translocation to peroxisomes and MDA5 translocation to mitochondria, it would suggest the additional utility of targeting NS3 with small molecule inhibitors, and the supplementary benefits of $DV2_{KIKP}$ as a possible vaccine.

Second, we proposed earlier that systematically disabling immune evasion mechanisms

of DV may allow rational design of live-attenuated DV vaccines. While we have successfully engineered a mutant virus that fails to antagonize RIG-I ($DV2_{KIKP}$), we envision that disabling additional immune evasion mechanisms in this background would further improve the safety profile and immunogenicity of the virus. Given that many other known immune evasion mechanisms of DV pertain to type I IFN-receptor signaling, disabling them in concert with $NS3_{KIKP}$ might present synergistic effects, as $DV2_{KIKP}$ elicits enhanced type I IFN induction.

Third, the molecular details of NS3-mediated degradation of RIG-I are poorly understood. In particular, how does NS3 target RIG-I for lysosomal degradation? While we proposed that K63-linked ubiquitination of RIG-I and autophagy may play important roles in RIG-I degradation, it is also possible that a completely unrelated mechanism is responsible. Since $NS3_{KIKP}$, which does not bind 14-3-3ε, fails to degrade RIG-I, it is likely that RIG-I-14-3-3ε interaction is critical for RIG-I stability. Preliminary experiments silencing 14-3-3ε or using the R18 peptide to block 14-3-3 interaction partners did not yield conclusive results on RIG-I degradation, especially since the former led to cytotoxicity. Future studies should be directed at understanding this process, and they may shed light on homeostatic regulation of RIG-I in the cell.

Fourth, the observation that IFITM proteins potently restrict ADE DV infection suggests that upregulation of IFITM activity may be effective against secondary DV infections. While IFITM proteins are ISGs that are strongly induced by IFN, it has been suggested that other cytokines can also induce IFITM expression [20]. In addition, small molecule libraries could also be screened for the ability to upregulate IFITM activity. These strategies may allow IFITM activity to be turned on temporarily, and may be particularly useful in cases of traveling to dengue-endemic areas.

## A POSTSCRIPT

The number of DV infections and severe disease cases worldwide is staggering and increasing with time. Vector control and supportive treatment are helpful but have proven inadequate in times of dengue outbreaks. Therefore, a key challenge for dengue immunologists is to better understand DV pathogenesis in order to design broadly effective vaccines and antivirals. We hope that the work described in this dissertation has furthered this goal and we eagerly await the development of much needed DV therapeutics.

## REFERENCES


1. Uchida L, Espada-Murao LA, Takamatsu Y, Okamoto K, Hayasaka D, et al. (2014) The dengue virus conceals double-stranded RNA in the intracellular membrane to escape from an interferon response. Sci Rep 4: 7395.

2. Morrison J, Aguirre S, Fernandez-Sesma A (2012) Innate immunity evasion by Dengue virus. Viruses 4: 397-413.

3. Jain B, Chaturvedi UC, Jain A (2014) Role of intracellular events in the pathogenesis of dengue; an overview. Microb Pathog 69-70: 45-52.

4. Schmid MA, Diamond MS, Harris E (2014) Dendritic cells in dengue virus infection: targets of virus replication and mediators of immunity. Front Immunol 5: 647.

5. Bidet K, Dadlani D, Garcia-Blanco MA (2014) G3BP1, G3BP2 and CAPRIN1 are required for translation of interferon stimulated mRNAs and are targeted by a dengue virus non-coding RNA. PLoS Pathog 10: e1004242.

6. Emara MM, Brinton MA (2007) Interaction of TIA-1/TIAR with West Nile and dengue virus products in infected cells interferes with stress granule formation and processing body assembly. Proc Natl Acad Sci U S A 104: 9041-9046.

7. Lee YR, Lei HY, Liu MT, Wang JR, Chen SH, et al. (2008) Autophagic machinery activated by dengue virus enhances virus replication. Virology 374: 240-248.

8. Pena J, Harris E (2011) Dengue virus modulates the unfolded protein response in a time-dependent manner. J Biol Chem 286: 14226-14236.

9. Halstead SB, Mahalingam S, Marovich MA, Ubol S, Mosser DM (2010) Intrinsic antibody-dependent enhancement of microbial infection in macrophages: disease regulation by immune complexes. Lancet Infect Dis 10: 712-722.

10. Chareonsirisuthigul T, Kalayanarooj S, Ubol S (2007) Dengue virus (DENV) antibody-dependent enhancement of infection upregulates the production of anti-inflammatory cytokines, but suppresses anti-DENV free radical and pro-inflammatory cytokine production, in THP-1 cells. J Gen Virol 88: 365-375.

11. Modhiran N, Kalayanarooj S, Ubol S (2010) Subversion of innate defenses by the interplay between DENV and pre-existing enhancing antibodies: TLRs signaling collapse. PLoS Negl Trop Dis 4: e924.

12. Chan KR, Ong EZ, Tan HC, Zhang SL, Zhang Q, et al. (2014) Leukocyte immunoglobulin-like receptor B1 is critical for antibody-dependent dengue. Proc Natl Acad Sci U S A 111: 2722-2727.

13. Diamond MS, Roberts TG, Edgil D, Lu B, Ernst J, et al. (2000) Modulation of Dengue virus infection in human cells by alpha, beta, and gamma interferons. J Virol 74: 4957-4966.

14. Diamond MS, Harris E (2001) Interferon inhibits dengue virus infection by preventing translation of viral RNA through a PKR-independent mechanism. Virology 289: 297-311.

15. Chase AJ, Medina FA, Munoz-Jordan JL (2011) Impairment of CD4+ T cell polarization by dengue virus-infected dendritic cells. J Infect Dis 203: 1763-1774.

16. Schoggins JW, Rice CM (2011) Interferon-stimulated genes and their antiviral effector functions. Curr Opin Virol 1: 519-525.

17. Villar L, Dayan GH, Arredondo-Garcia JL, Rivera DM, Cunha R, et al. (2015) Efficacy of a tetravalent dengue vaccine in children in Latin America. N Engl J Med 372: 113-123.

18. Capeding MR, Tran NH, Hadinegoro SR, Ismail HI, Chotpitayasunondh T, et al. (2014) Clinical efficacy and safety of a novel tetravalent dengue vaccine in healthy children in Asia: a phase 3, randomised, observer-masked, placebo-controlled trial. Lancet 384: 1358-1365.

19. Odendall C, Dixit E, Stavru F, Bierne H, Franz KM, et al. (2014) Diverse intracellular pathogens activate type III interferon expression from peroxisomes. Nat Immunol 15: 717-726.

20. Bailey CC, Huang IC, Kam C, Farzan M (2012) Ifitm3 limits the severity of acute influenza in mice. PLoS Pathog 8: e1002909.